Spintronic devices

P.P.Freitas

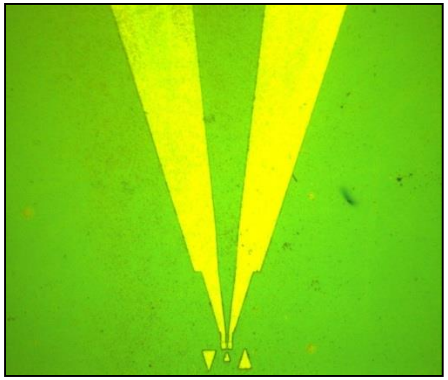

INESC-Microsistemas e Nanotecnologias/
Instituto Superior Técnico (Lisbon,PT)
and
International Iberian Nanotechnology Laboratory
(Braga, PT)

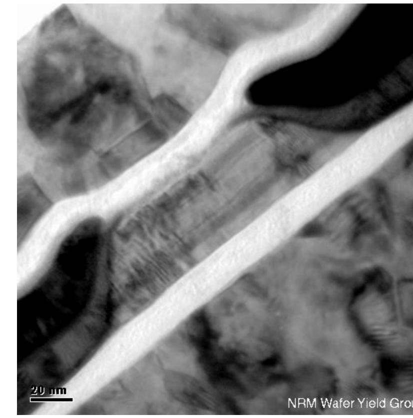

http://www.inesc-mn.pt

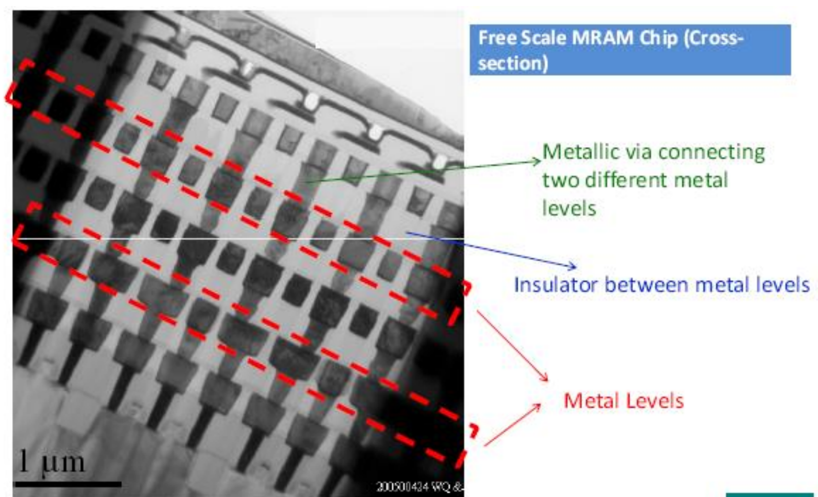

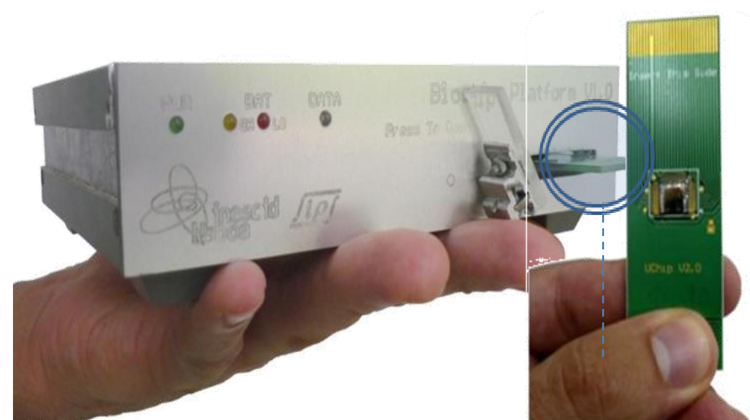

Frontiers on Magnetism, Benasque, February 2014

-Present markets:

Data storage : PC+consumer electronics

Sensors: automotive: current, power, position-linear and angular, battery cell monitoring
navigation systems-digital compass

MRAM: 1st generation

-Emerging markets:

NVM: STT-RAM (MRAM), M-FPGA (integrated Sensor + CMOS)

-New sensor markets:

Low power (<mW) , low noise (nT/sqrt(Hz),medium landscape (<5mm2) integrated sensors

-point of care biosensor arrays (MR sensor arrays, microfluidics, CMOS, packaging)

-scanning sensor arrays (high resolution current imaging, non destructive testing)
(MR, CMOS, packaging)

-remote sensor networks (hybrid RF antenna-MR sensor microsystems)

Very low noise -pT/sqrt(Hz)-integrated sensors for low frequency (1Hz) applications

-MCG/MEG-hybrid MEMS-flux guide-MR sensor arrays

-smart microelectrode arrays for neuroelectronics

1-Data Storage

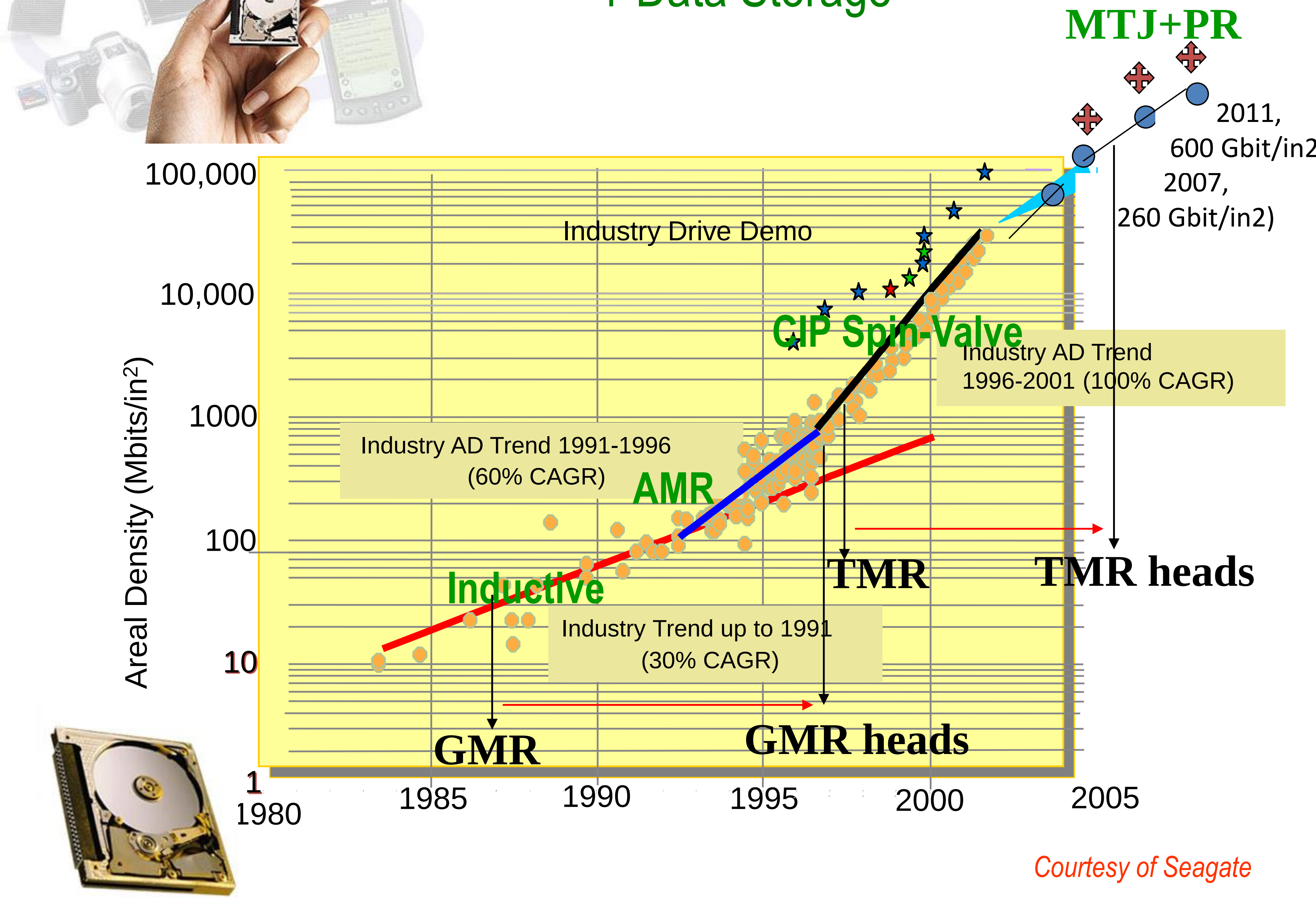

Courtesy of Seagate

Technology Transitions in Magnetic Recording

CPP Transducers
Tunneling and SV

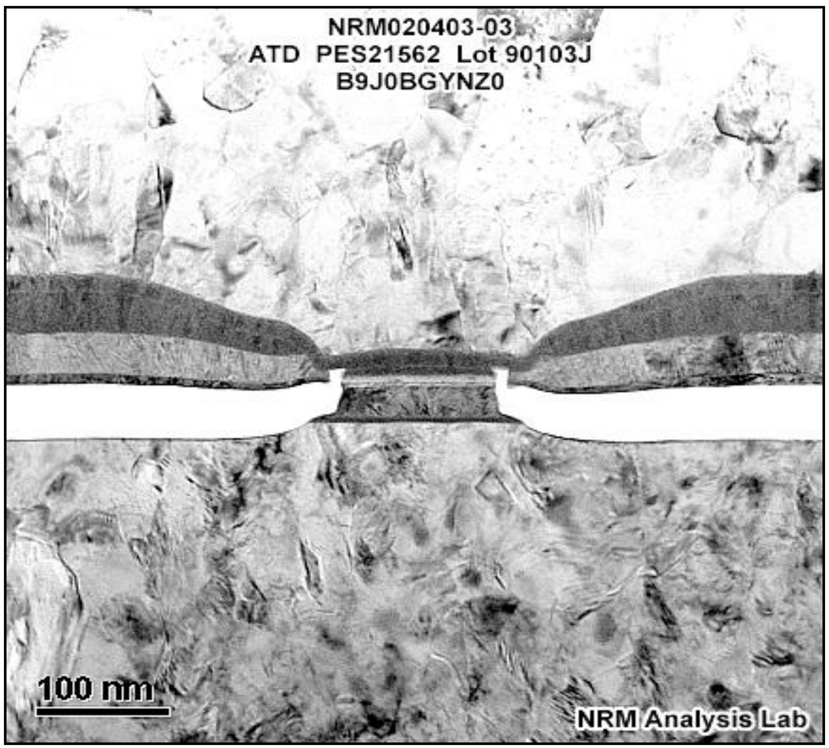

Perpendicular Recording

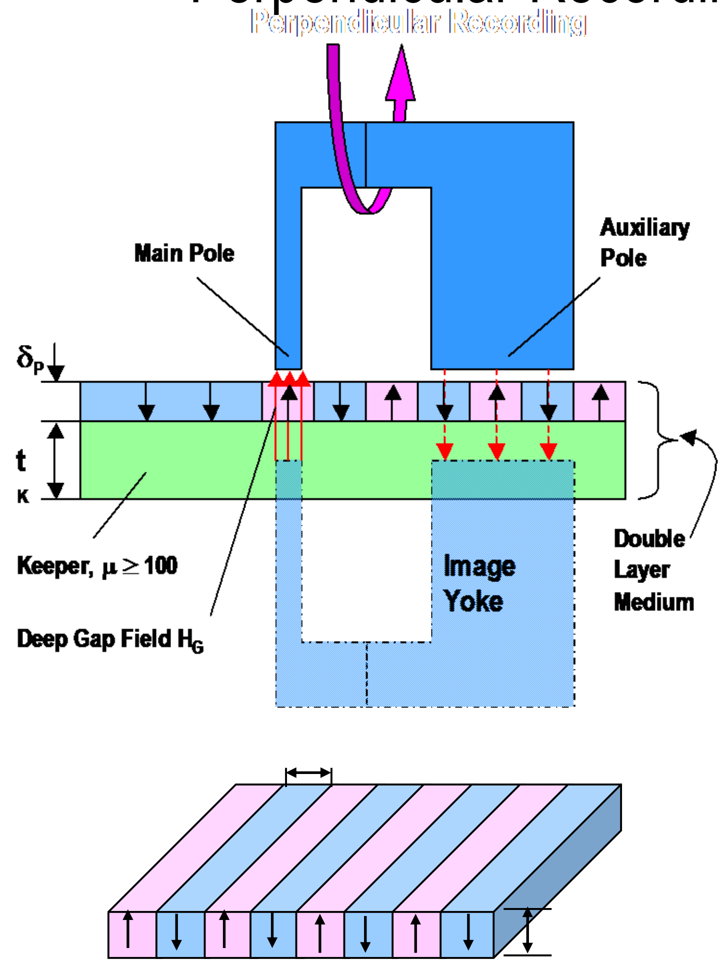

MTJ-MRAM

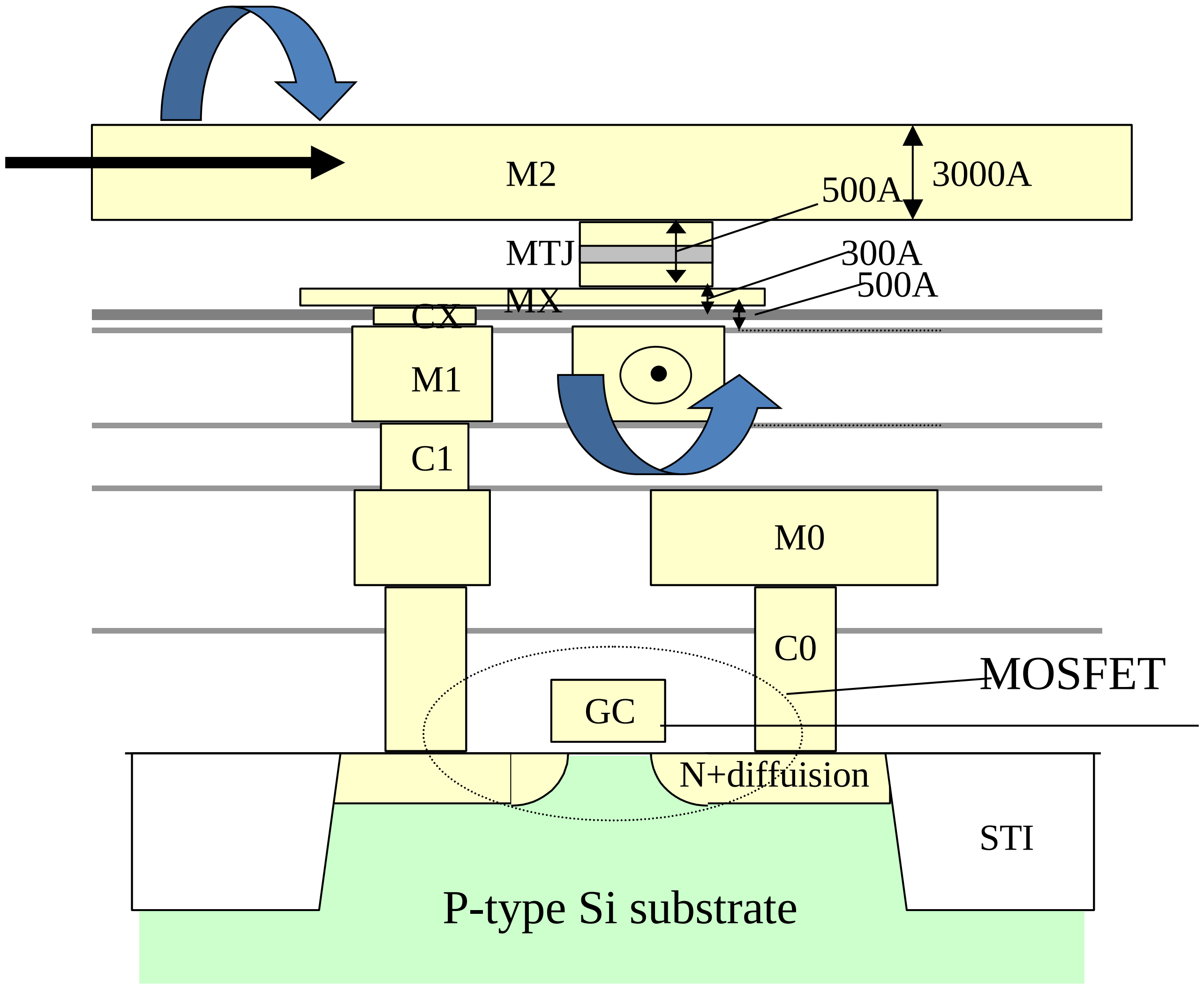

M2
3000A
500A
MTJ
300A
500A
MX
CX
M1
C1
M0
C0
MOSFET
GC
N+diffuision
STI
P-type Si substrate

3 MRAM Approaches

	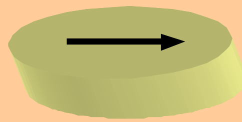	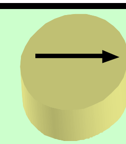	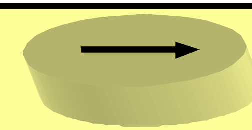
	FIMS writing	TAS+ FIMS writing	CIMS writing
Stabilization scheme	Shape anisotropy	Exchange biased storage layer	Shape anisotropy
Bit shape	Elliptic with AR~1,5	Circular	Elliptic with AR~1,5
Writing current	$I_W \#(AR-1).t.M_s/\sqrt{L}$	$I_w \# J_h.L^2$	$I_w \# J_c.L^2/AR$
Writing speed	~1-2ns	~1-2ns	<0,5ns
Useable range	L>200nm(no toggle)	35nm<L<200nm	25nm<L<150nm
Superparamagnetic limit	25nm	35nm	25nm

NEXT MRAM project (2000-2005)

III) Magnetoresistive Sensors in Automobile Applications, other industrial applications

At least 15 different types of sensors using magnetoresistive devices are already being integrated in automobiles

*Information from Sensitec website

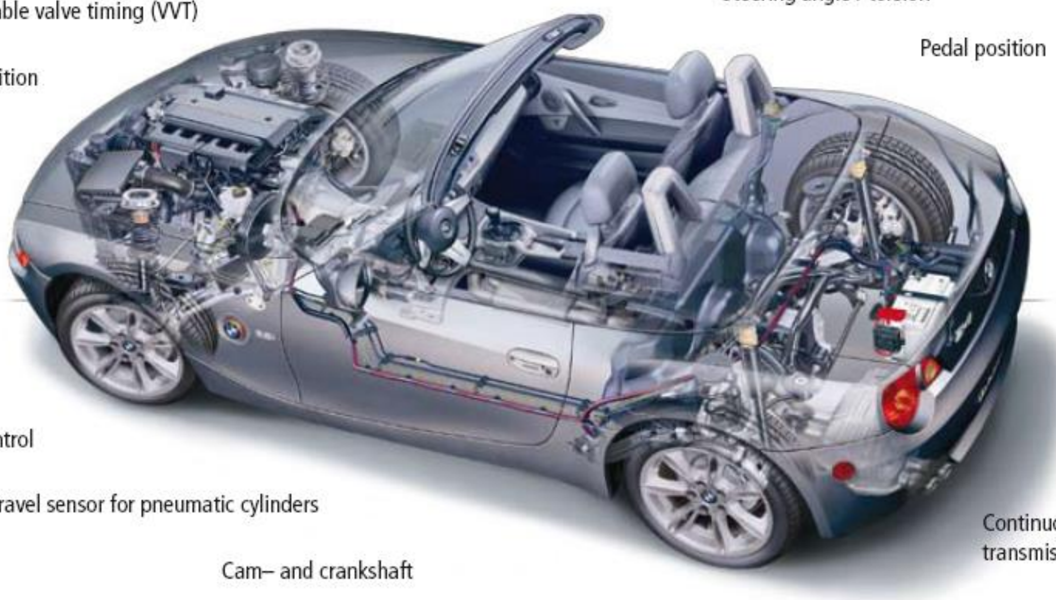

Advantages:

- Contactless, wear-free operating principle for angular and linear measurement
- Large air gap
- Large permissible air gap tolerances
- Withstands extreme operating conditions
- Full redundancy possible
- Failsafe design
- Flexible integration
- High bandwidth for measurements in time slots of less than 100 ms

+ Navigation Systems

+ Electric Batteries Safety Systems

+ Acceleration Sensors for Airbags (MEMS+Magnetoresistive)

IV-MagnetoResitive (MR) Biochips: diagnostics

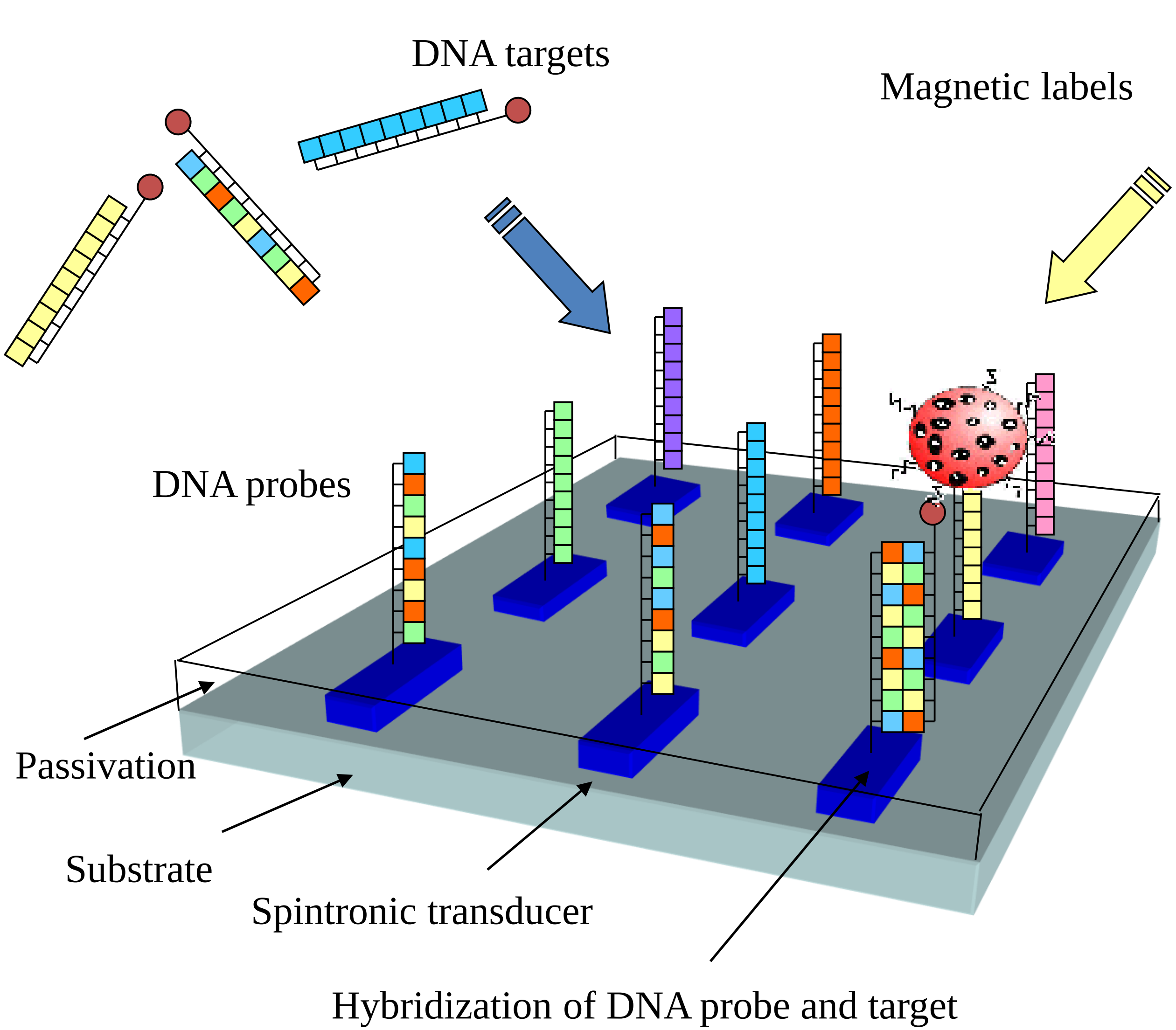

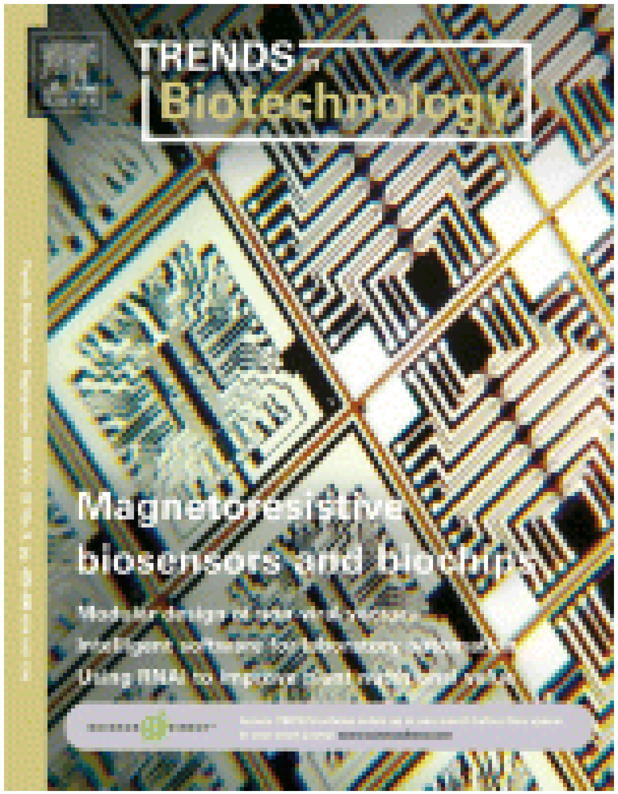

Trends in Biotechnology, August 2004

V-Biomedical imaging applications

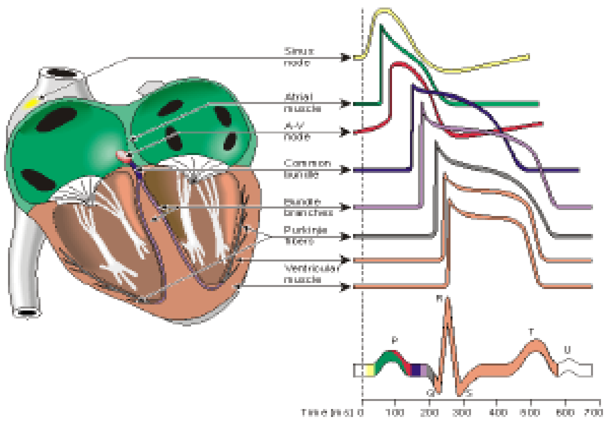

- Requirements:
- Magnetoencephalography-**fT**
- Magnetocardiography –**pT**
- Low field MRI-**fT**

- Increase GMR/TMR sensitivity, decrease noise background

- Devices:
- GMR/TMR + fluxguide hybrid sensors
- MEMS + GMR/TMR hybrid sensors

MR sensors: basics
1-Anisotropic Magnetoresistance
(intrinsic property)

Non spherical
3d wave functions

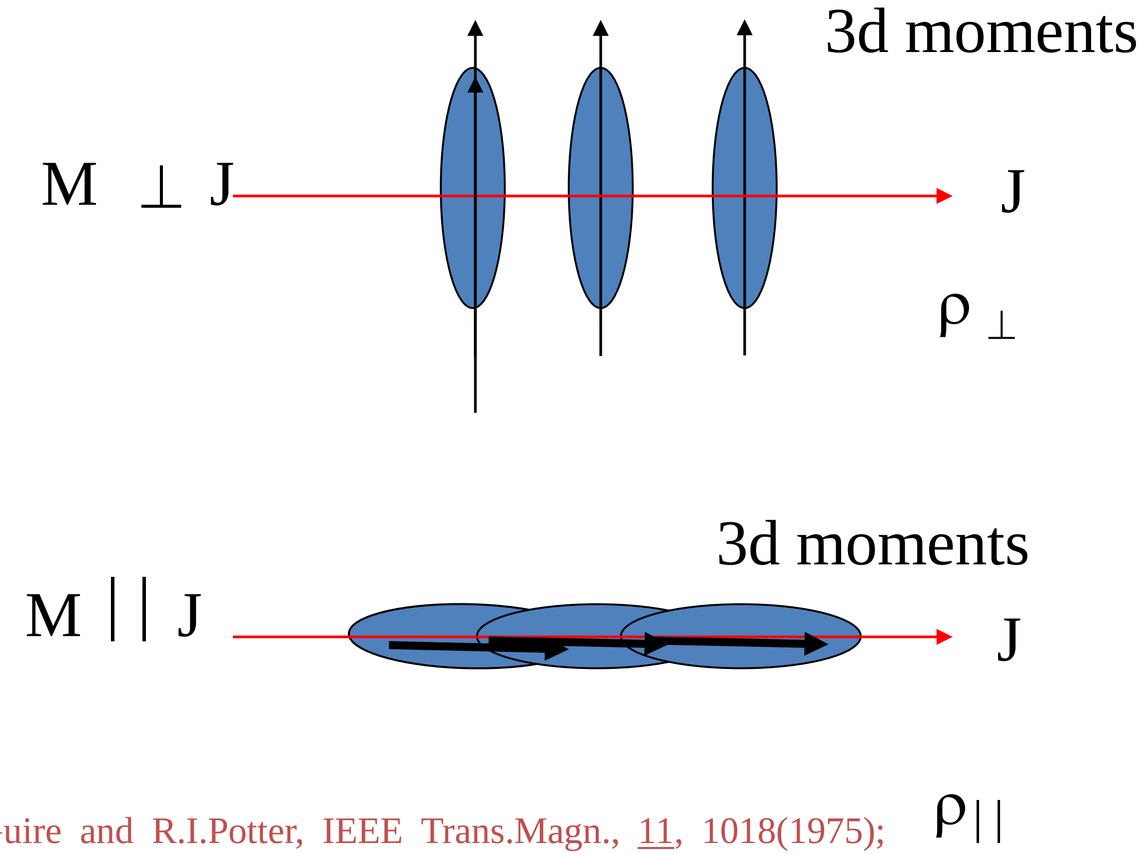

Different Scattering
cross sections

J.Smit, Physica 16, 612 (1951); T.R.McGuire and R.I.Potter, IEEE Trans.Magn., 11, 1018(1975); O.Jaoul, I.A.Campbell, and A.Fert, J.Magn.Magn.Mater., 5, 23(1977); L.Berger, AIP Conf.Proc., .34, 355(1976); L.Berger, P.P.Freitas, J.D.Warner, and J.E.Schmidt, J.Appl.Phys., .64, 5459 (1988).

AMR in thin $Ni_{80}Fe_{20}$ films

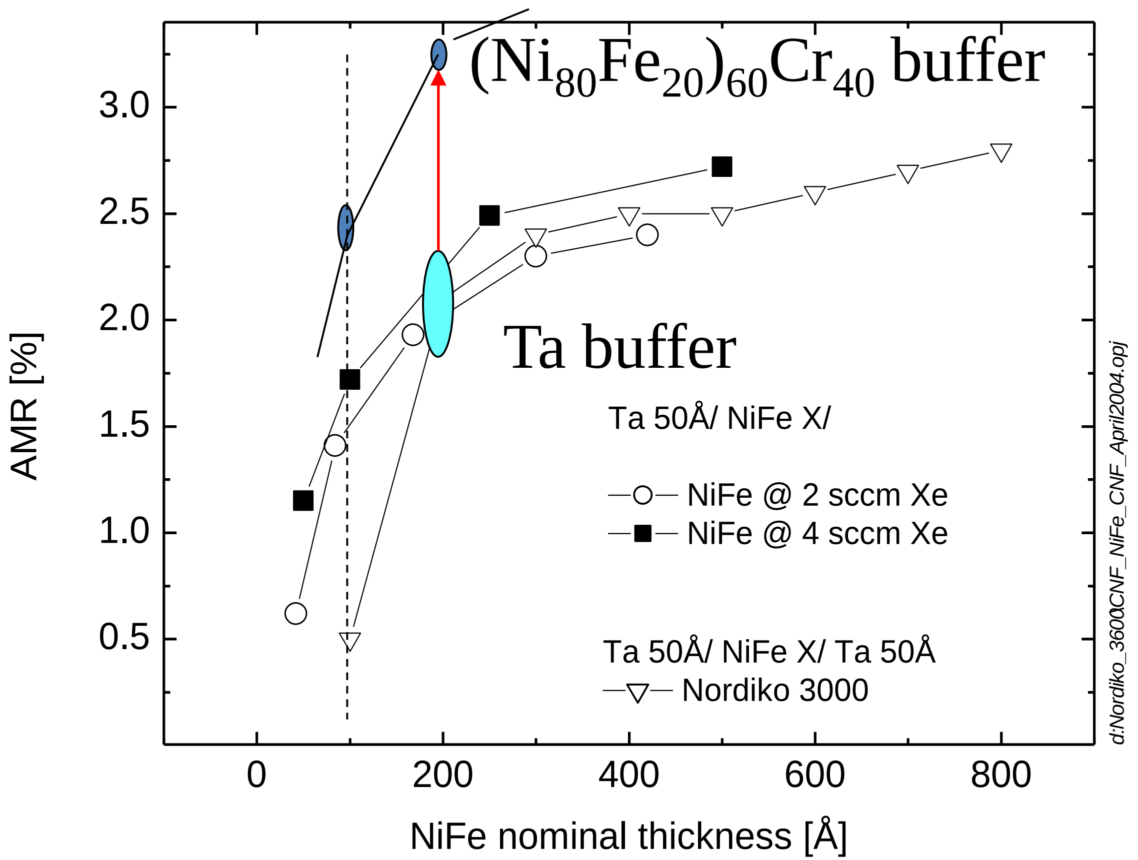

Buffer controls grain size, mean free path and specularity

How to make an AMR sensor?

1-Control the magnetics of the thin NiFe slab:

Magnetic Energy of a semi-infinite thin film **(w>>h,t)**

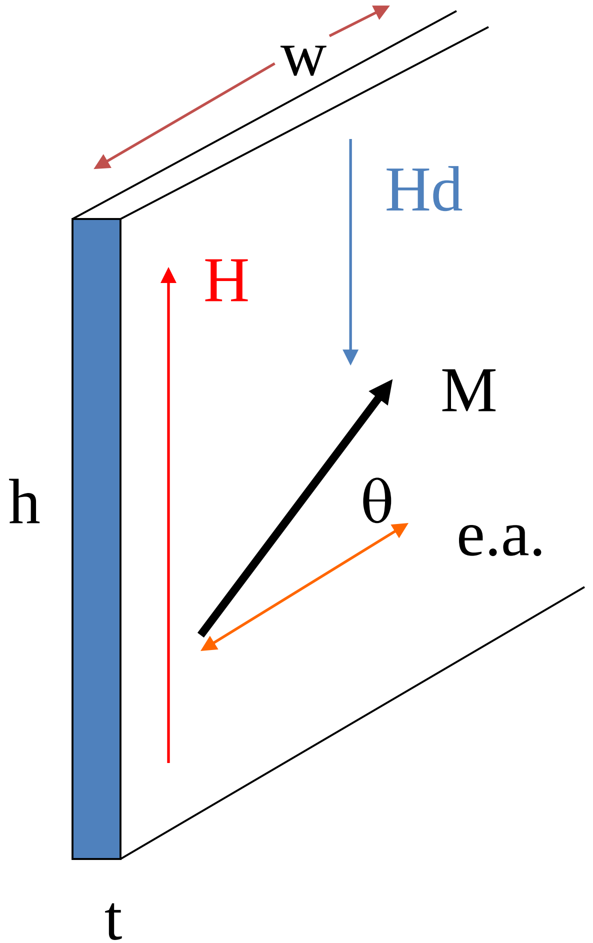

$$E/V = -\mu_o H.M + K \sin^2\theta - \tfrac{1}{2}\mu_o H_d.M$$

Where $Hd_y = -M_y N_y$

Minimizing energy:

$$\sin\theta = \mu_o H M_s / 2 K_{eff}$$

$$K_{eff} = K + \tfrac{1}{2}\mu_o M_s^2 N_y$$

$$Ny \cong (t/\pi h) \ln [(h-\Delta)/\Delta]$$

B.D.Cullity(1972) Introduction to Magnetic Materials, A.W, MA

Theory Magnetic Recording, N.Bertram, p.172

2- R vs H response for a single NiFe stripe

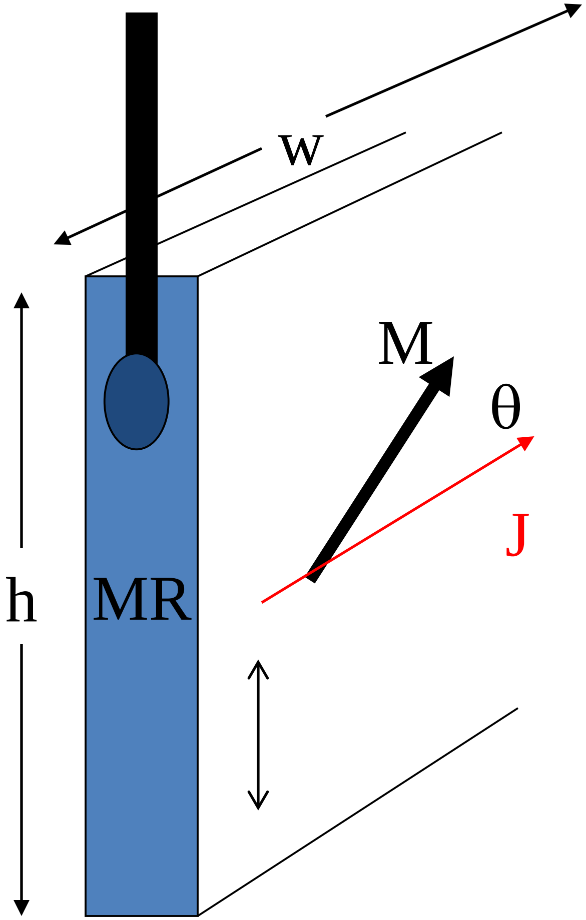

$$R = R_{per} + \Delta R \cos^2 \theta$$

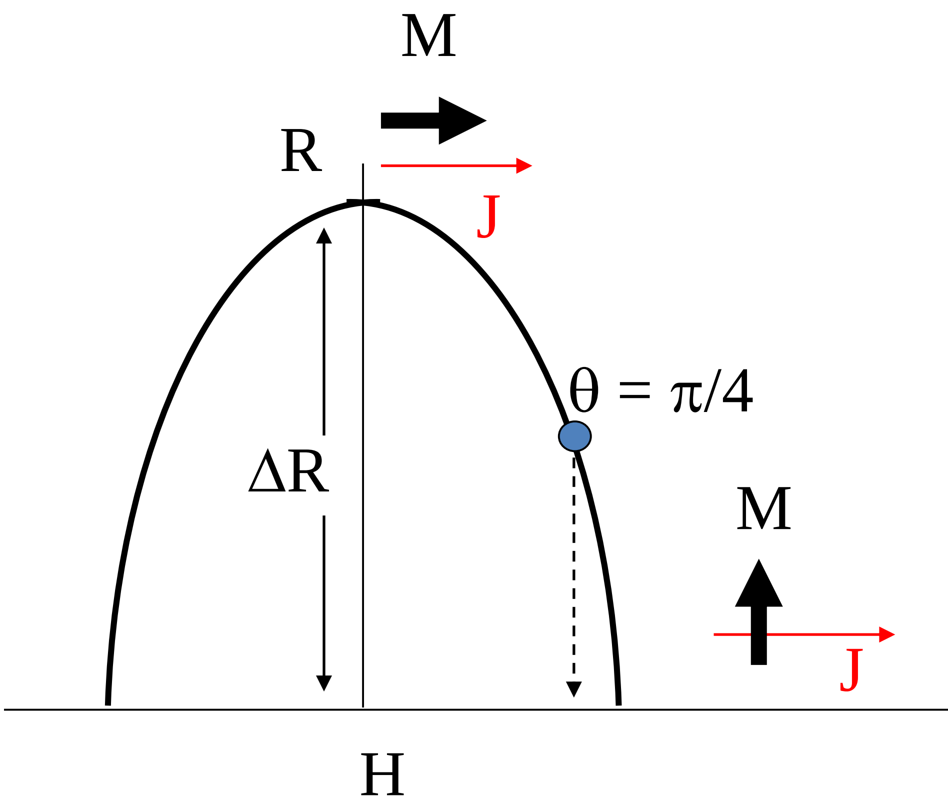

NON linear near H = 0

Chapter 7, Theory of Magnetic Recording, N.Bertram, 1994
N.Smith, IEEE Trans.Magn., 23, 259, 1987

3-Biased Soft Adjacent Layer AMR sensor

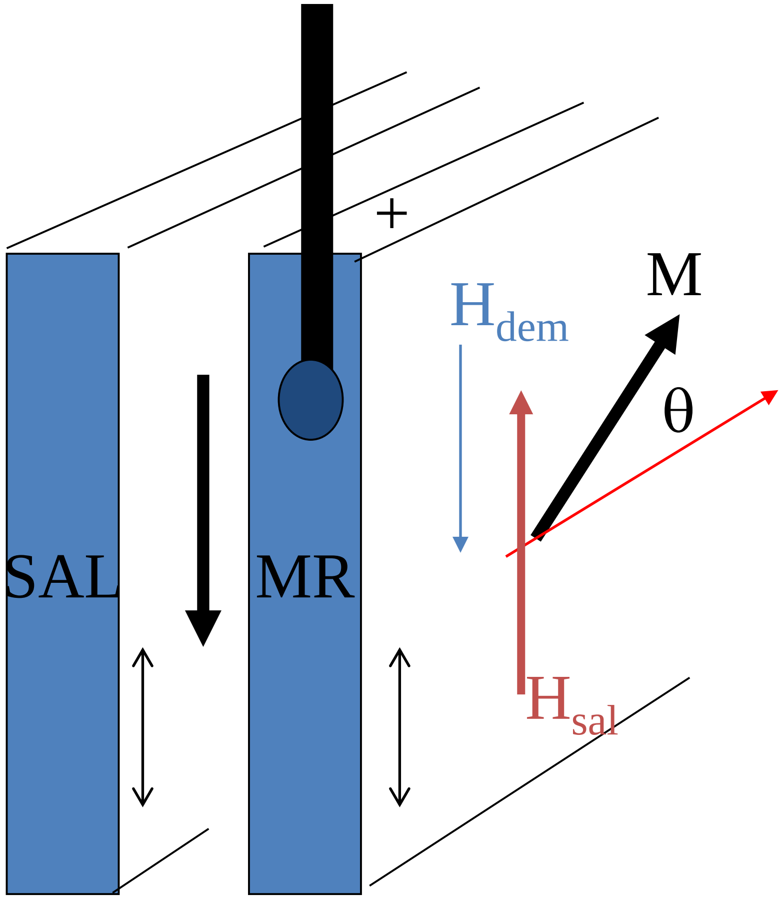

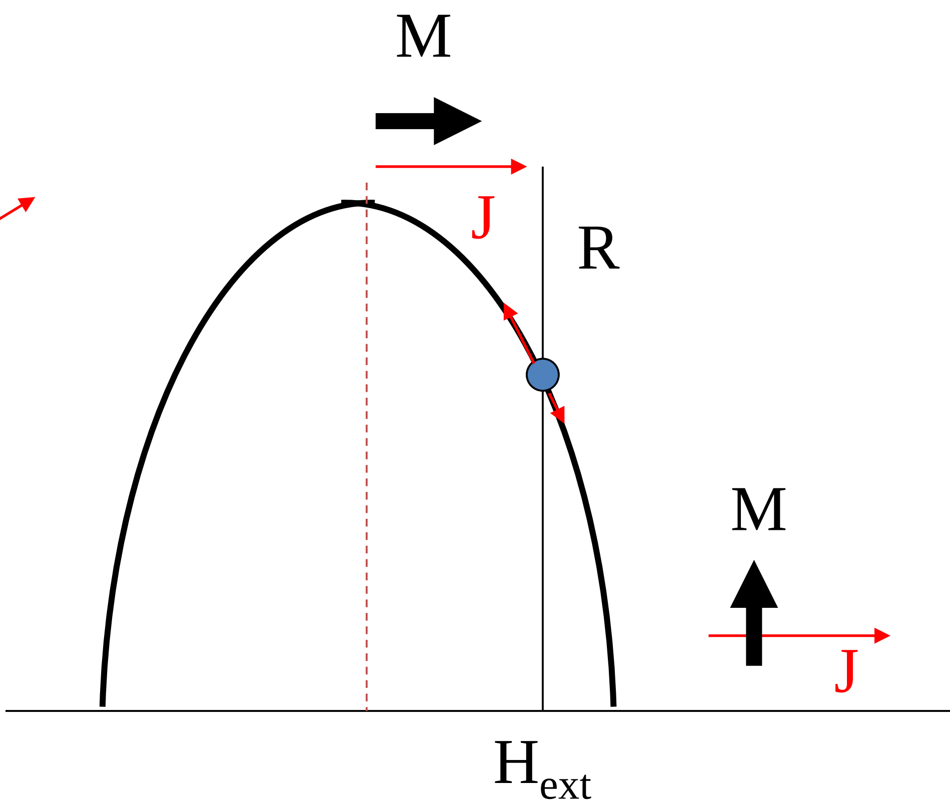

Linearized output

Chapter 7, Theory of Magnetic Recording, N.Bertram, 1994
N.Smith, IEEE Trans.Magn., 23, 259, 1987

Micromagnetic simulation for SAL and MR layers

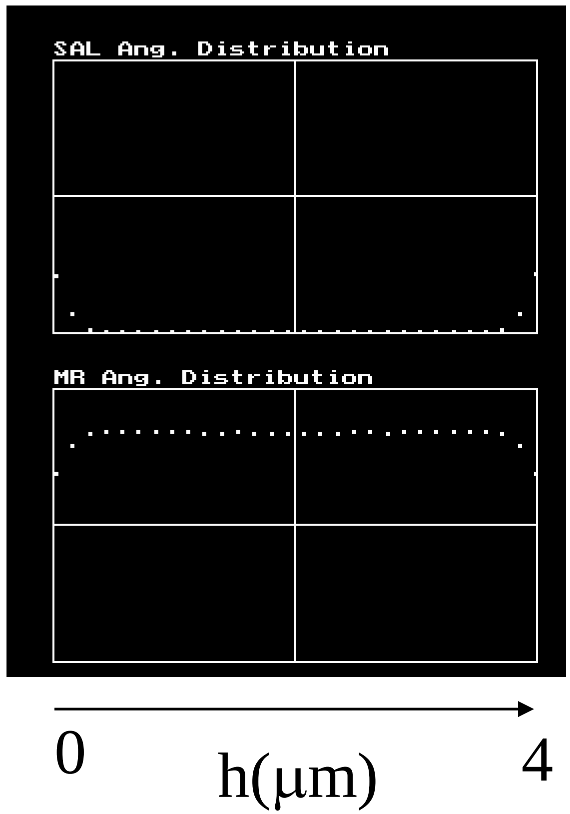

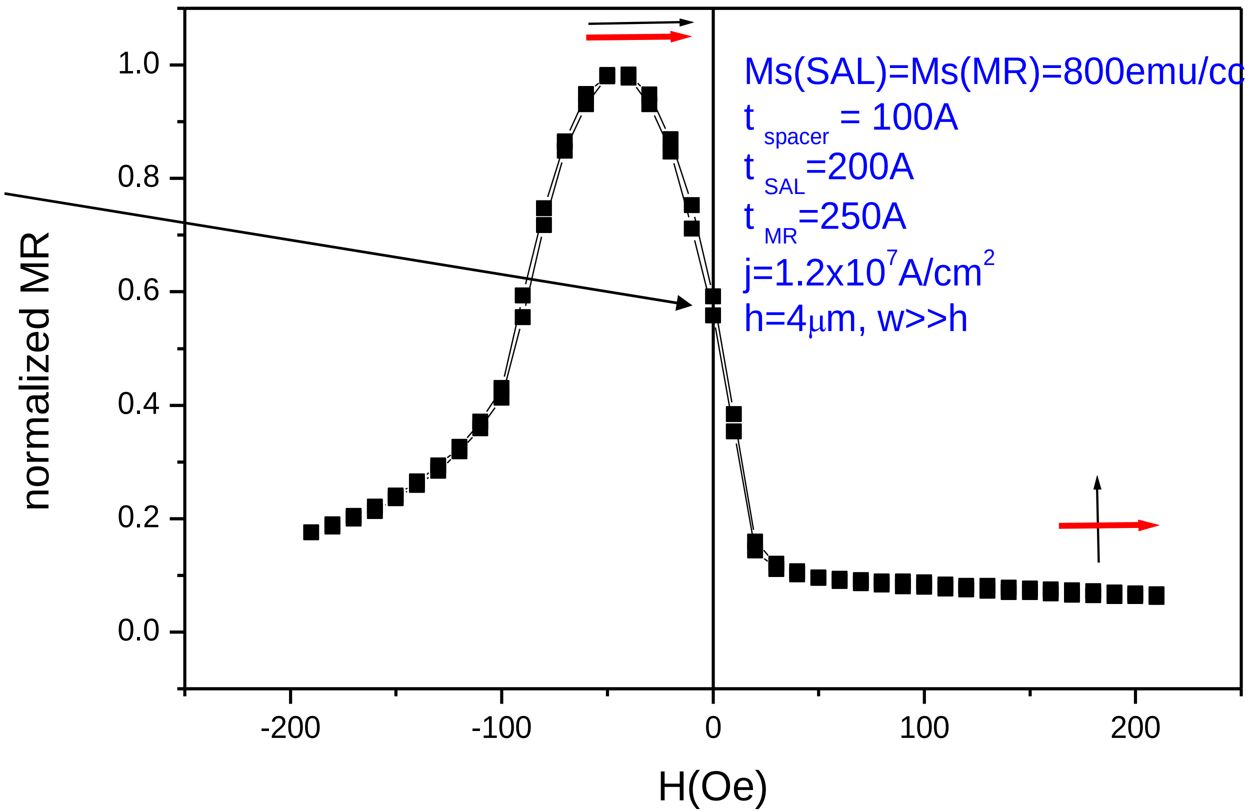

AMR heads used till 1995 in HDD and still in use for tape recording

• The Spin Valve Sensor

GMR effect, spin dependent scattering
At NM/M interfaces and in the bulk
(1986)

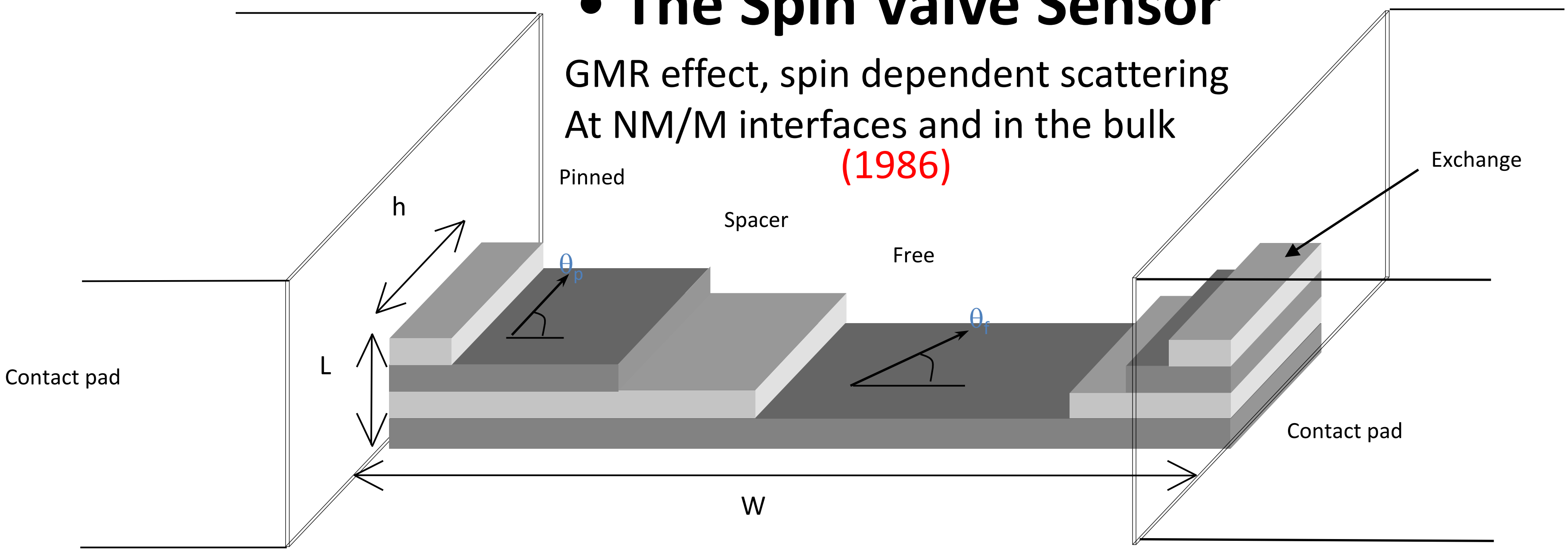

$$\Delta V = ½ (\Delta R/R).I.Rsq.(W/h) <1\text{-}\cos(\theta_f - \theta_p)>$$

1-C.Tsang, R.E.Fontana, T.Lin, D.E.Heim, V.S.Speriosu, B.A.Gurney, and M.L.Williams, IEEE Trans.Magn., 30, 3801 (1994).

3- B.Dieny, V.S.Speriosu, S.S.Parkin, B.A.Gurney, D.R.Wilhoit, and D.Mauri, Phys.Rev.B, 43, 1297(1991).

4- D.E.Heim, R.E.Fontana, C.Tsang, V.S.Speriosu, B.A.Gurney, and M.L.Williams, IEEE Trans.Magn.., 30, 316 (1994); P.P.Freitas, J.L.Leal, L.V.Melo, N.J.Oliveira, L.Rodrigues, and A.T.Sousa, Appl.Phys.Lett., 65, 493 (1994);

J.L.Leal, N.J.Oliveira, L.Rodrigues, A.T.Sousa, and P.P.Freitas, IEEE Trans.Magn., 30, 3031(1994).

Spin Valve sensors-magnetic response

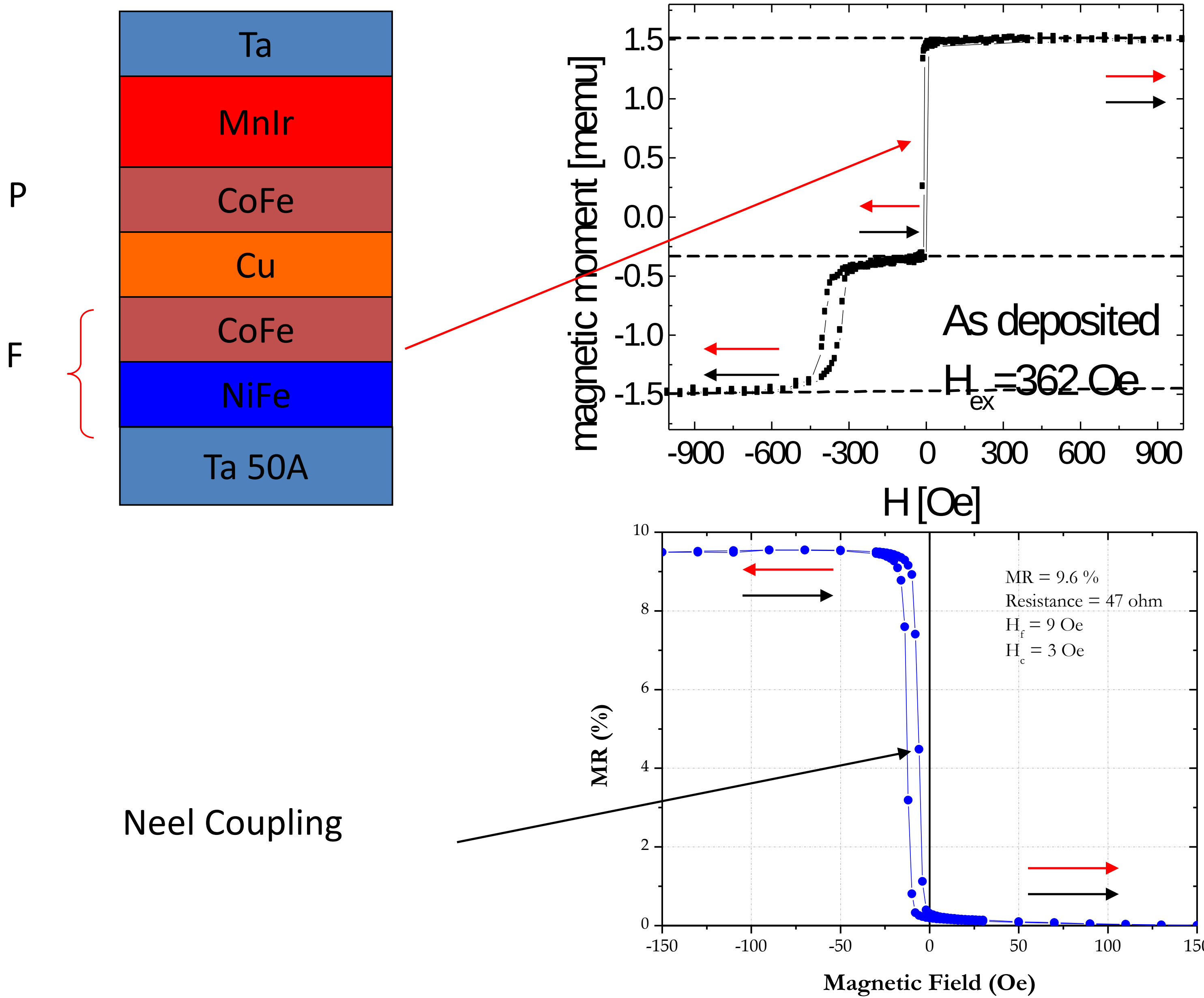

SV materials

Basic stack(94-97)

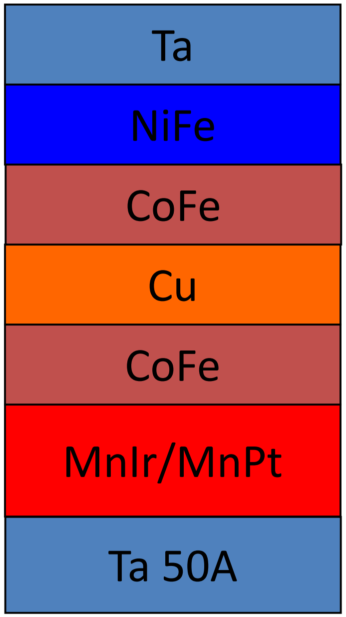

8%<MR<10%

Hc < 2Oe

Hf < 10 Oe

Hex > 600 Oe(MnIr)

 > 1000 Oe (MnPt)

SAF+NiFeCr(97-02)

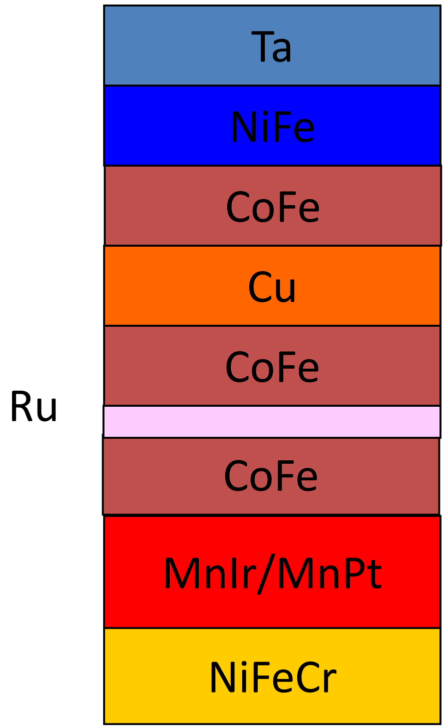

10%<MR<15%

Hex > 3000 Oe

Specular SAF(01-)

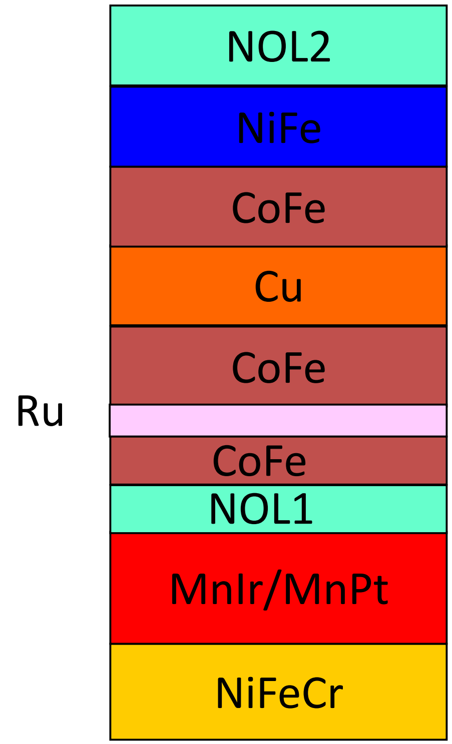

14%<MR<16(20)%

Spin Valve Sensor: biasing

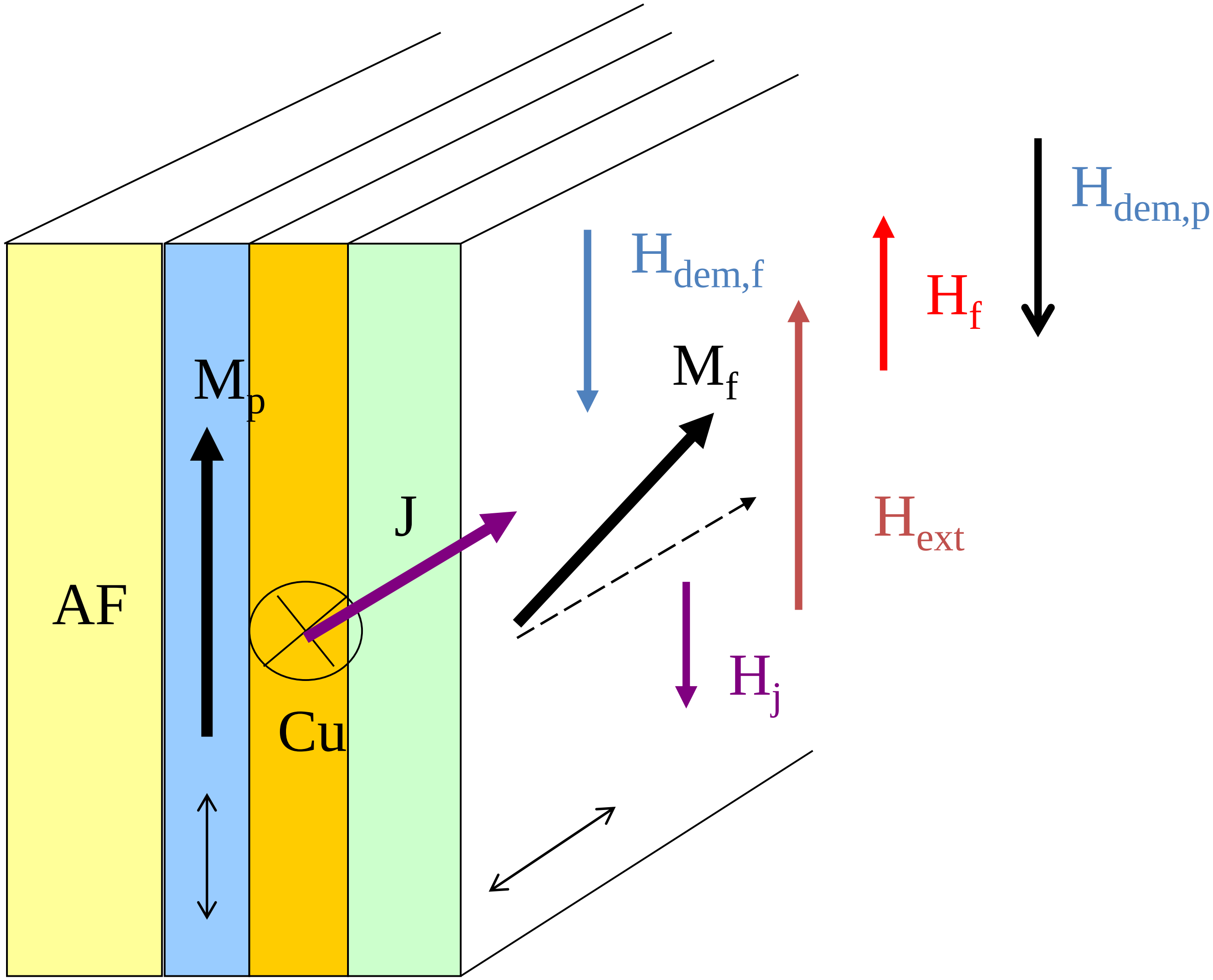

$$\sin\theta_f = \mu_o \,[H_{ext} - H_j - H_{dem,p} + H_f\,]\, M_s / 2\, K_{eff}$$

Sensor design issues

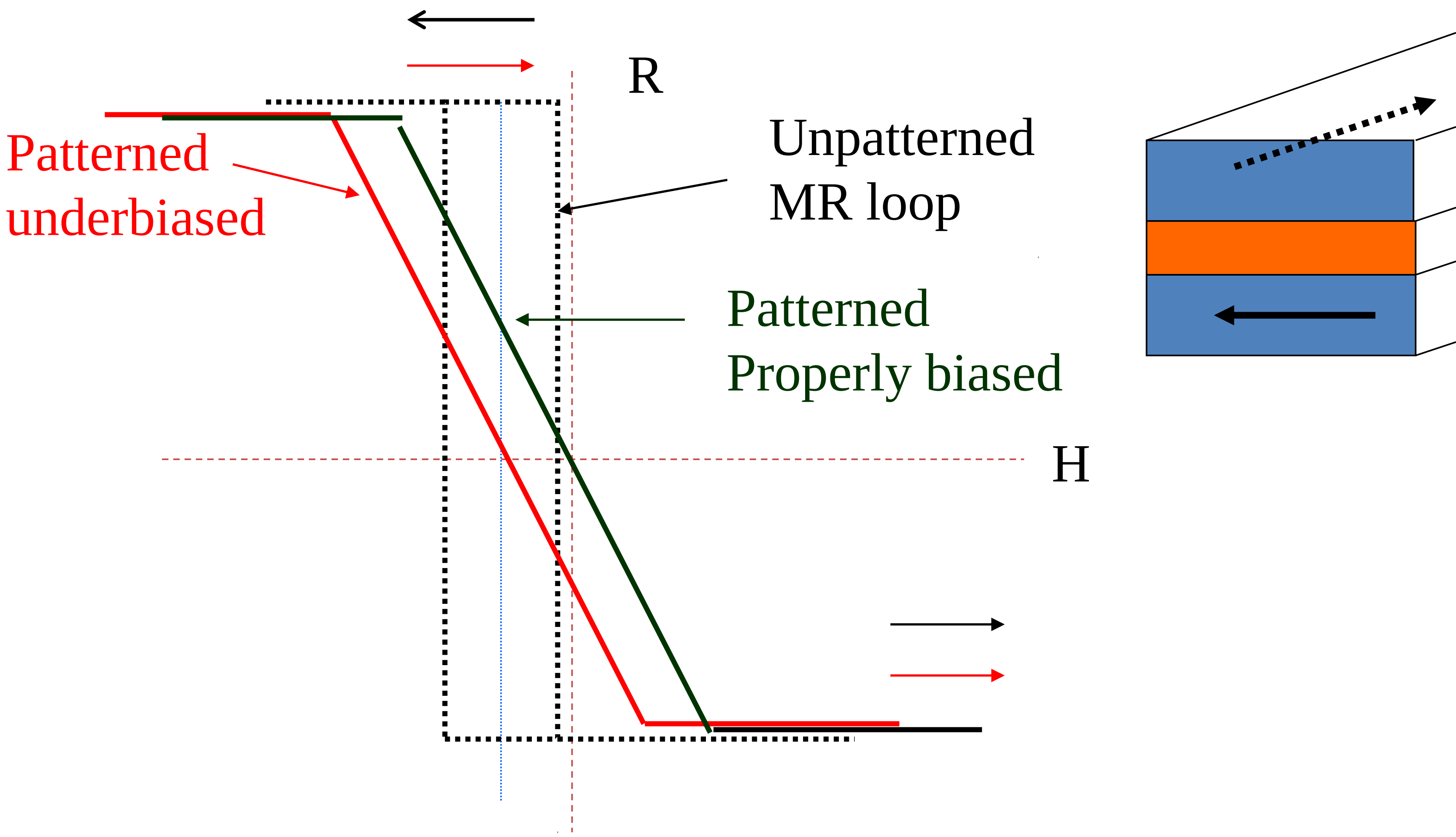

Micromagnetic simulation for SV sensor

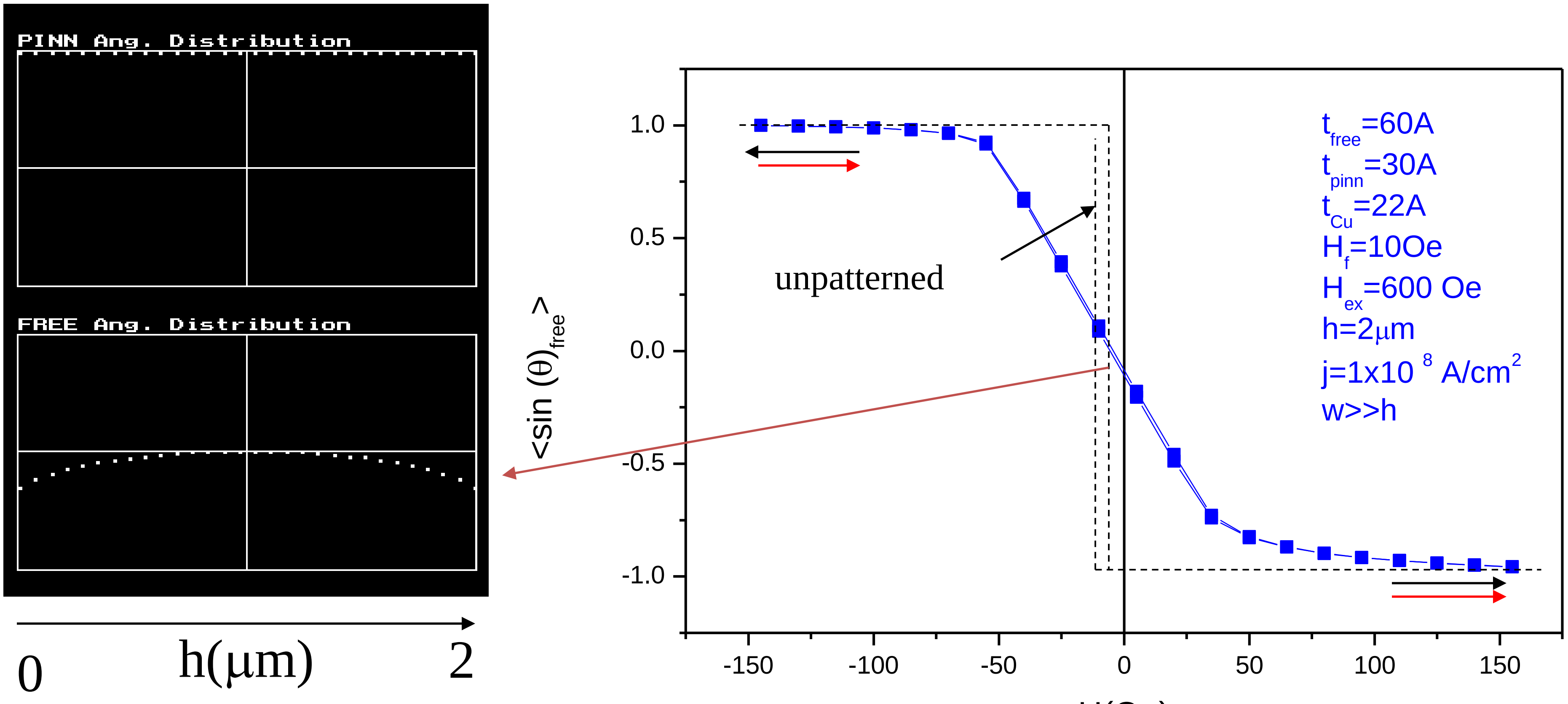

Spin Valve Sensor Transfer Curve

Ta20Å/NiFe30Å/CoFe20Å/Cu28Å/CoFe25Å/MnIr60Å/Ta25Å

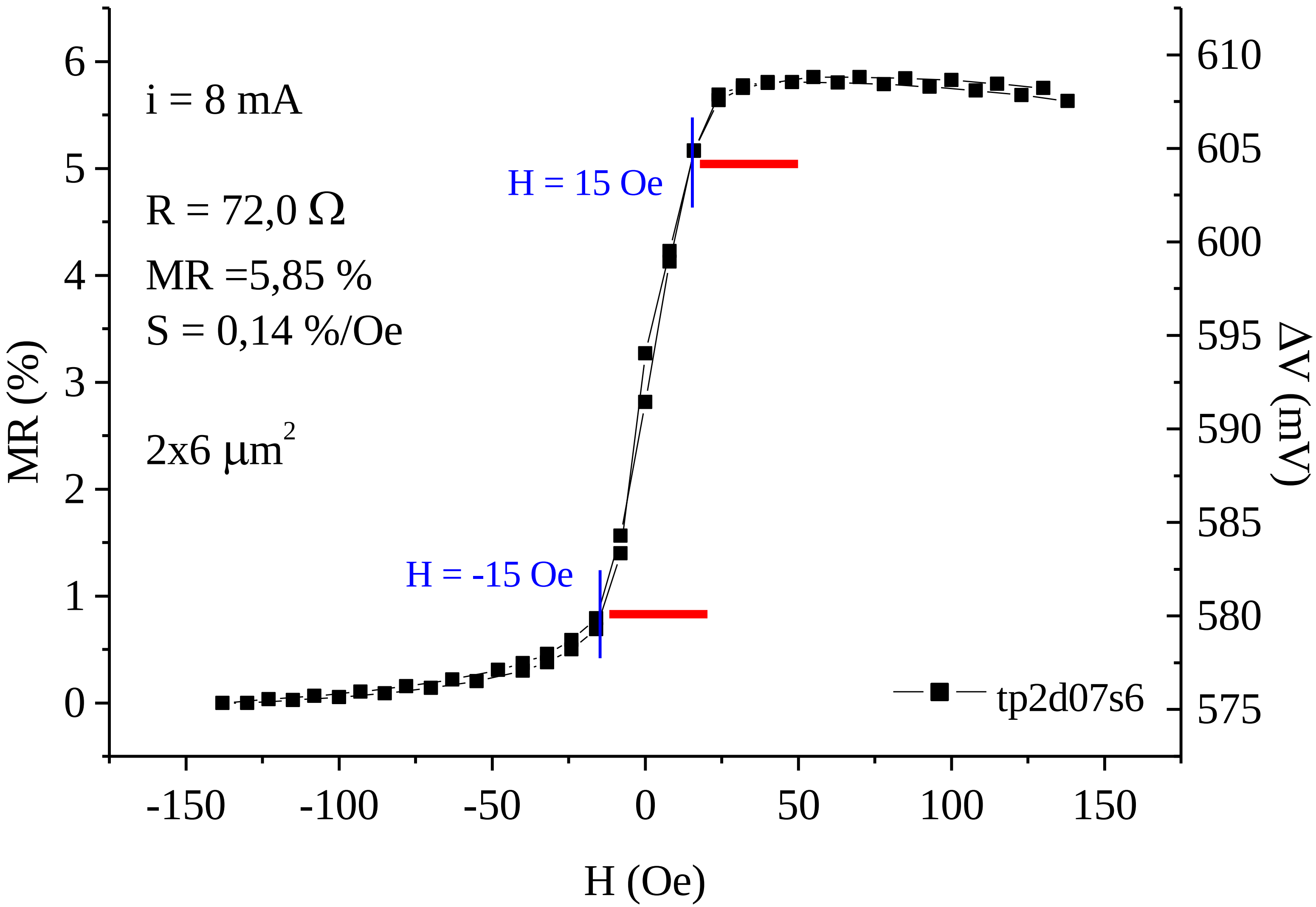

How to chose the best sensor? Noise spectrum

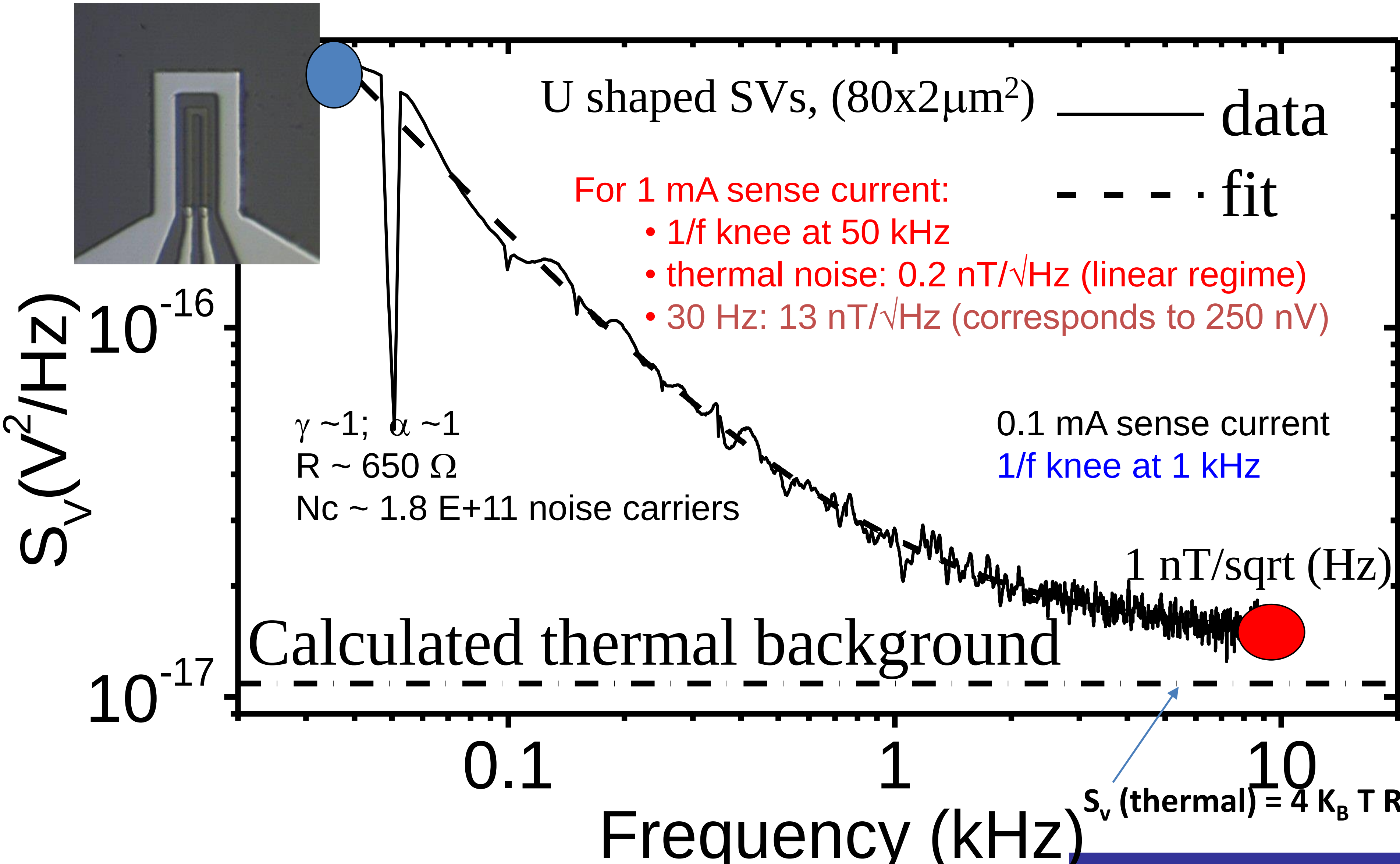

The Magnetic Tunnel Junction-I

incoherent tunneling through an amorphous barrier

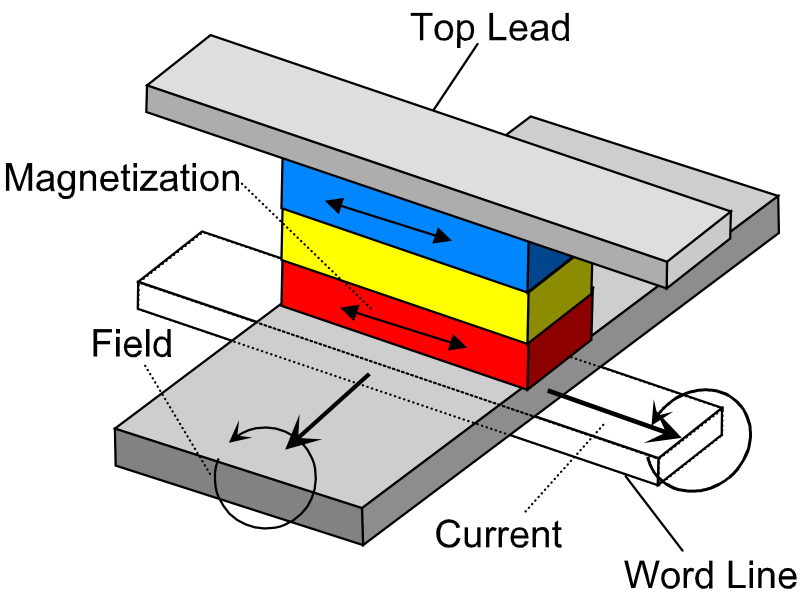

Julliere´s model for incoherent tunneling
Accross amorphous barriers (AlOx, TiOx)

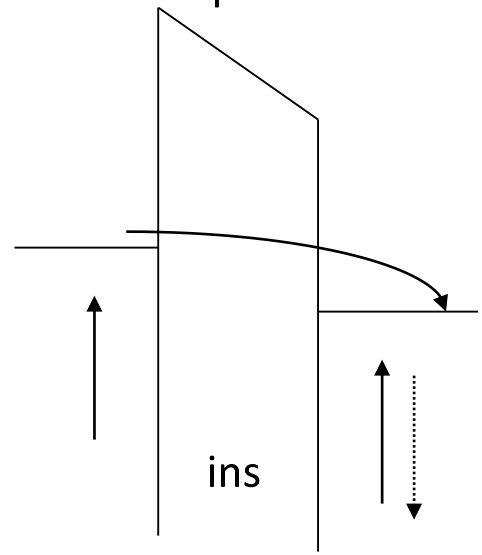

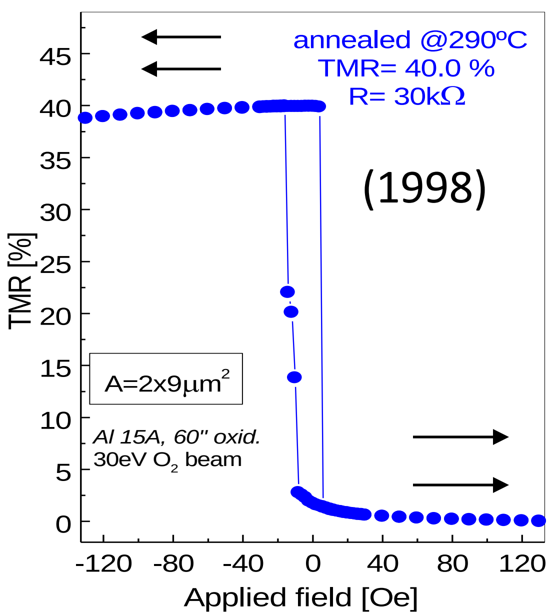

$TMR = 2P_1P_2/1+P_1P_2$

$P = [D_\uparrow(\varepsilon_F) - D_\downarrow(\varepsilon_F)] / [D_\uparrow(\varepsilon_F) + D_\downarrow(\varepsilon_F)]$

Max TMR (RT) 70%

P	%
CoFe	55
half metal	100

Tunnel Junctions deposited by Ion Beam

Nordiko 3000 deposition system

INESC-MN

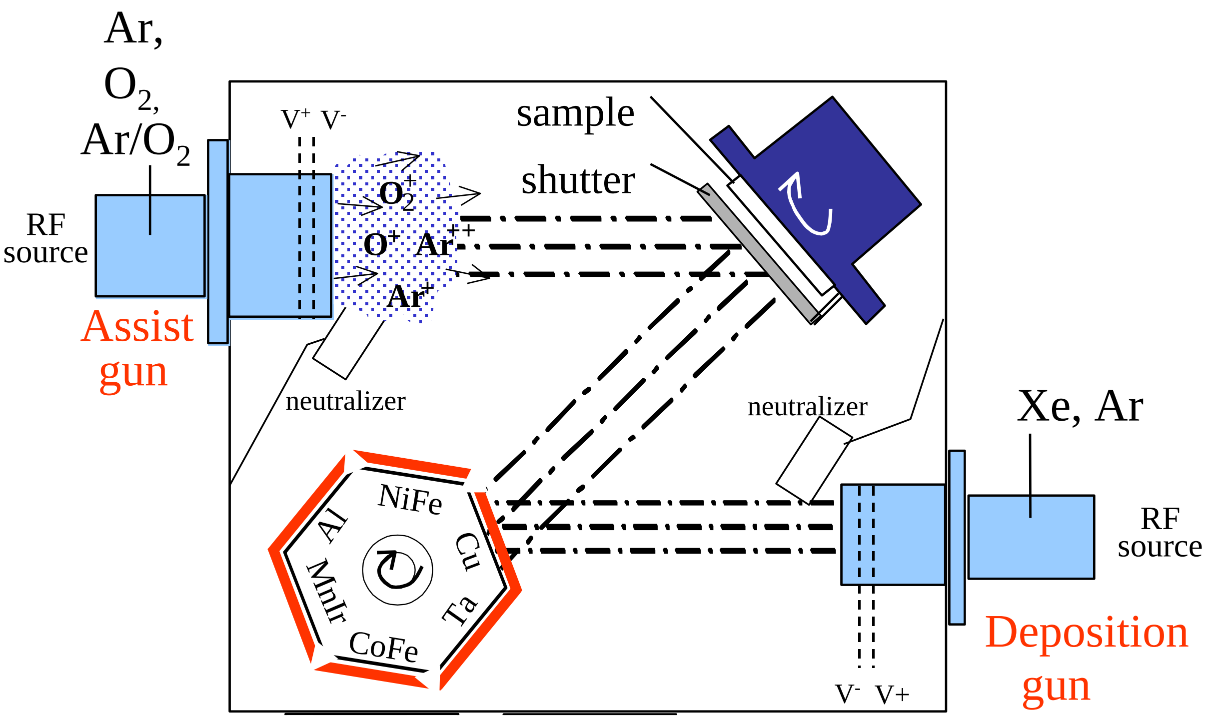

Deposition Conditions

RF plasma
33 mA Xenon beam:
Acceleration = +1450 V
Deceleration = -300V

Dep. pressure: 3.5 x10^{-5}Torr

Table rotation: 15 rpm
Table tilt: 80°

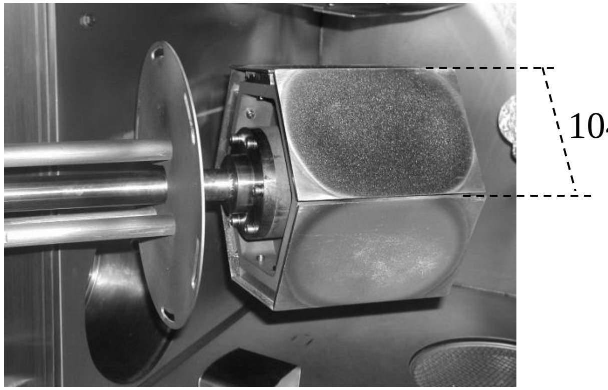

Target assembly (shield removed)

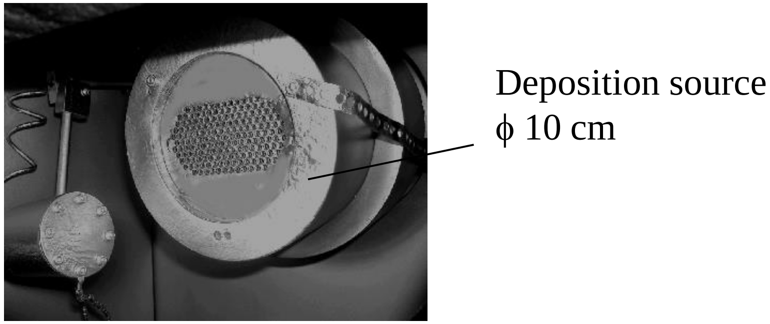

1nm thick barriers for read heads

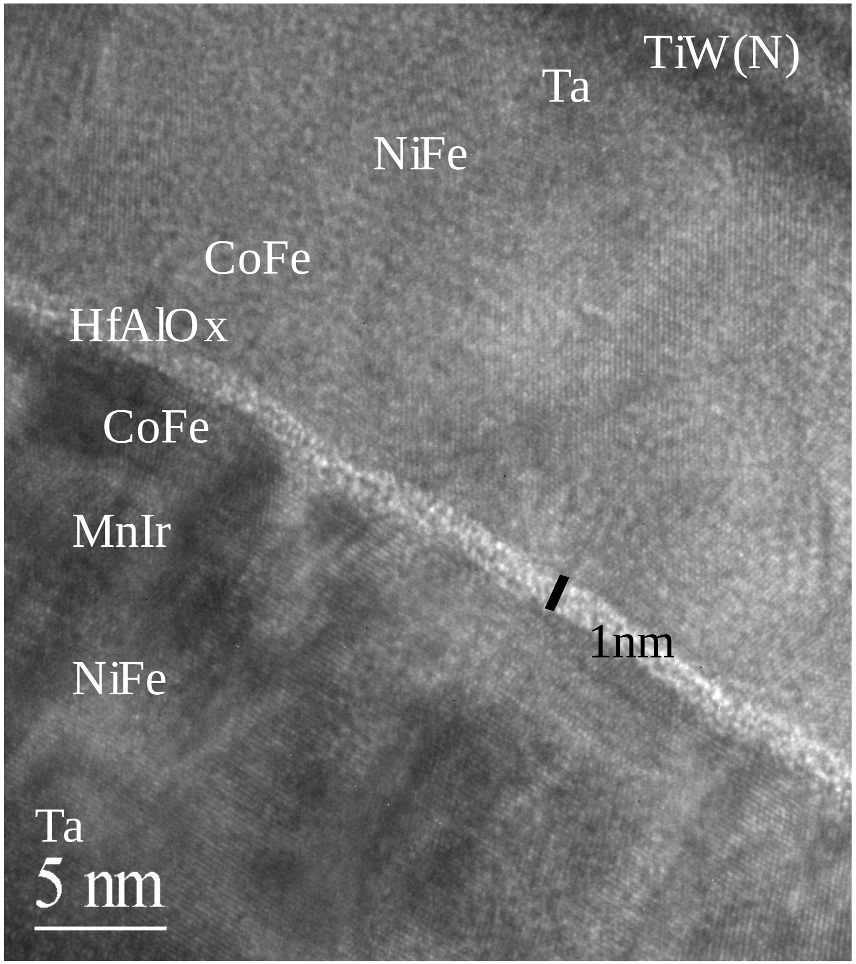

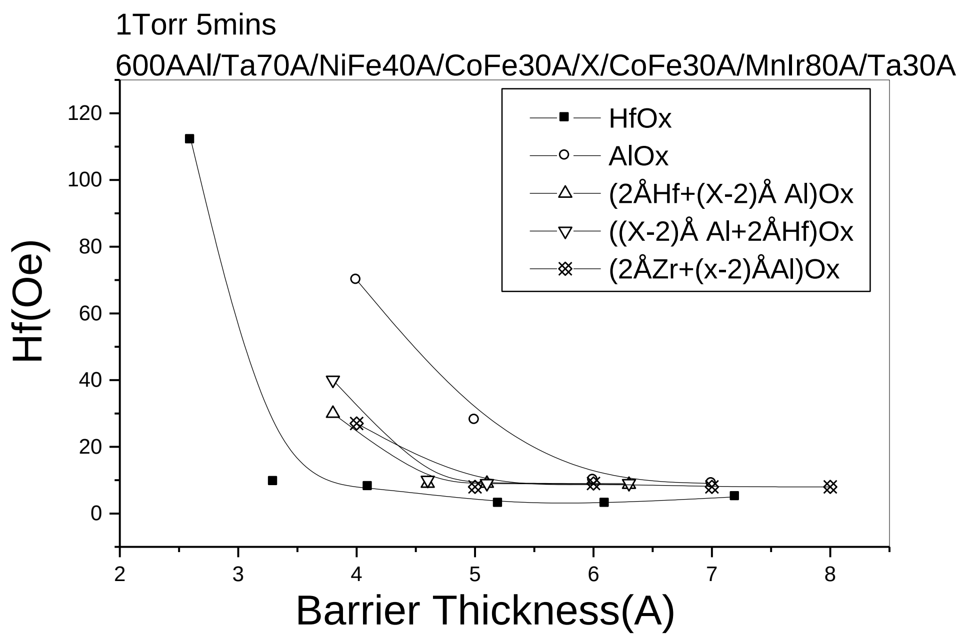

Tunnel Junctions Characterization

Automatic Measurement of Transport Properties

INESC-MN

Automatic Measurement Setup

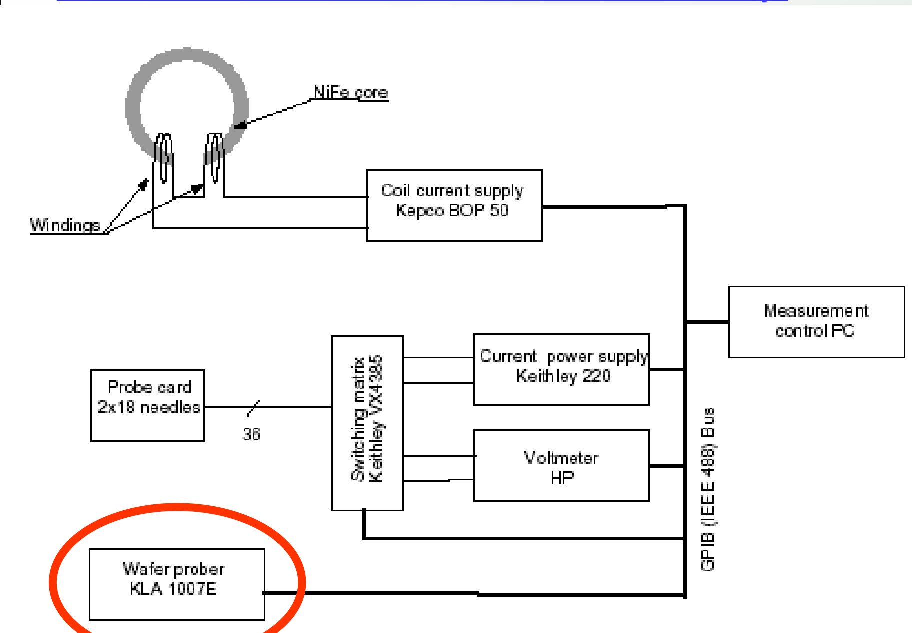

Fully Automatic Measurement of magneto-transport properties :

- Resistance
- Magnetoresistance Transfer Curve
- Current-Voltage Characteristic
- MR Bias Voltage Dependence
- Breakdown Voltage
- Current Induced Switching

Integrated Data Analysis Software

6" Wafers measurement capability (2 or 4 contacts)

KLA 3700

Probe Station

Probe Card

36 Kelvin Needles

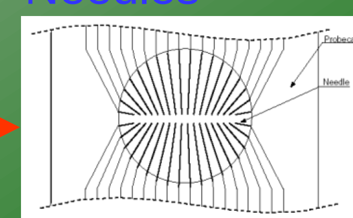

Patterned Junctions Transport Properties
TMR(%)

INESC-MN

Bottom electrode

Ta 90Å/ NiFe 50Å/ MnIr 90Å/ CoFeB 40,50,60Å/ Al 9Å

Oxidation:

20´´ *RF power=110W*remote 0/-0V
4 sccm Ar + 40 O_2

Top electrode

CoFe 30/NiFe 40/Ta 30/TiWN2

60Å CoFeB

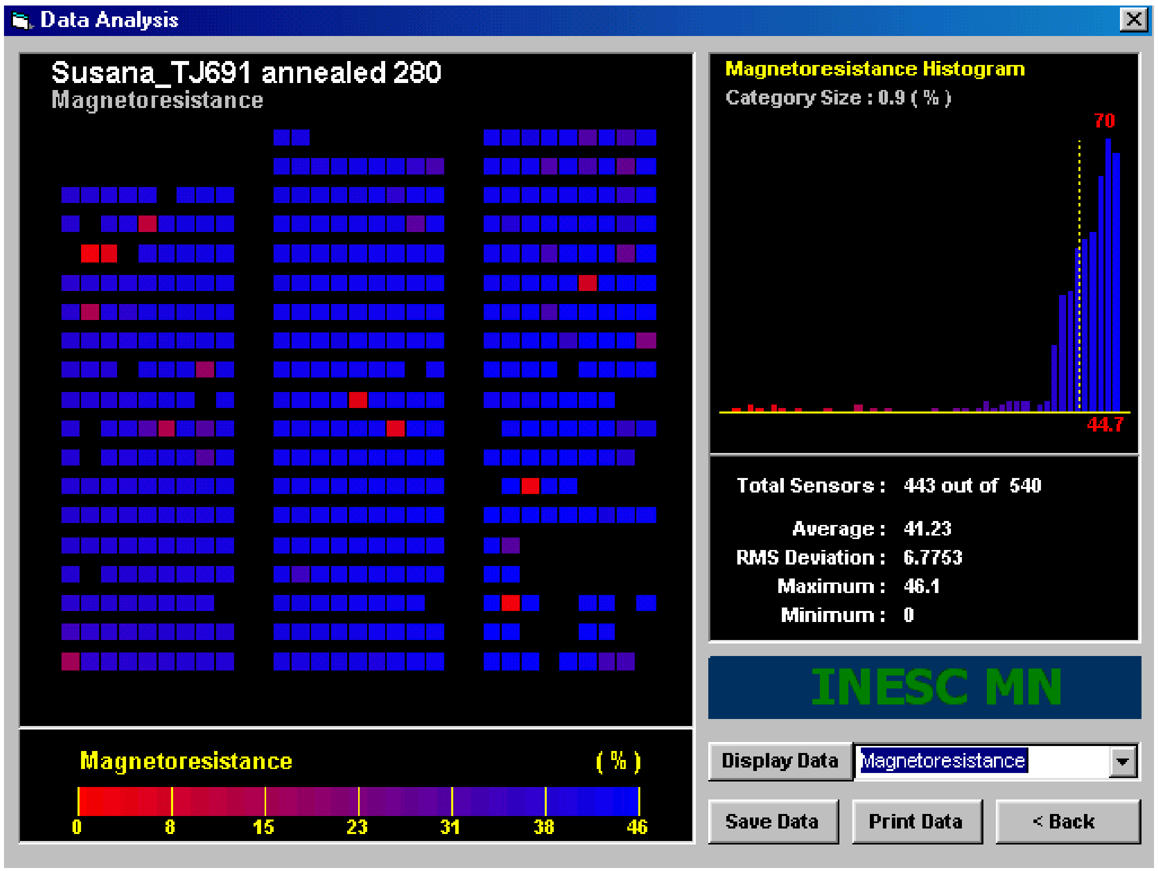

50Å CoFeB

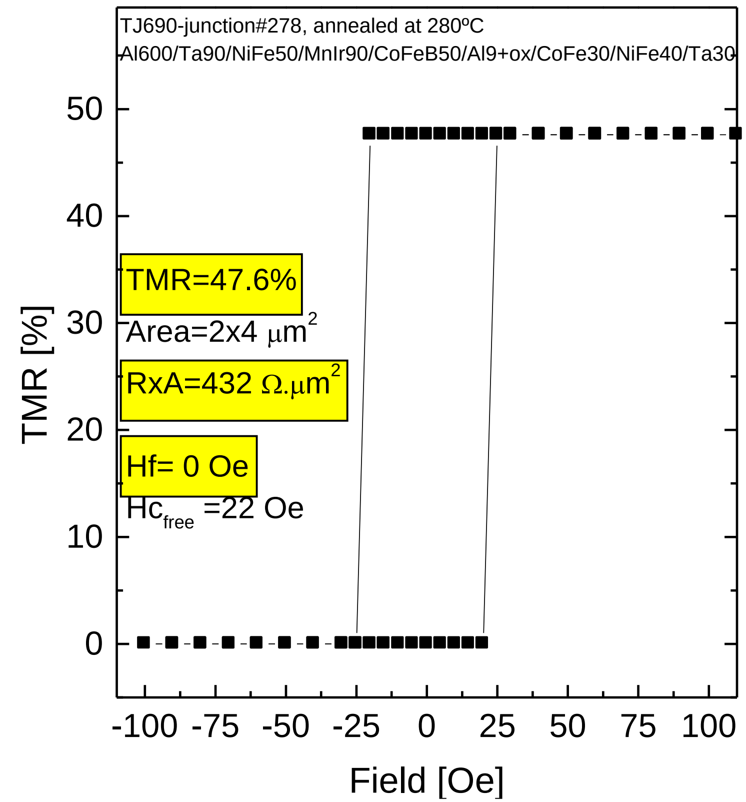

Hf < 2Oe, TMR > 50%, RA < 500 Ohm μm^2,Therm.Stab. 320 to 350C

The Magnetic Tunnel Junction-II

Coherent tunneling through a crystalline MgO barrier

2) Magn Anneal

1) Stack dep
(10 target PVD)

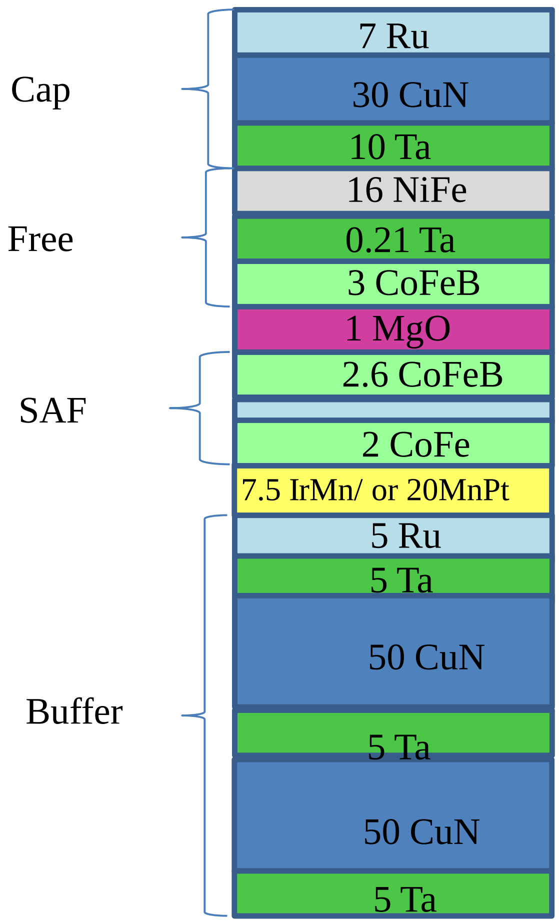

0.85 Ru

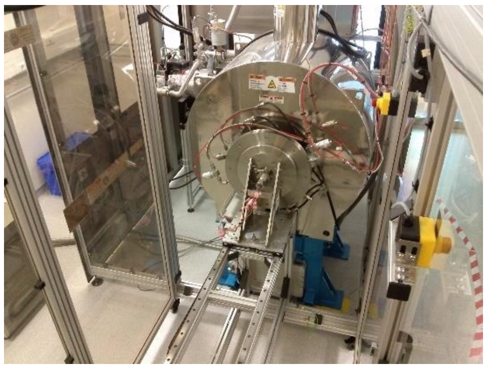

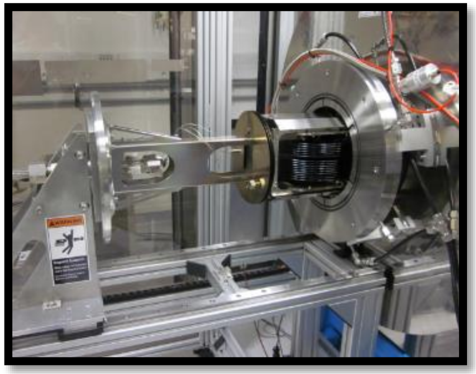

1h, 330ºC, 1T

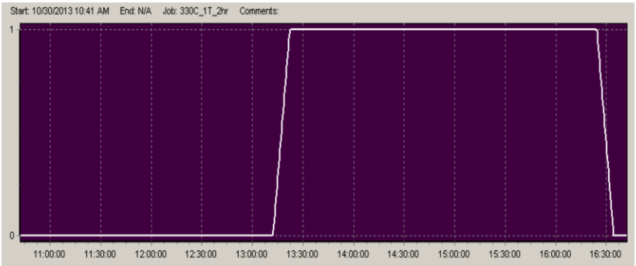

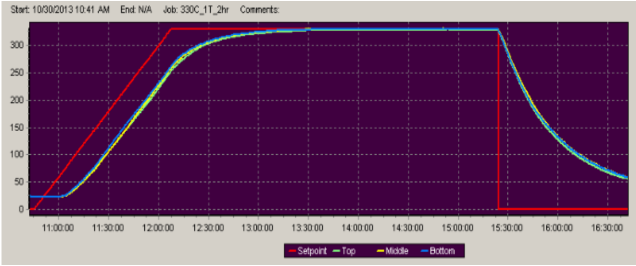

The TMR device: process

4) stack magn. characterization

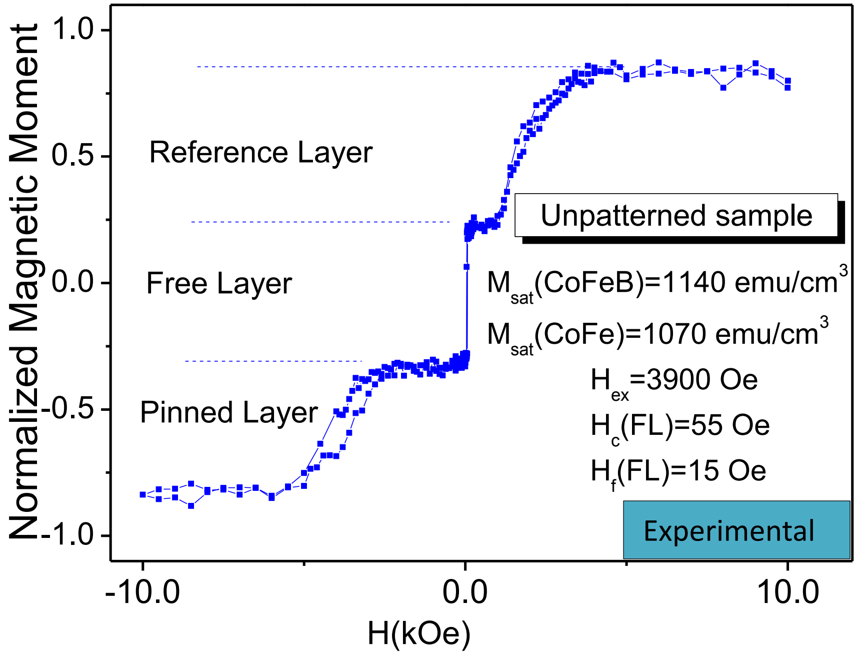

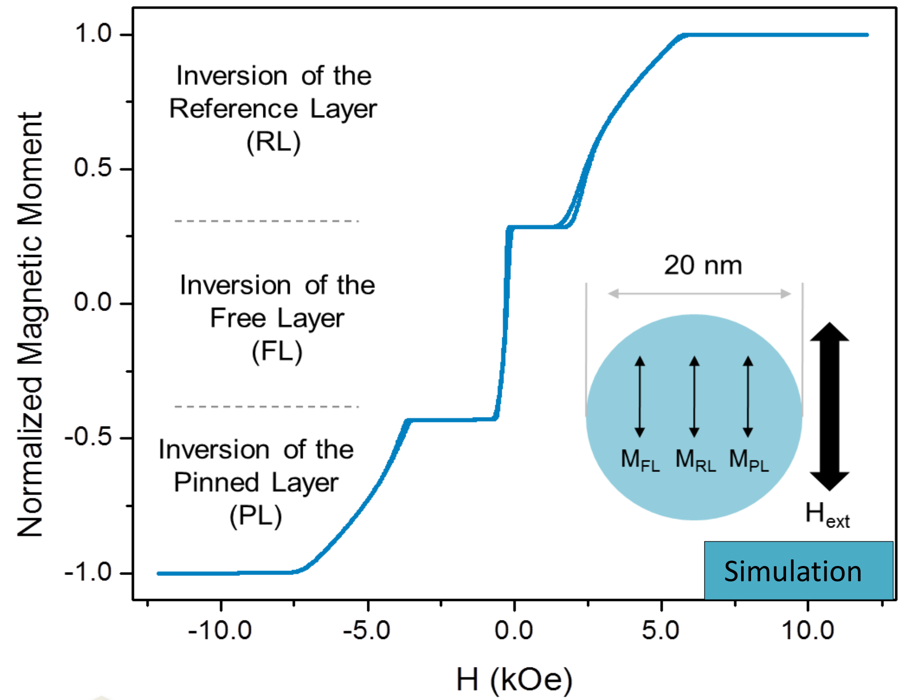

Micromagnetic Simulations:

Performed using time independent solutions of the LLG equation.

Interfacial/interlayer Surface Coupling constants	(erg/cm²)
Exchange coupling between PL and AFM	0.34
Antiferromagnetic coupling for the SAF (PL/spacer/RL)	-0.53
Ferromagnetic coupling between SAF and FL	0.02

Magnetic Parameters:

Layer	M_s (emu/cm³)	t (nm)	l_{ex} (nm)	H_k (Oe)
FL	1140	2.5	3.5	15
Barrier	-	1	-	-
RL	1140	2.5	3.5	15
Spacer	-	0.85	-	
PL	1070	2.3	3	15
AMF	-	15	-	-

Linear response optimization: 2nd annealing temperature
VSM plots obtained in a matrix of annealing temperature vs NiFe thickness

INTERNATIONAL IBERIAN NANOTECHNOLOGY LABORATORY

5 Ta / 15 Ru / 5 Ta / 15 Ru / 5 Ta / 5 Ru / 17 PtMn / 2.0 $CoFe_{30}$ / 0.85 Ru / 2.6 $CoFe_{40}B_{20}$ / MgO 4x123 3kW 600sccm / 3.0 $CoFe_{40}B_{20}$ / 0.21 Ta / 8 NiFe / t_{MnIr} / 2 Ru / 5 Ta / 10 Ru

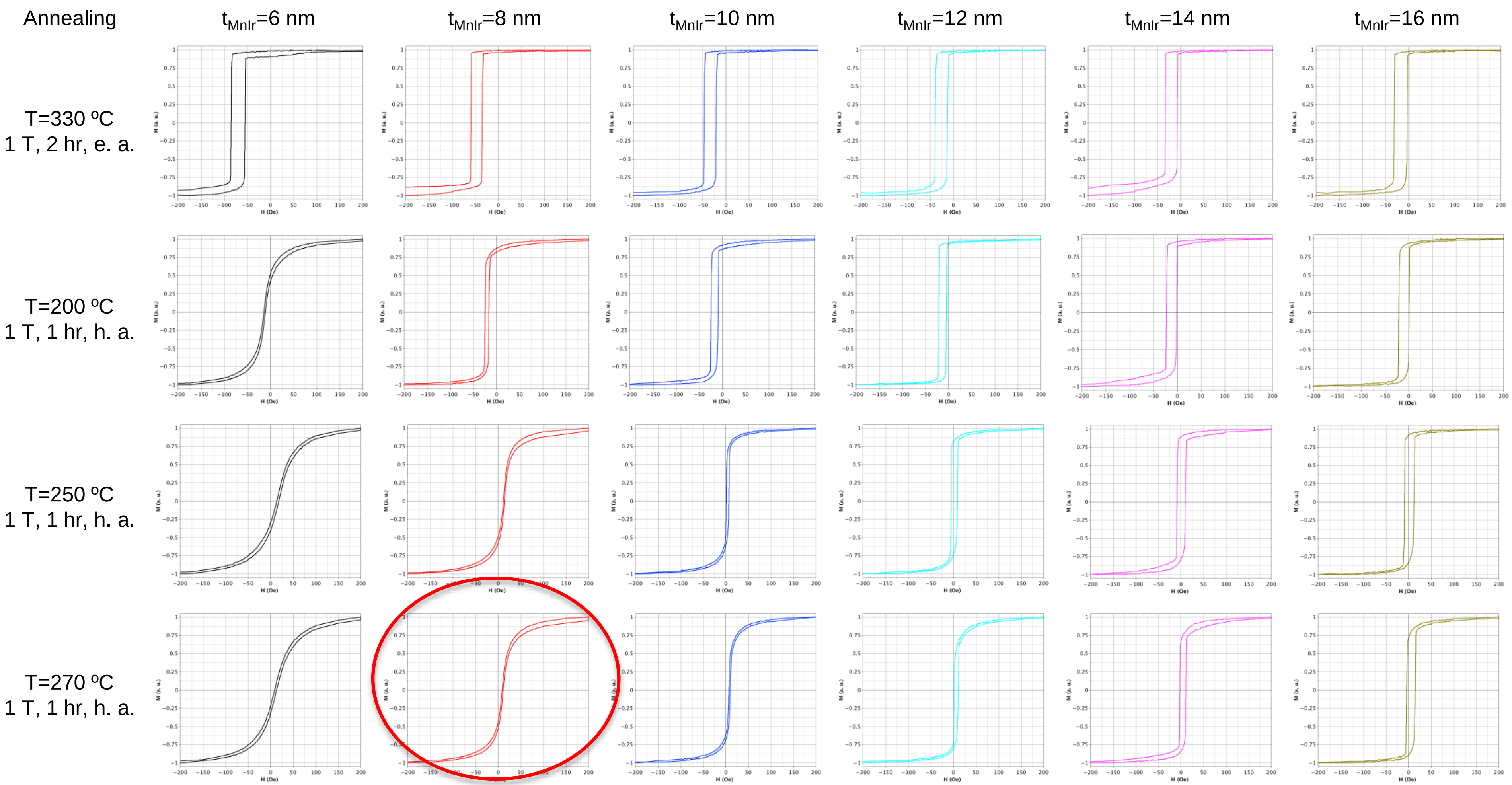

The annealing temperature used to produce the linear response must be optimized for each stack : notice that Hf, Hc and Hk change with the temperaure even after obtaining linear response.

The basic TMR device: process

5) CIPT transfer curve characterization

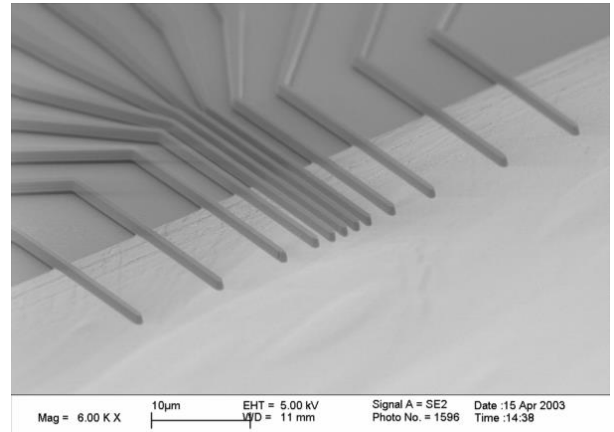

CIPT Transfer Curve for a specific probe spacing

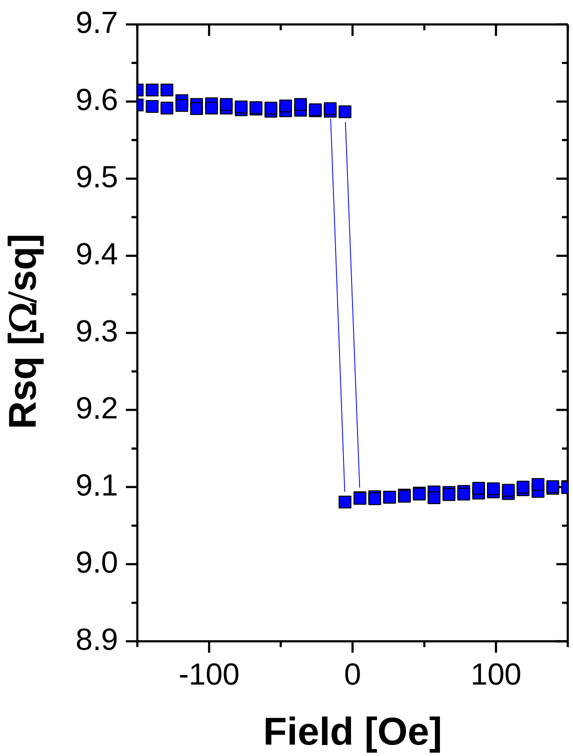

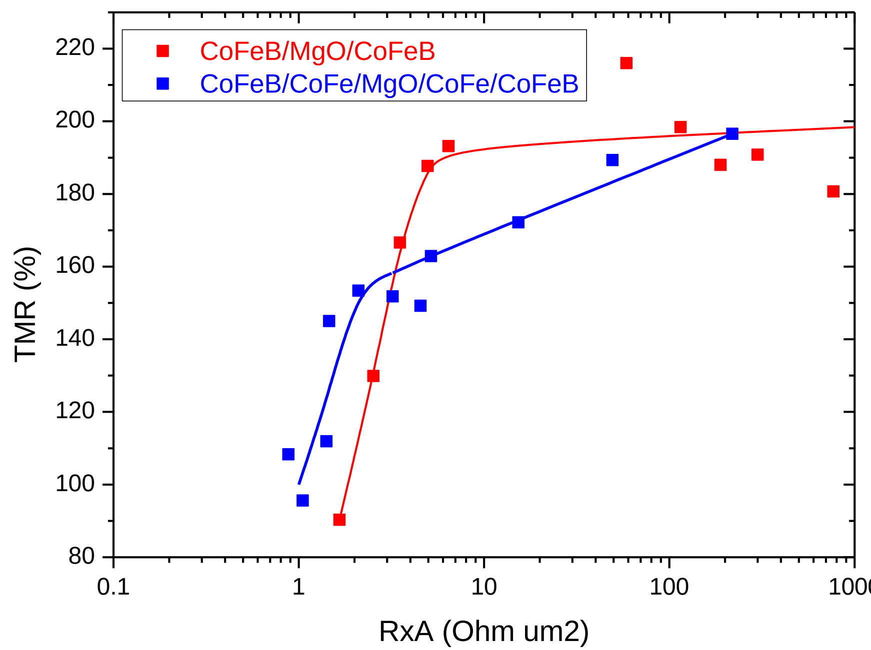

The TMR device: process

6) MPW , Wafer map, die layout

NDT testing

6 TMR
10x4 μm^2

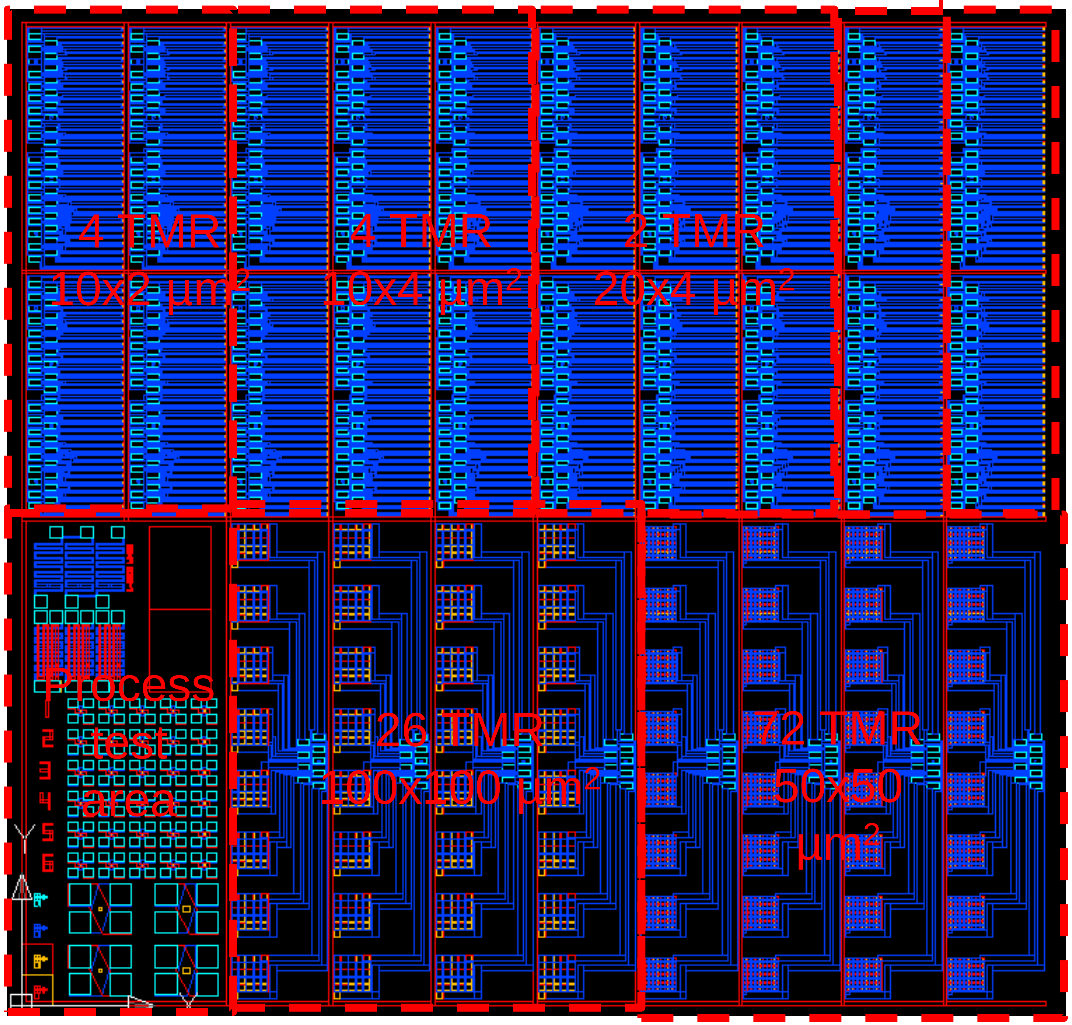

4 TMR
10x10
μm^2

Surface
defects

Buried
defects

The TMR device-process

7) MTJ ion milling , w/wo SIMS end point detection

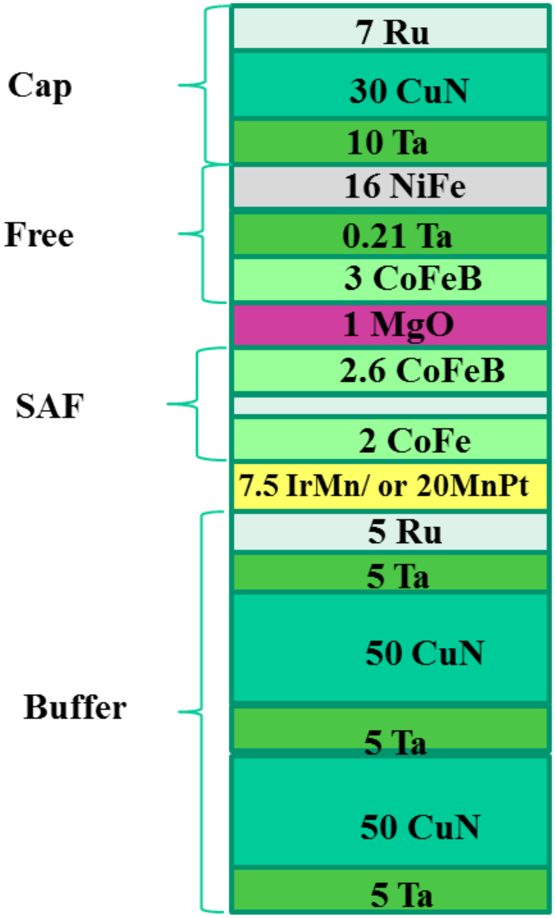

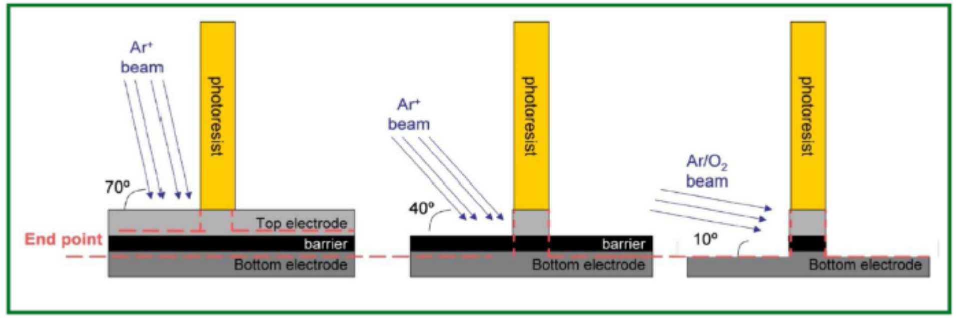

Early Etching Stage : Large incident angle reduces shadow effects, but results in heavy redeposition

At the level of the barrier: Shallow incident angle increases the etching in the sidewalls of the pillar, reducing the amount of redeposited material

Final oxidation step: Any material deposited in the sidewalls of the junction is oxidized, becoming an insulator.

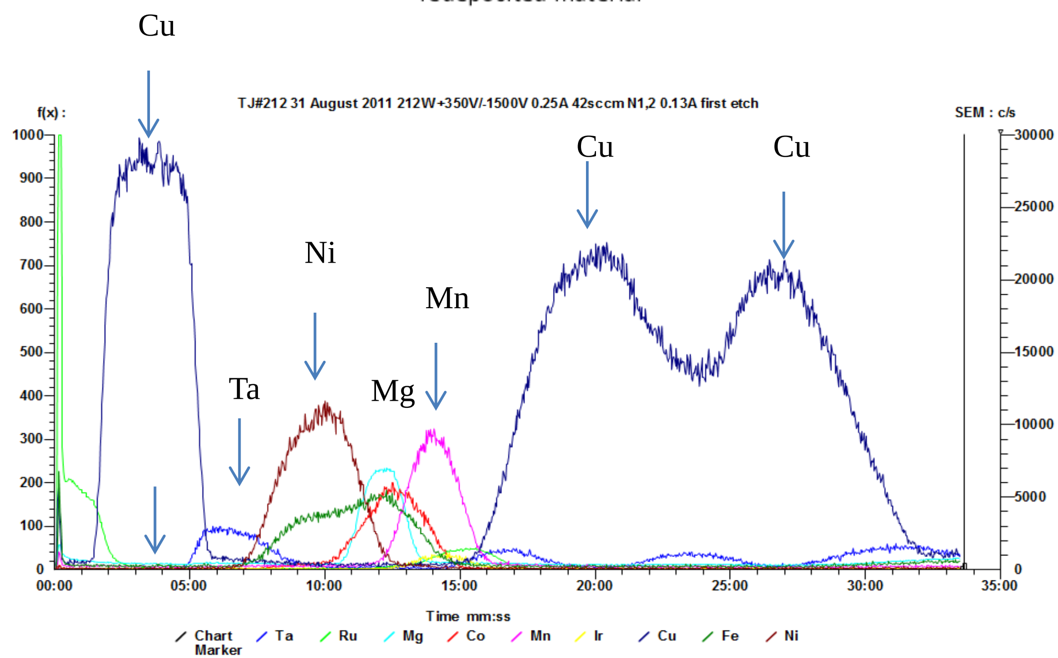

Multiproject Wafer Service (200mm and 150mm, INL and INESC MN)

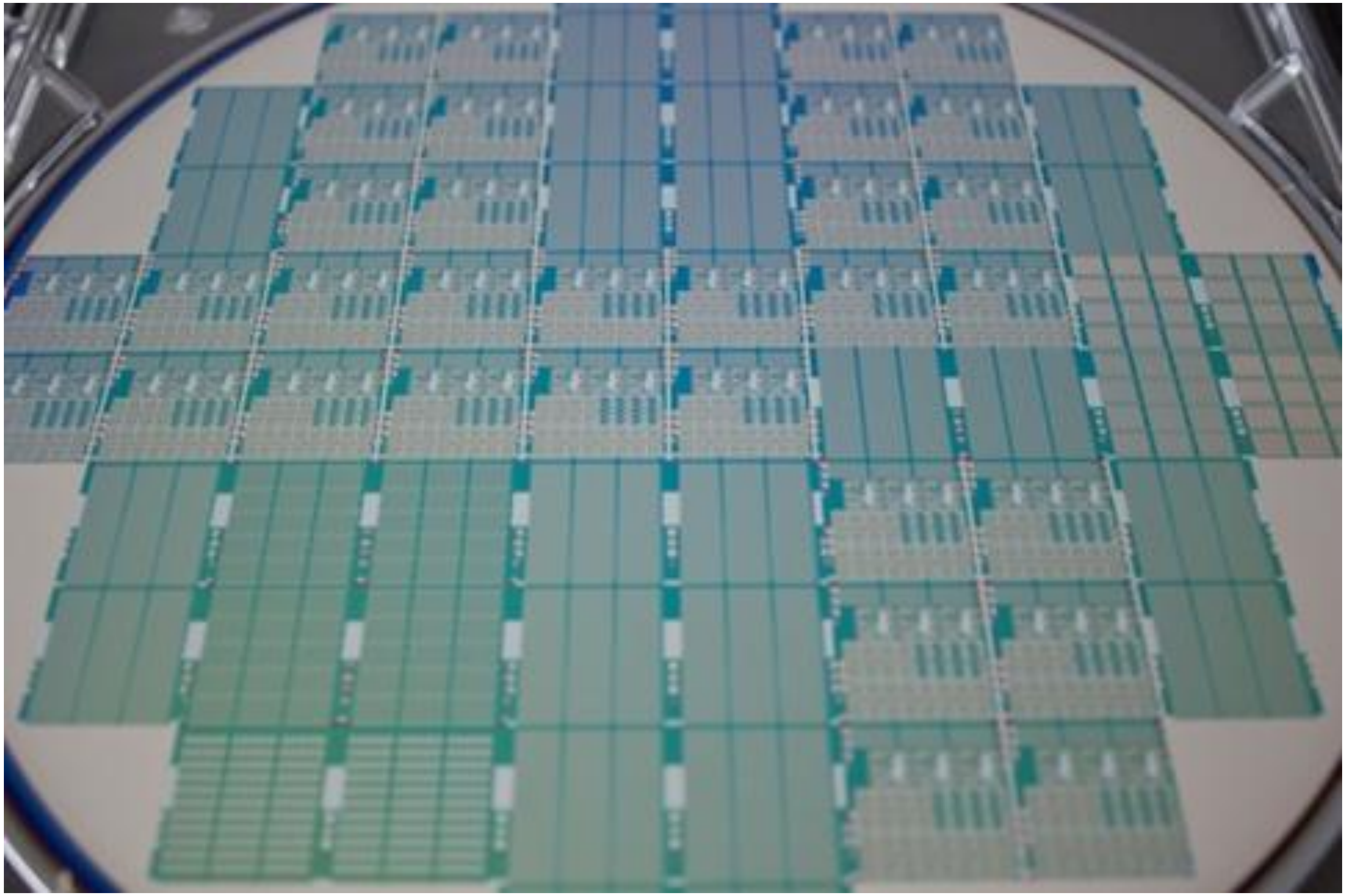

MTJ stacks deposited on Si/SiO_2 blank wafers and patterned with minimum feature sizes of 1µmm

Process extension to 100 nm features available

TMR sensor: output, noise, detectivity

noise power $S^2_v(f) = 2\,e\,I\,R^2 \coth\left(\frac{eV}{2K_BT}\right) + \alpha\frac{V^2}{A}\frac{1}{f}$ (V²/Hz)

sensor output $\Delta V = \left(\frac{\Delta R}{R}\right)\left(1 - \left(\frac{V_b}{V_0}\right)^n\right) V_b \langle H\rangle/(2\,H_k^{eff})$ (V)

Defining $\gamma = \Delta V/\langle H\rangle$ (V/T)

Then minimum field detectable is

$D^2 = S^2/\gamma^2 = (1/\gamma^2)\,[(2eR/V)\,\coth(eV/2K_BT) + \alpha\frac{1}{A\,f}]$ (T²/ Hz)

For a series of N sensors

$D^2 = S^2/\gamma^2 = (1/\gamma^2)\,[(2eR/V_{tot})\,\coth(eV/2NK_BT) + \alpha\frac{1}{A\,N\,f}]$

(T²/ Hz)

For $V_{tot}/N \ll K_B T$, $D^2 = S^2/\gamma^2 = (1/\gamma^2)\,(4NRK_BT/V_{tot}^{\;2} + \alpha\frac{1}{A\,N\,f}]$

Full Wheatstone Bridge
Magnetic sensor requirements

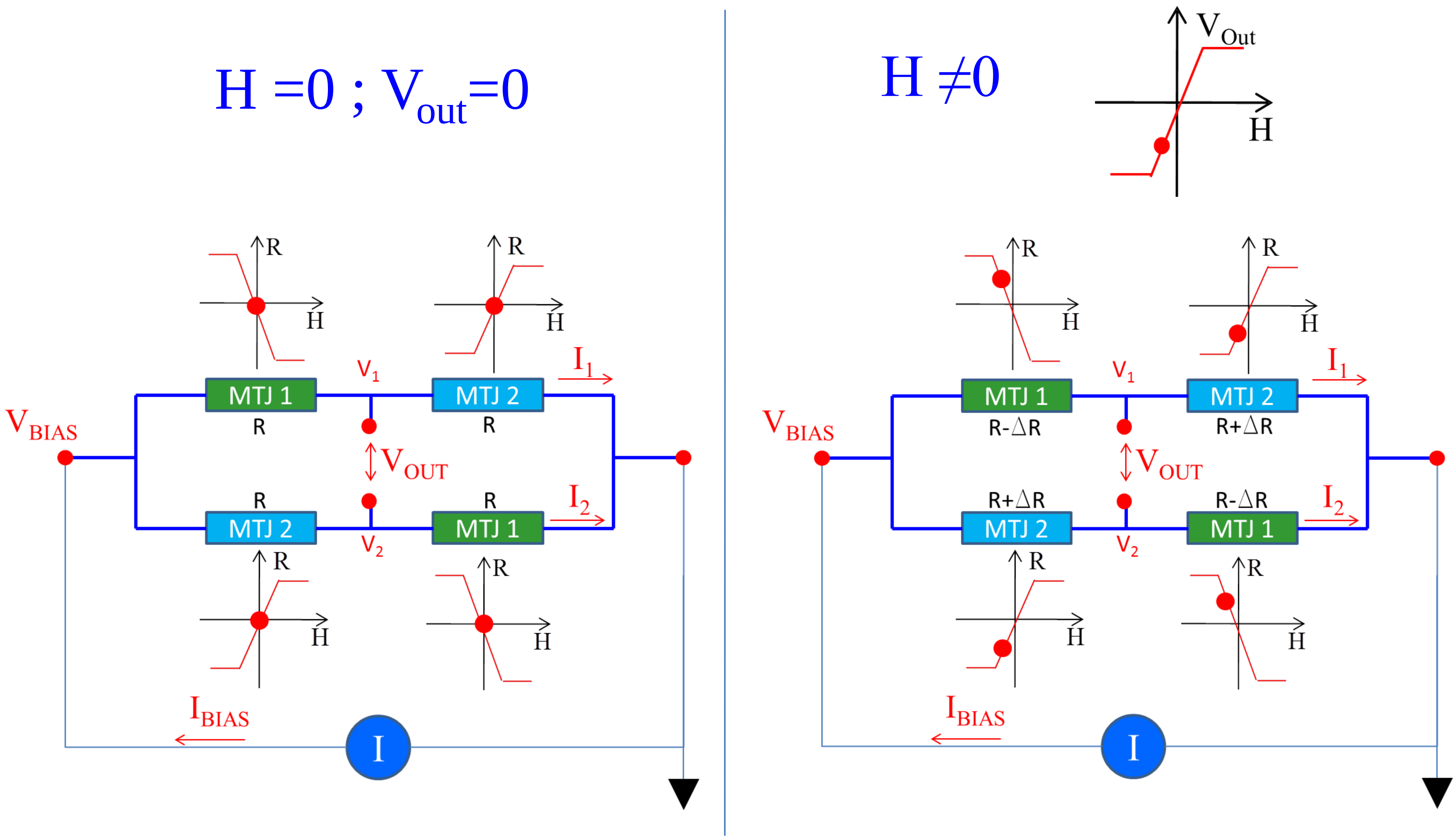

Bridge output is immune to thermal drifts

Final Device Geometry
Full Whetstone Bridge Incorporating MTJs connected in Series

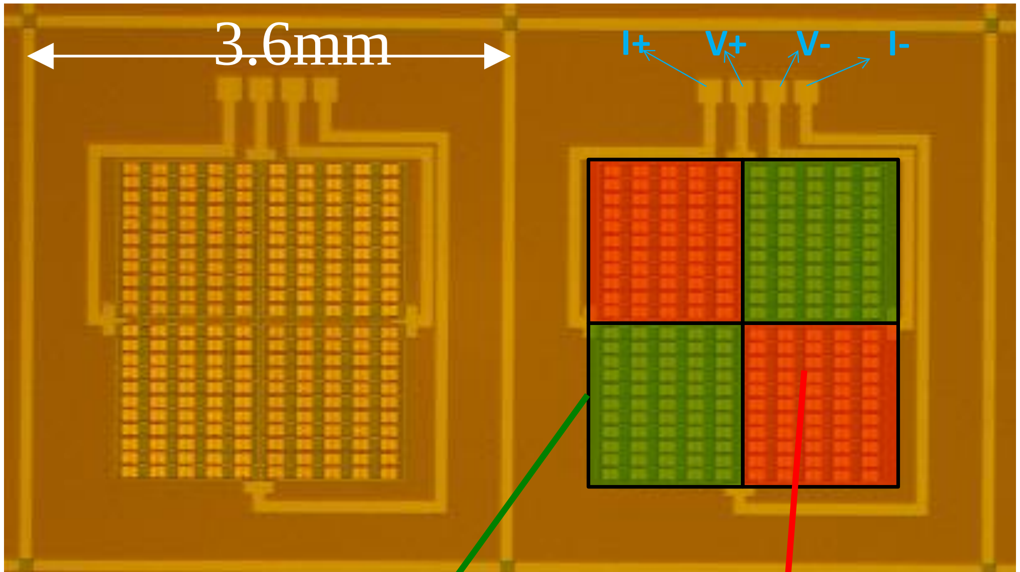

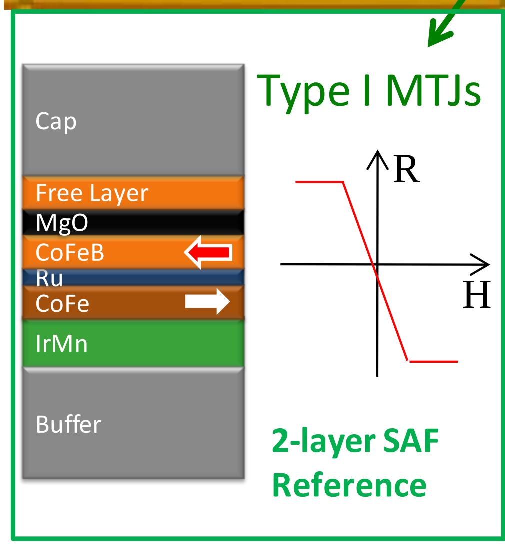

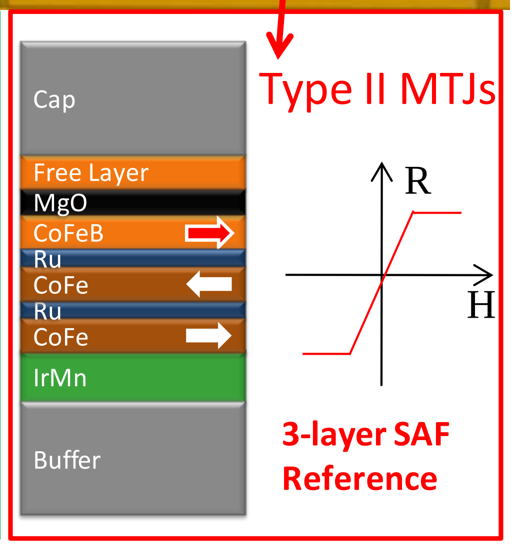

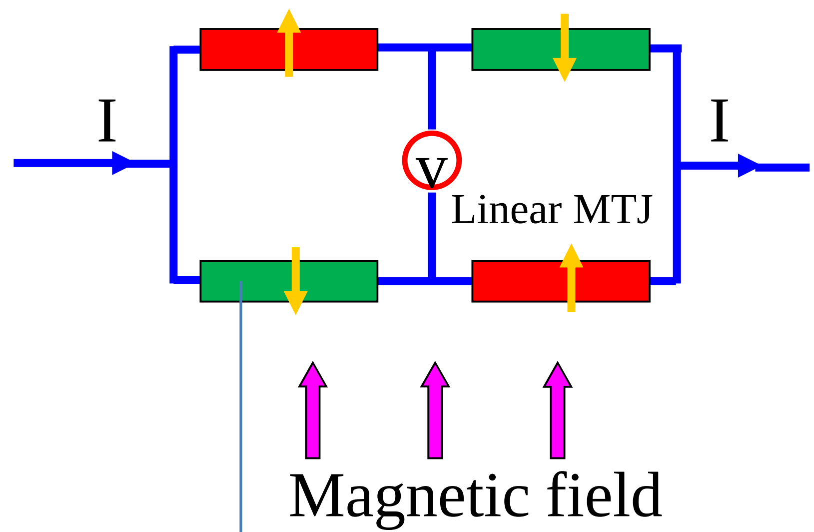

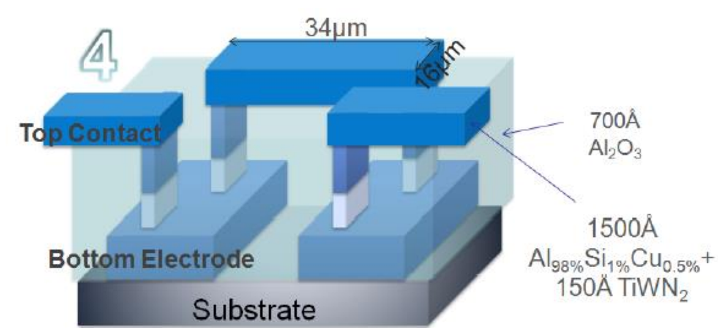

Individual MTJ Area: 5x70 μm^2
MTJ Elements in series: 110 per arm

Current in plane Transfer Curves
MTJ Stack I vs. MTJ Stack II after annealing

STEP #7 : Magnetic Annealing

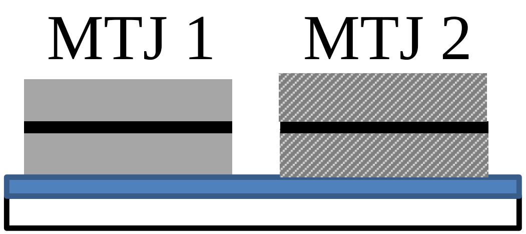

$T_{annealing}$ = 330C
Dwell Time : 2h
Cool down field : 1T

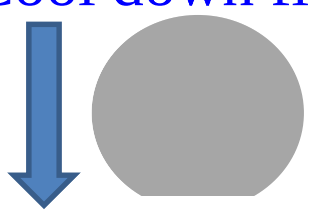

TMR after Annealing ~175%

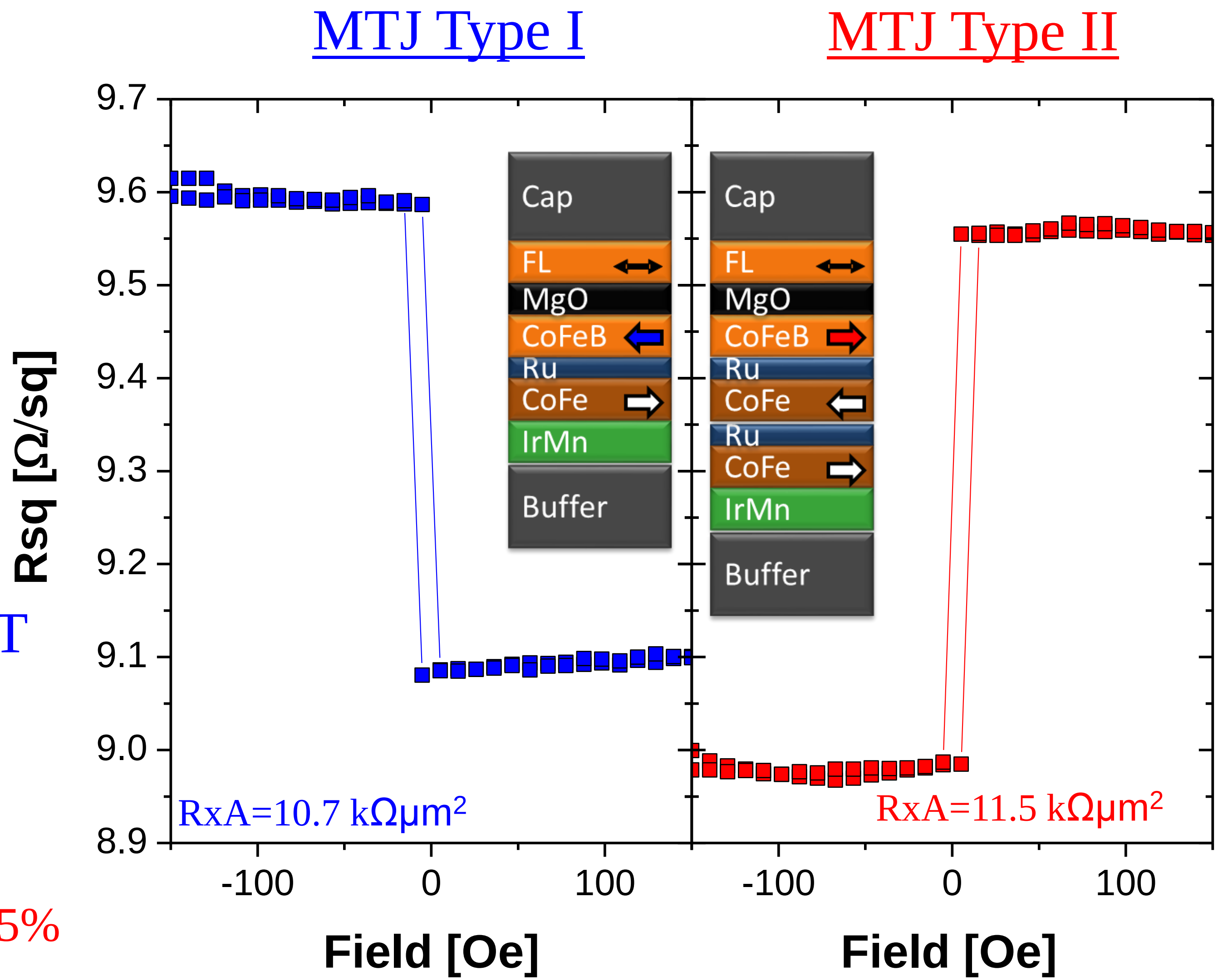

2D Magnetometers
Output from two orthogonal bridges

ENIAC-JTI

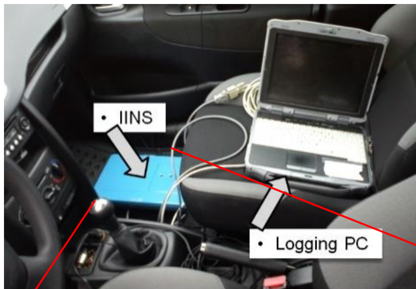

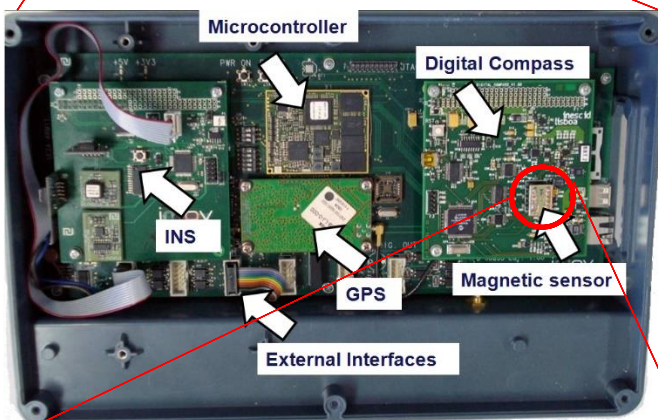

XX Component Sensor

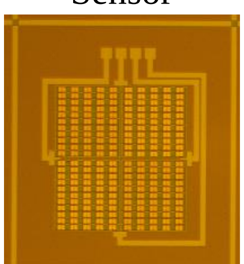

YY Component Sensor

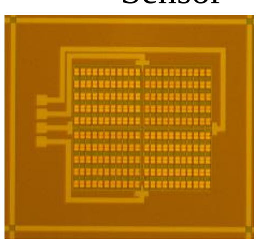

Sensor output during a 360° rotation

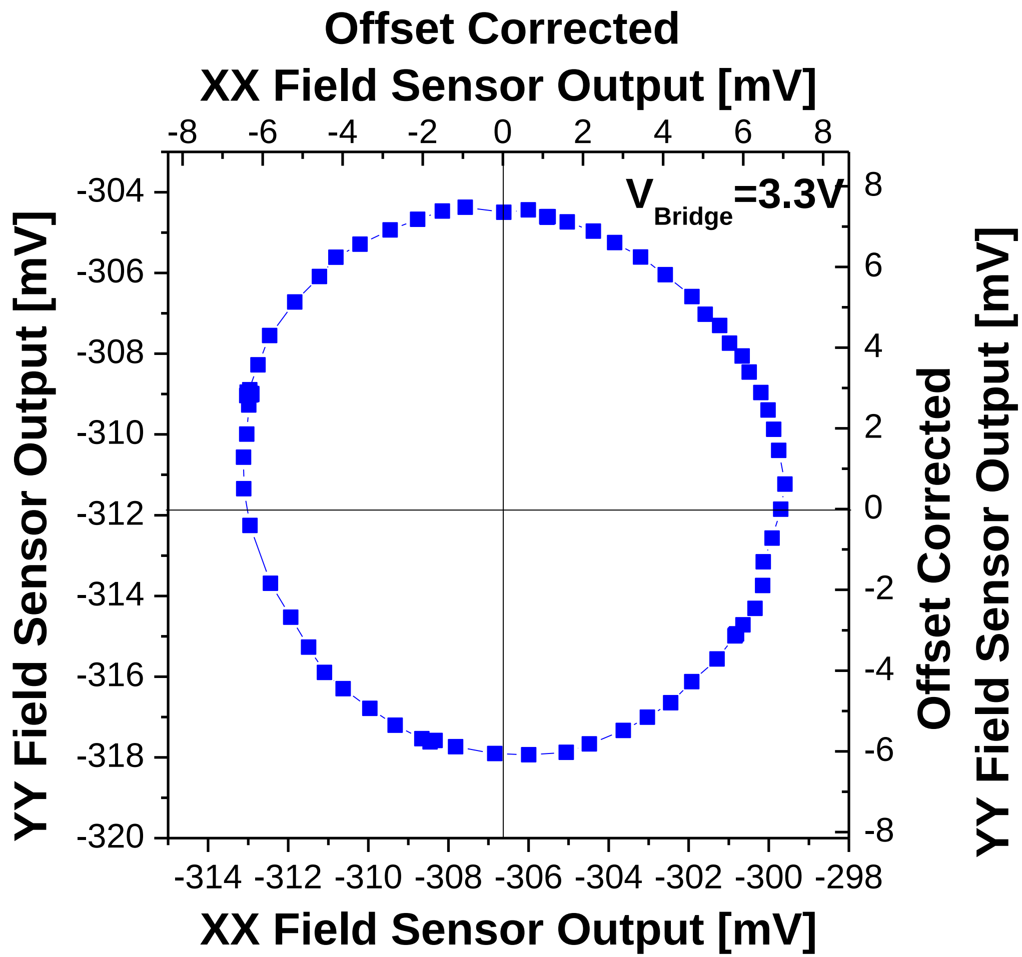

13.3 mV/V/Oe sensitivity → 0.31 Oe field

NDT Testing with TMR sensors

In collaboration with INESC ID

FP7-IMAGIC

Aluminum Mock-up with a width of 100 µm and a depth ranging of 0.2, 0.5 and 1 mm

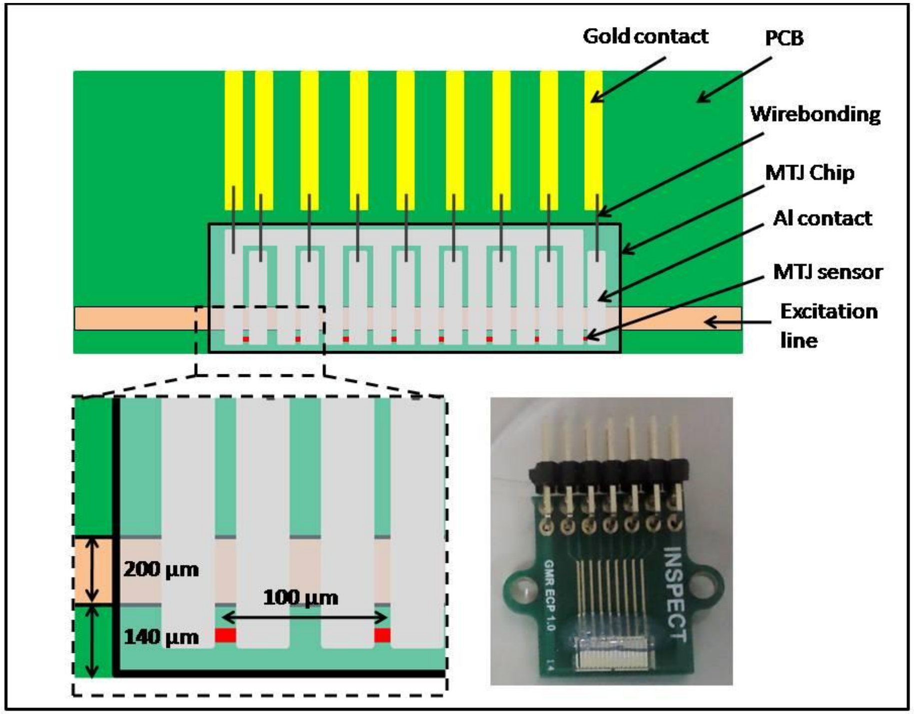

MINIMIZING INTERCONNECT RESISTANCE IN LARGE MTJ SERIES, stack 4

TJ933 – Si / Al_2O_3 (100nm) / [5 Ta / 25 CuN]x6 / 5 Ta / 5 Ru / 20 IrMn / 2 $CoFe_{30}$ / 0.85 Ru / 2.6 $CoFe_{40}B_{20}$ / MgO 2x41 / 2 $CoFe_{40}B_{20}$ / 0.21 Ta / 4 NiFe / 0.20 Ru / 6 IrMn / 2 Ru / 5 Ta / 10 Ru

200mm wafer processed at INL

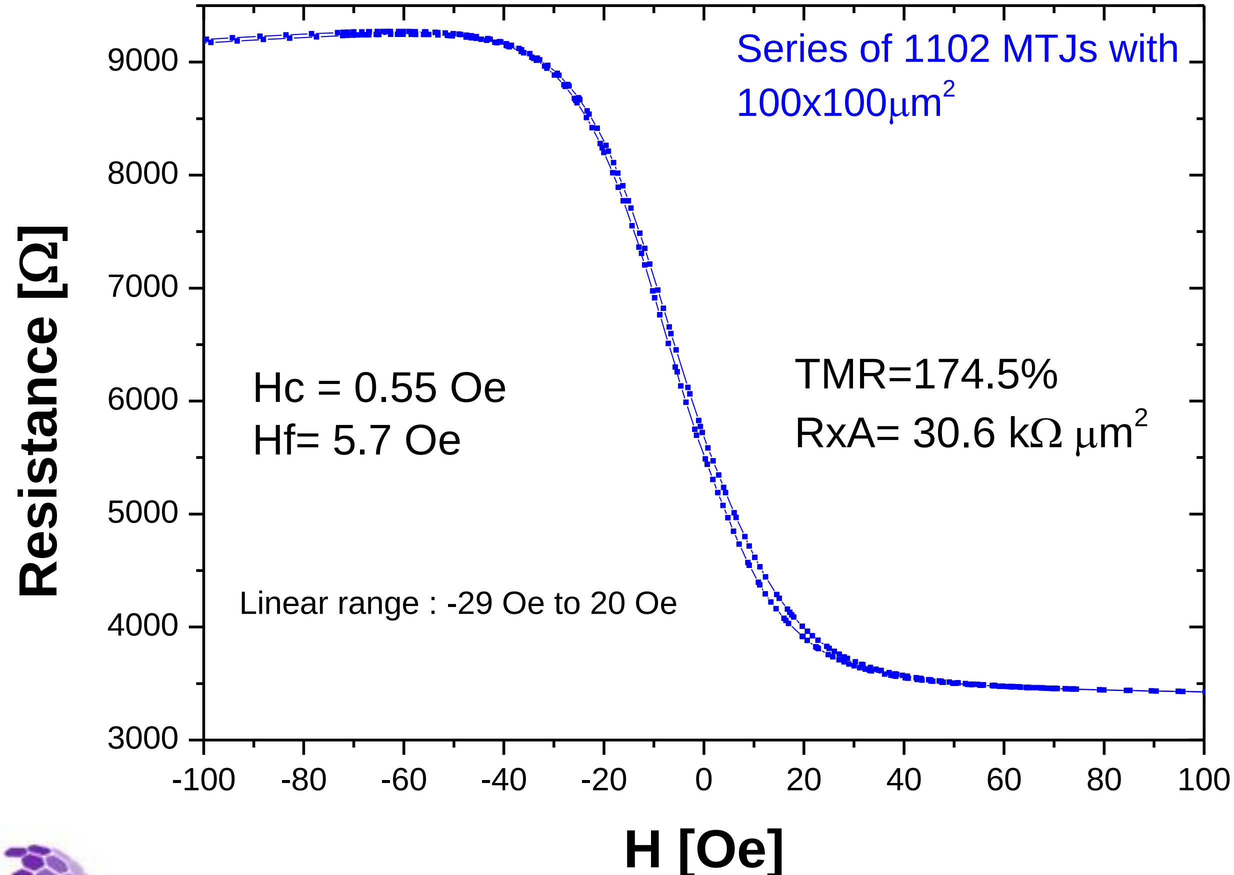

(Ta/Cu) x n Buffer minimizes Interconnect resistance contribution

INTERNATIONAL IBERIAN NANOTECHNOLOGY LABORATORY

Previous results – Buried defects

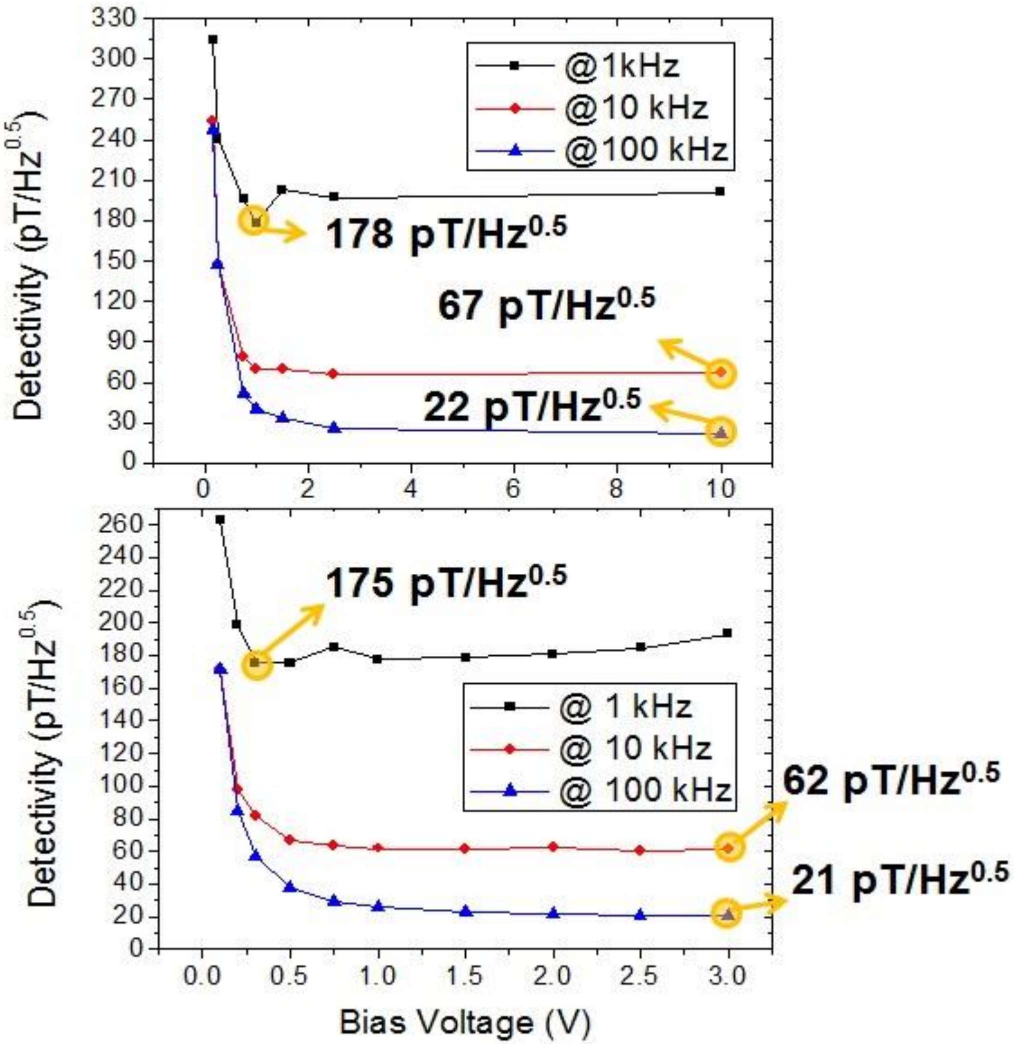

72 MTJ in series 50x50 µm²

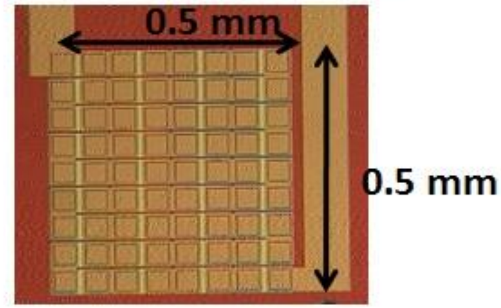

R_{sensor} = 990 Ω

26 MTJ in series 100x100 µm²

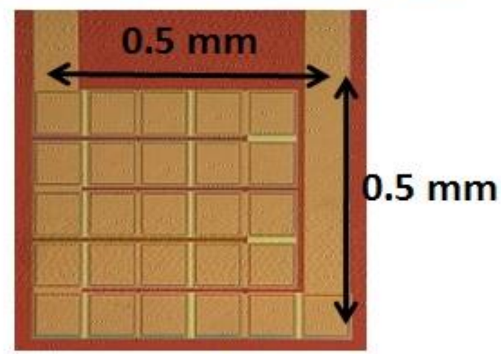

R_{sensor} = 130 Ω

Internal TMR probe tests at INESC MN

f_{meas} =1 kHz

f_{bias}=999kHz

I_s = 100 µA $_{0\text{-}p}$

$f_{excitation}$ = 1000 kHz

I_{exc} = 1 A $_{0\text{-}p}$

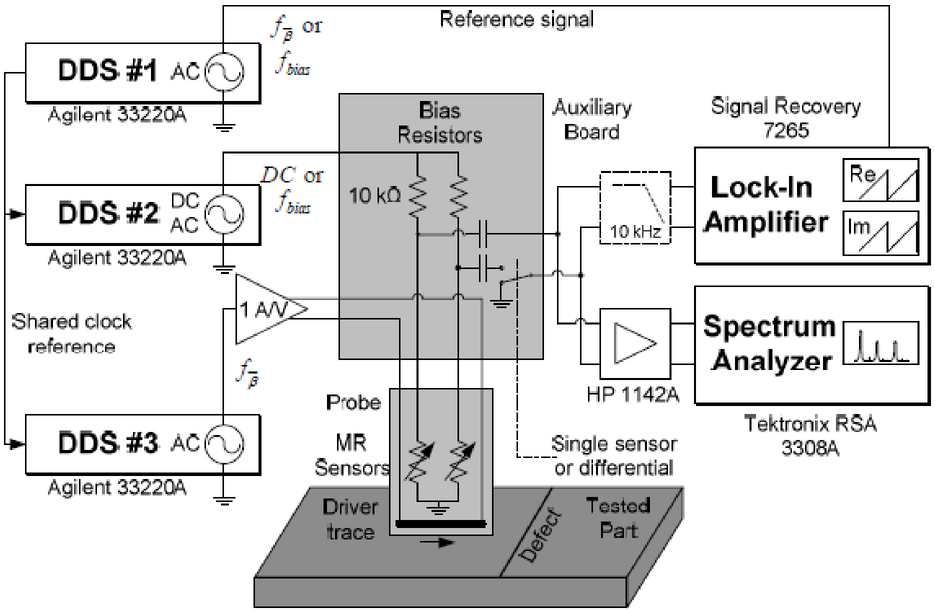

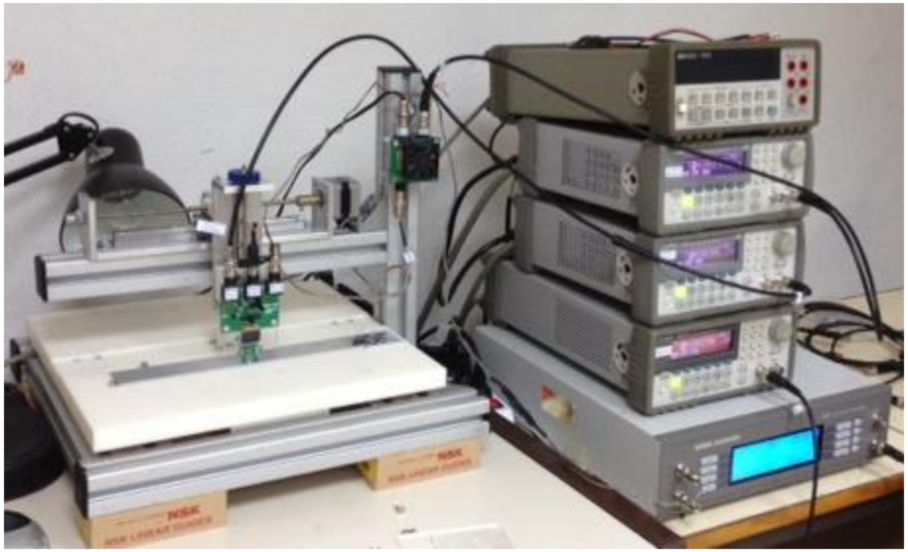

Friction Stir Welding detection

Top view
(scanning side)

Bottom view
(Welding side)

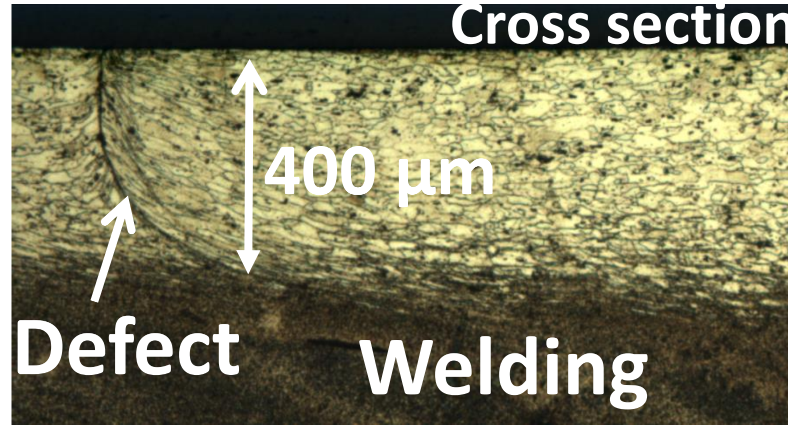

TMR - Single ended

Signal (µV)

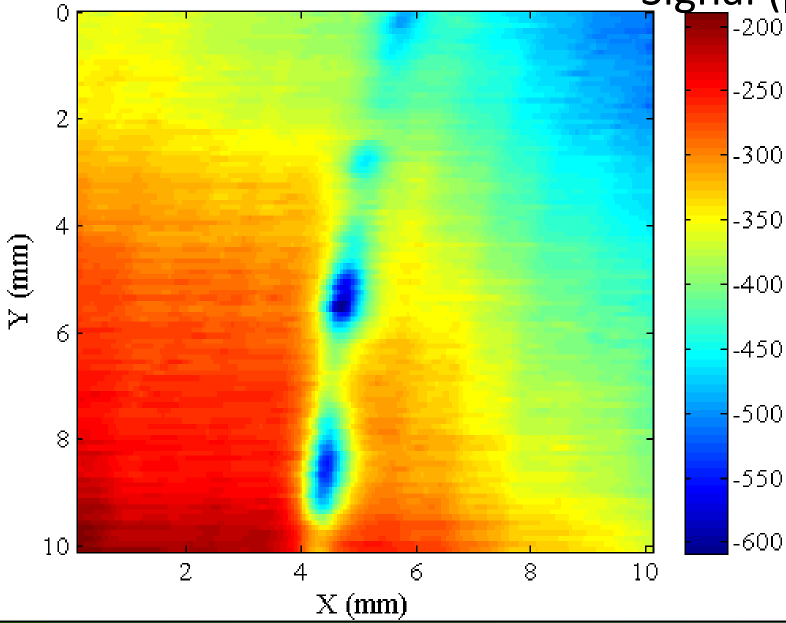

TMR - differential

Signal (µV)

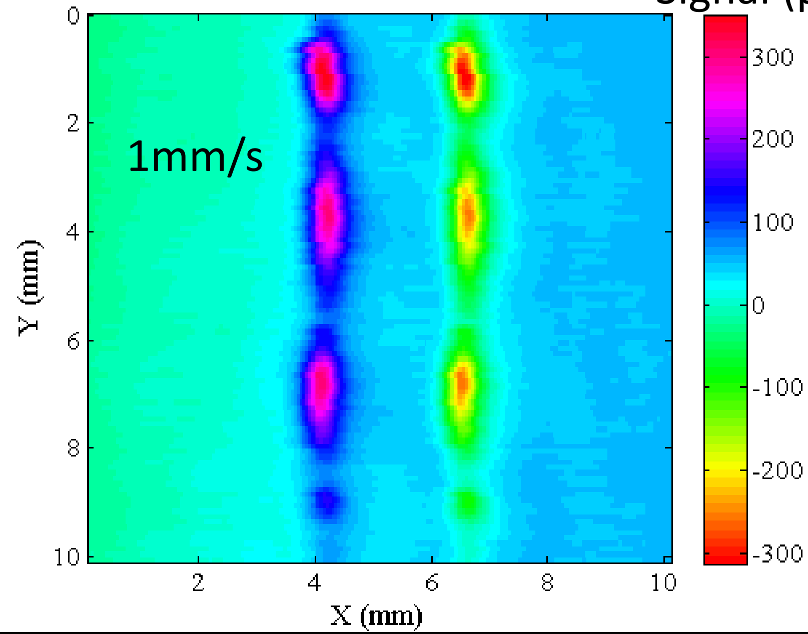

Scanning probes

current imaging in Ics

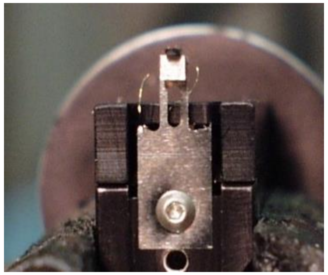

INESC MN-NEOCERA

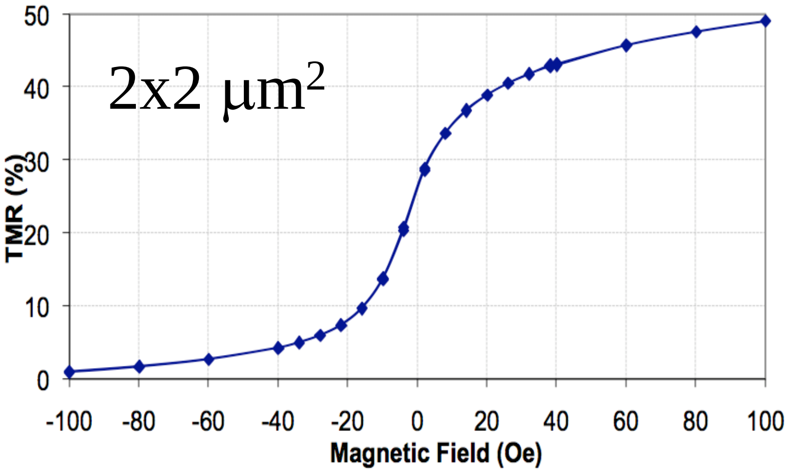

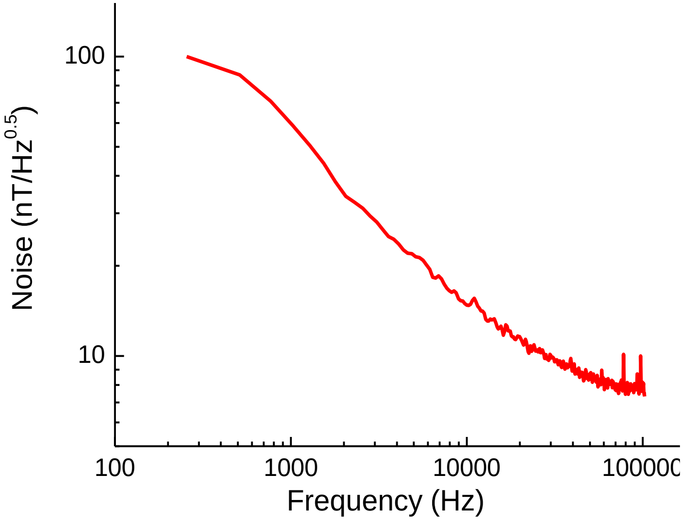

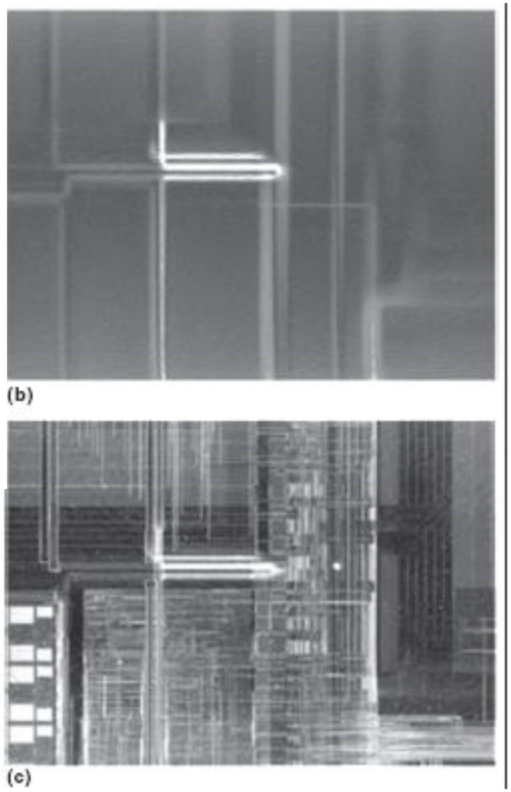

SPIN, 2011

TMR sensor linearization strategies
2: thin CoFeB (out of plane)

glass/Ta 5/Ru 18 /Ta 3/PtMn 18/CoFe 2.2/ Ru 0.9/ CoFeB3/MgO1.35/CoFeB 1.55 / Ru 5/Ta 5

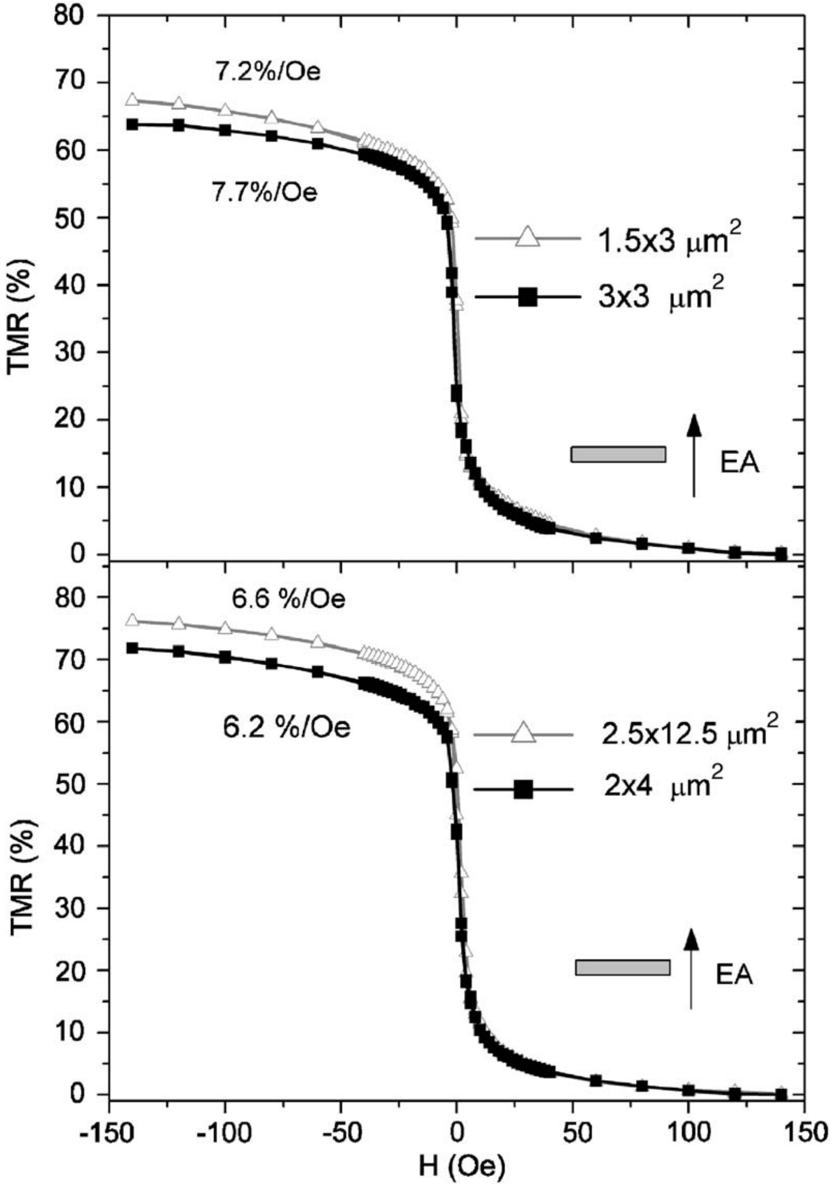

P. Wiśniowski et al, JAP 103,07A910 (2008)

P. Wiśniowski et al, IEEE Trans. Mag.,44(11), 2551-2553 (2008)

	Thick Free layer
TMR @ 20°C	76%
Sensitivity @ 0 Oe & 20°C	250 V/V/Tesla
Linear range @20°C	[-5 Oe; 5 Oe]
Voltage Noise @ 10 kHz & 20°C	700 nV/√Hz (for single TMR)
Voltage Noise @ 10 MHz & 20°C	70 nV/√Hz (for single TMR)
Field Noise @ 10 kHz & 20°C	6 nT/√Hz (for single TMR)
Field Noise @ 10 MHz & 20°C	0.6 nT/√Hz (for single TMR)

Reaching pT detectivity with MR sensors

Magneto Cardiography

Magneto-CardioGraphy :
Amplitude: 10^{-11} - 10^{-10} T
Frequency: 0,1 – 1kHz
Temporal resolution: 1ms

Contactless (no electrodes) and non invasive technique
Cartography of circulating currents
Additional information to Electro-Cardiography

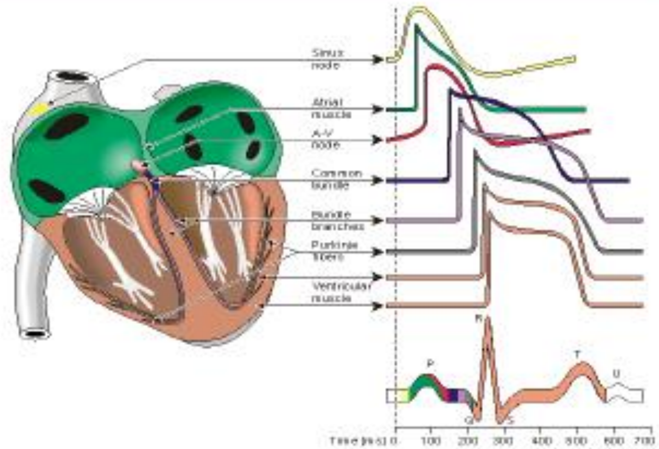

Magnetically Shielding Room – Neurospin

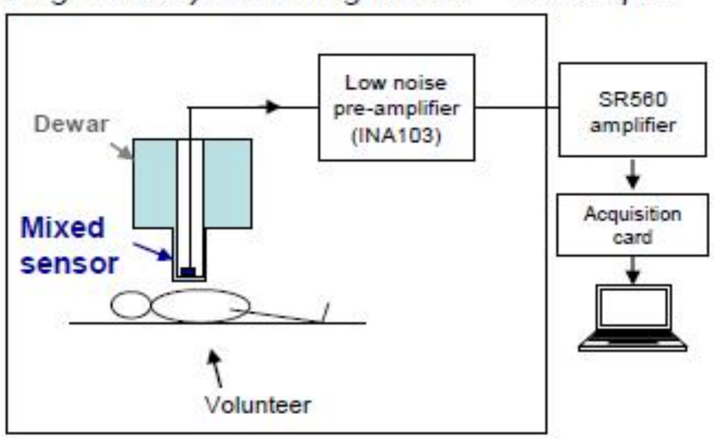

With permission from M.Pannetier, C.Fermon

MCG recordings at various locations

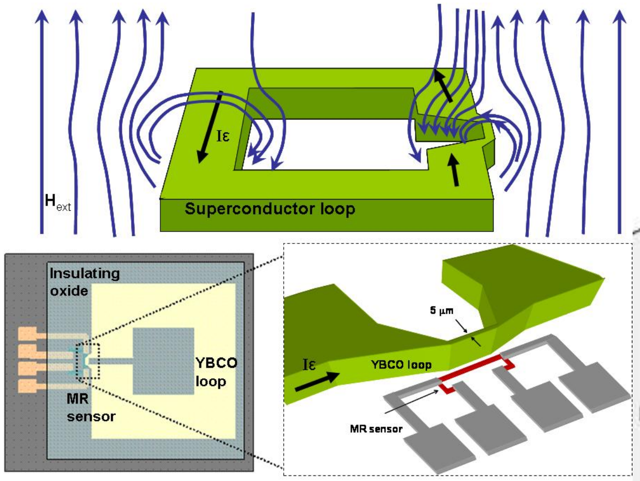

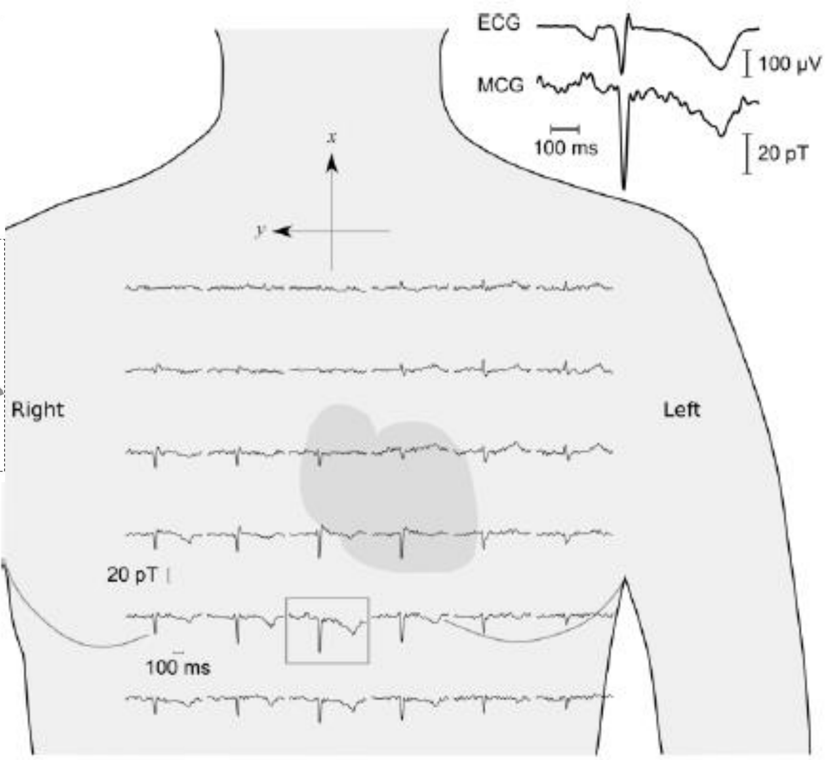

With permission from M.Pannetier, C.Fermon

Hybrid MTJ+flux guide structures: towards pT detection at RT and low freq.

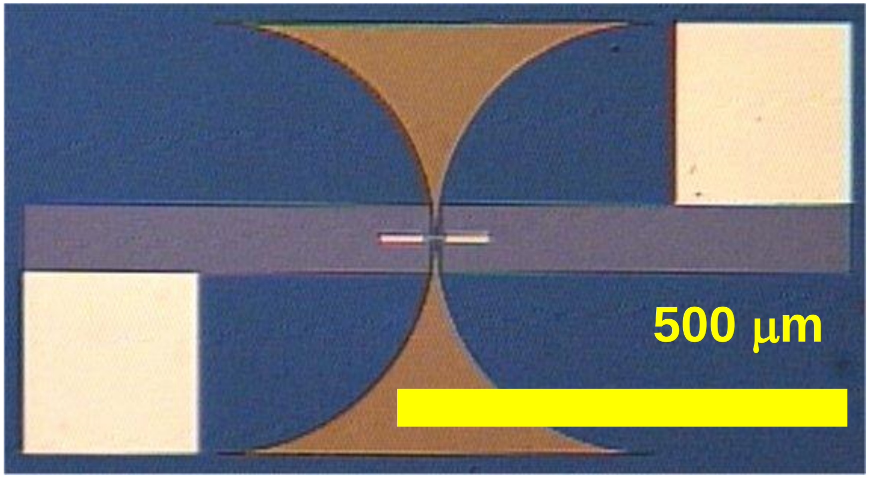

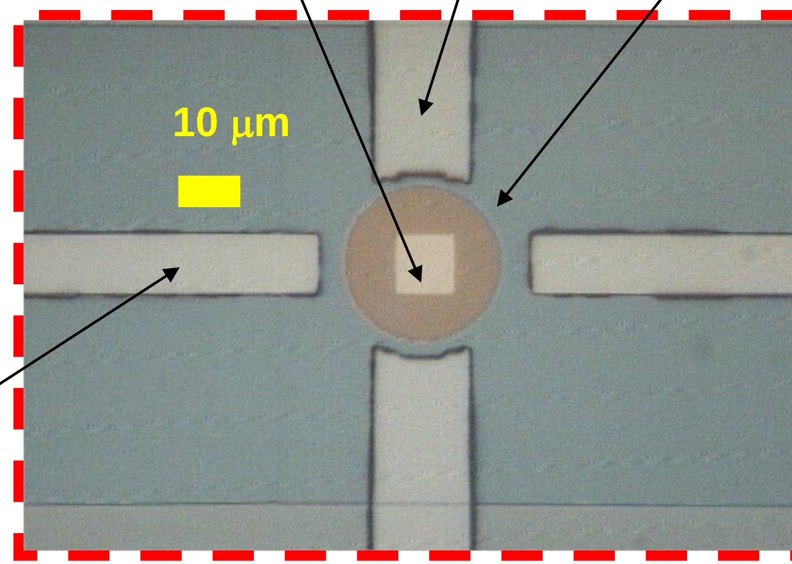

Goal: increase volume of free layer-reduce magnetic 1/f noise
increase junction area-decrease barrier 1/f noise
increase sensitivity: flux guides + MgO MTJ

Noise characteristics

Field Resolution α_H=3.2 E-9 μm^2

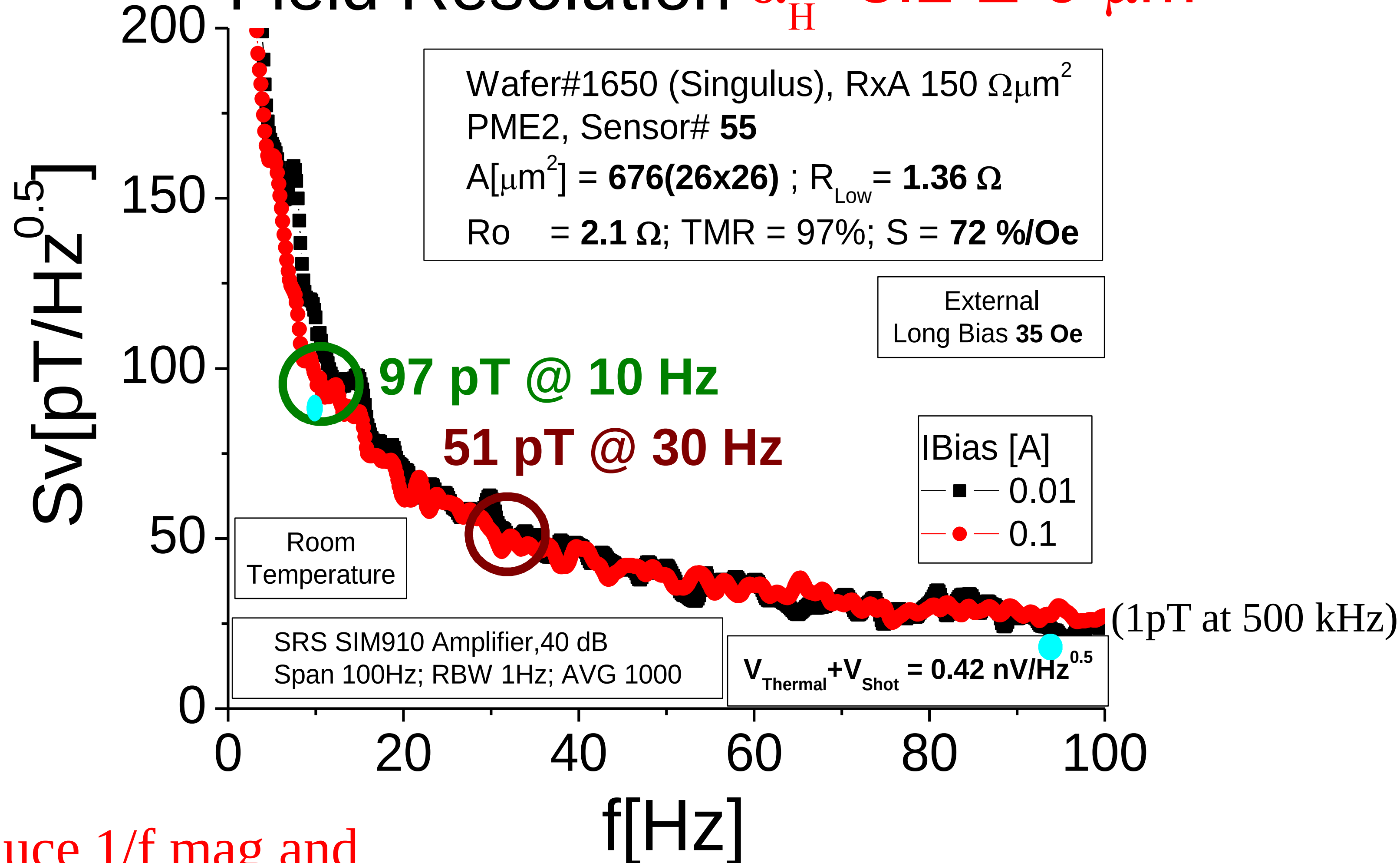

Need reduce 1/f mag and white mag noise

Appl. Phys.Lett., 91, 102504, August 2007

INL approach to picoTesla field detection

Large Arrays of linear MTJs integrating large area MTJs

Detection of very weak magnetic fields at INL :

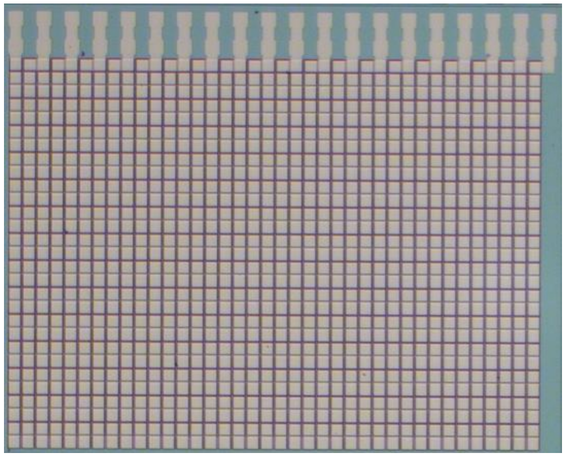

Array of 1102 MTJs connected in series with an individual area of 100x100 μm^2

Total Area : 4x6 mm^2

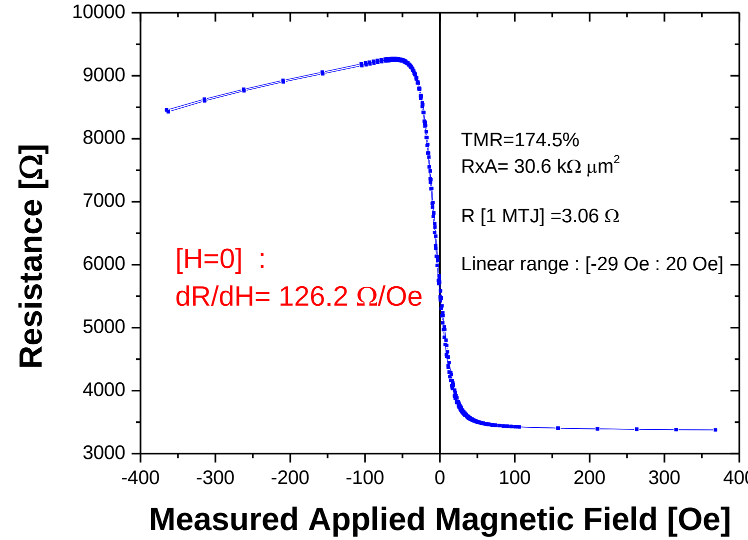

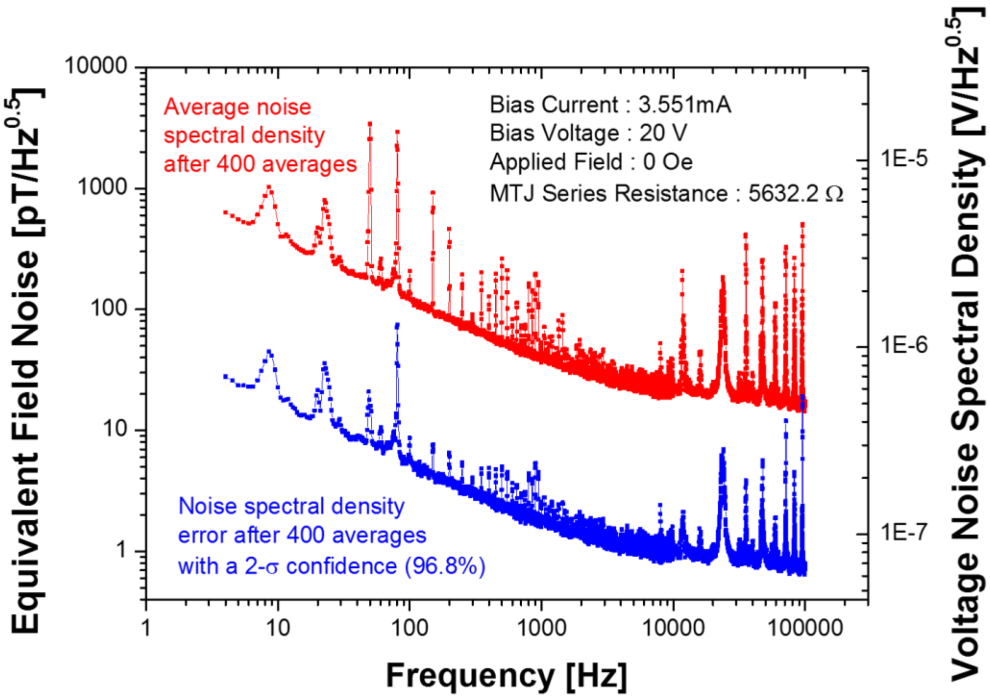

Direct detection of weak magnetic fields obtained WITHOUT magnetic shielding.

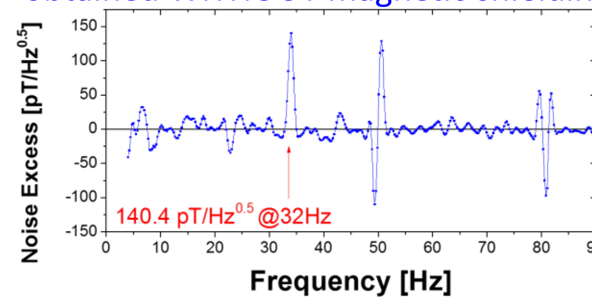

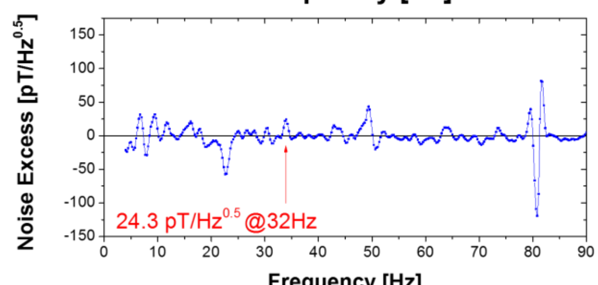

INESC-MN's static, multiplexed MR biochip

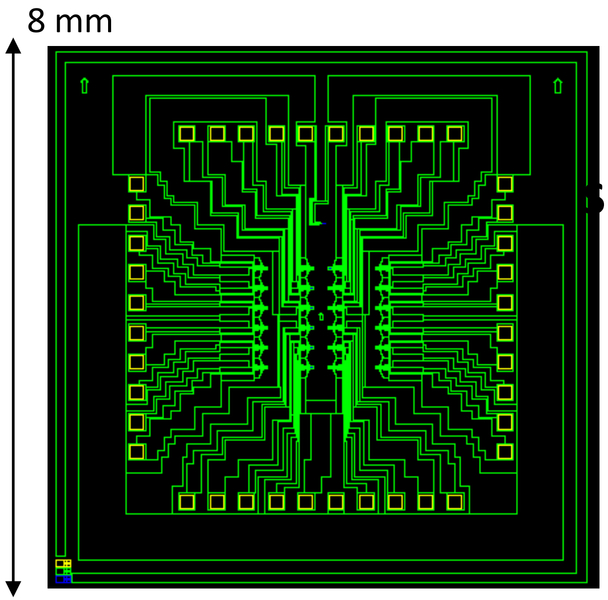

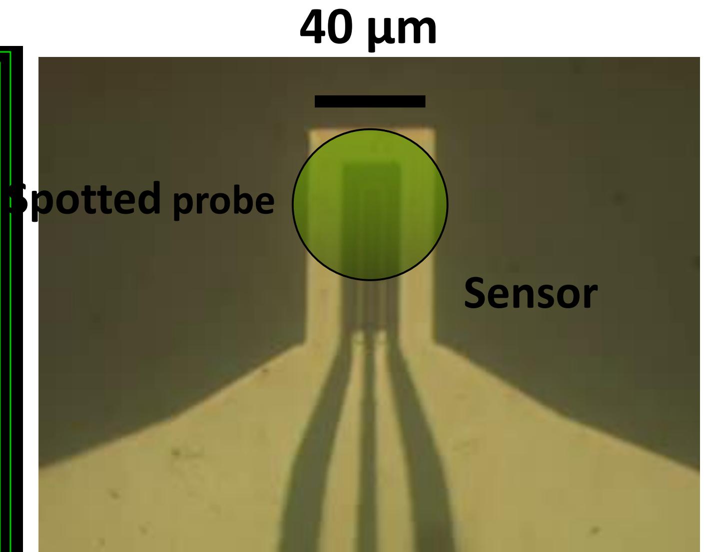

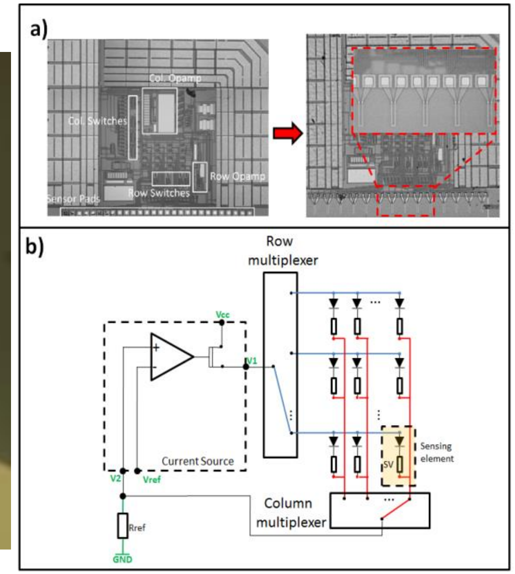

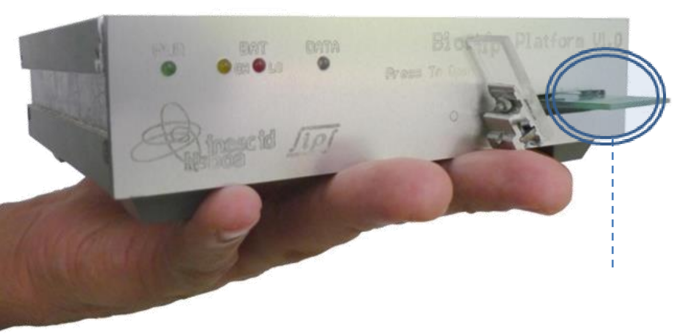

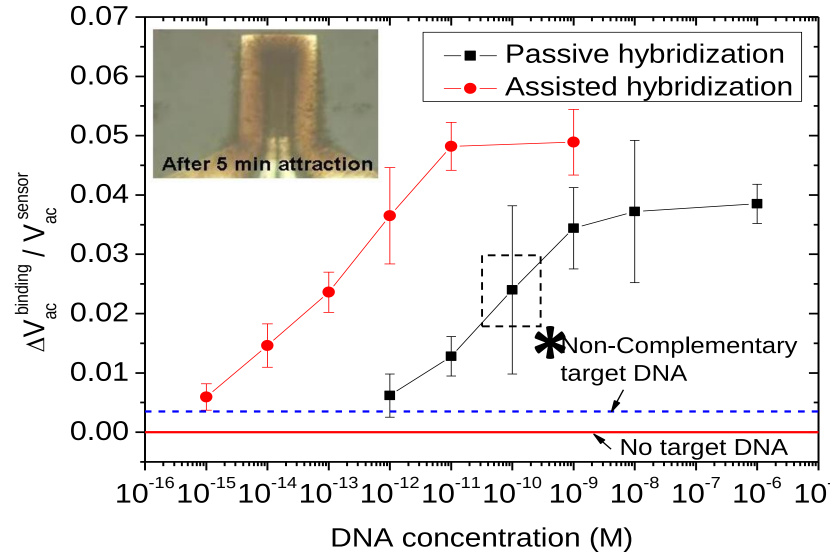

ftmolar sensitivity (DNA chip)
multiplexed analysis
CMOS, microfluidics, sensors

Tech review, Lab On Chip 2012

1-d) Spotting biological targets on the biosensing platform

Spotting site

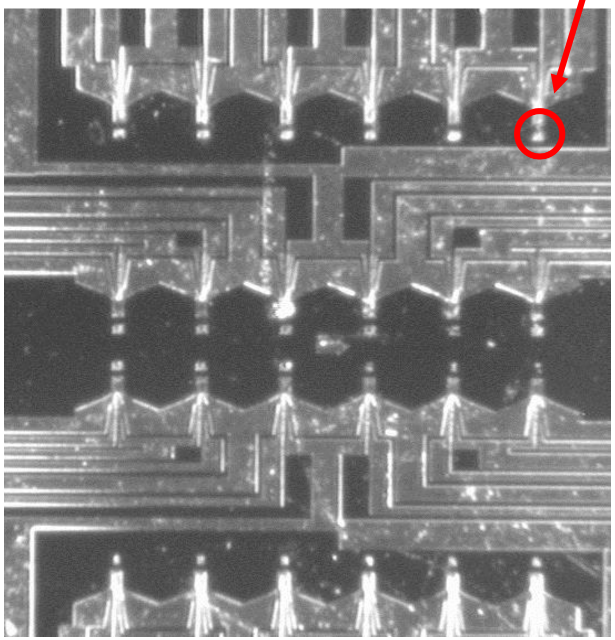

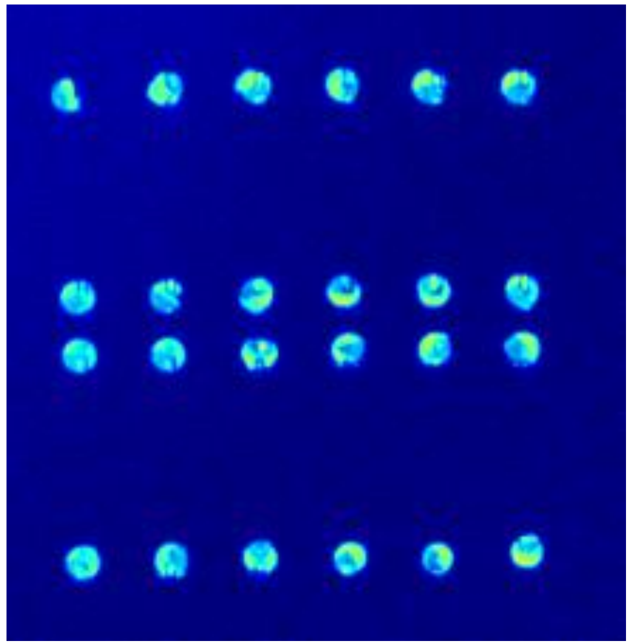

1 μM Oligo solution, Cy5 labeled
200 pL droplets

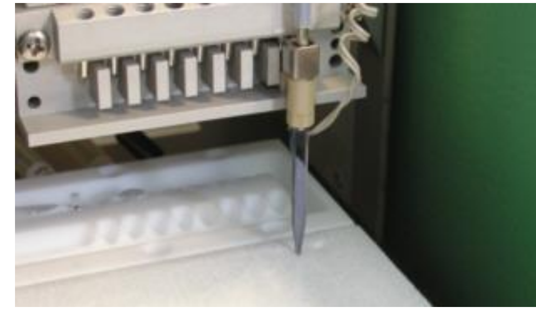

Gesim spotter

Disposable biochip

Protein/DNA Biochip

Blood finger-prick

Sample preparation step
separation of plasma
from blood cells

Plasma injected in
the detection chip

Measurement of the chip

Cell free DNA detection in blood
As cancer biomarker

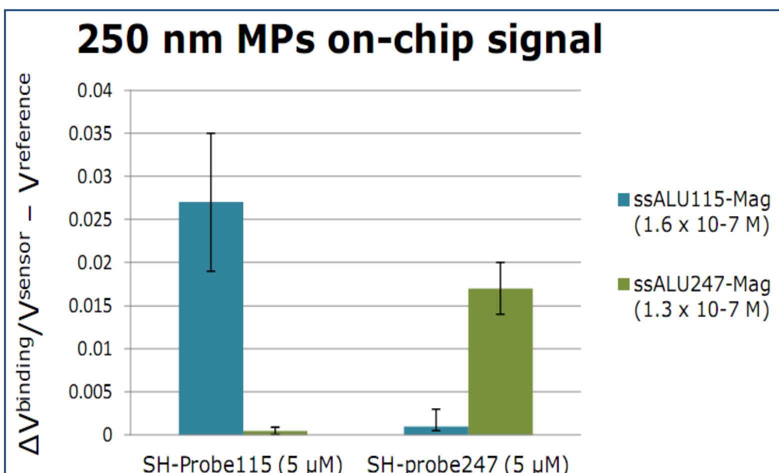

Also used for protein and immuno assays

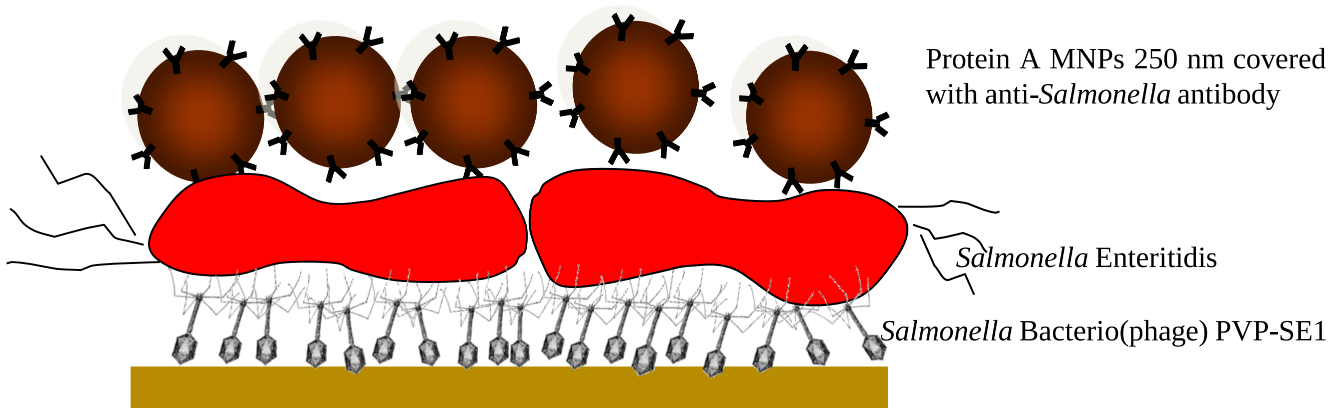

The signal obtained…

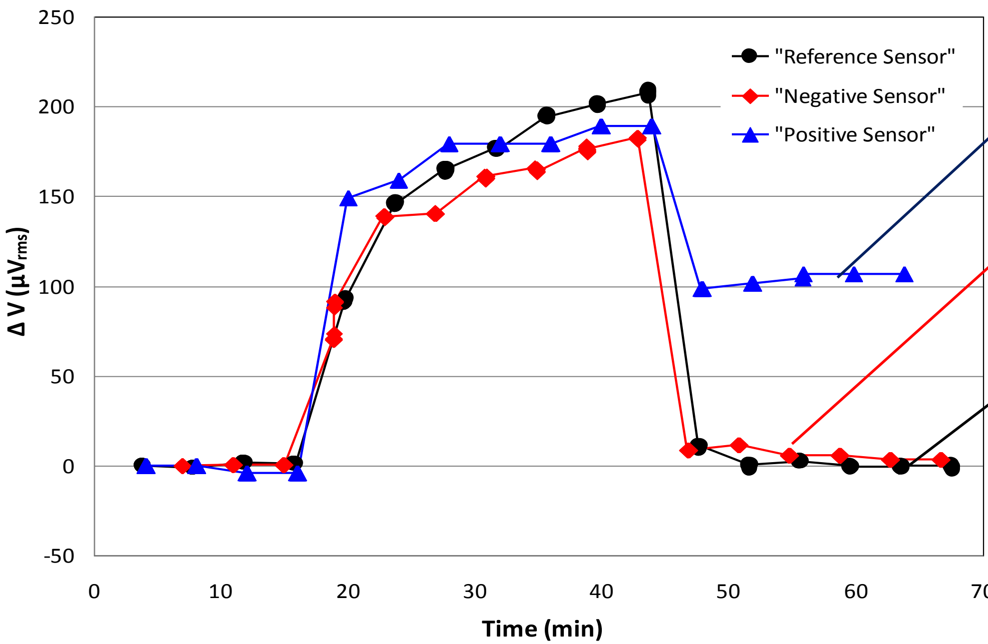

Affinity of the specific phage was about 20 times higher (average absolute value of 100 μV against 5 μV).

Detecting labelled cells in flow

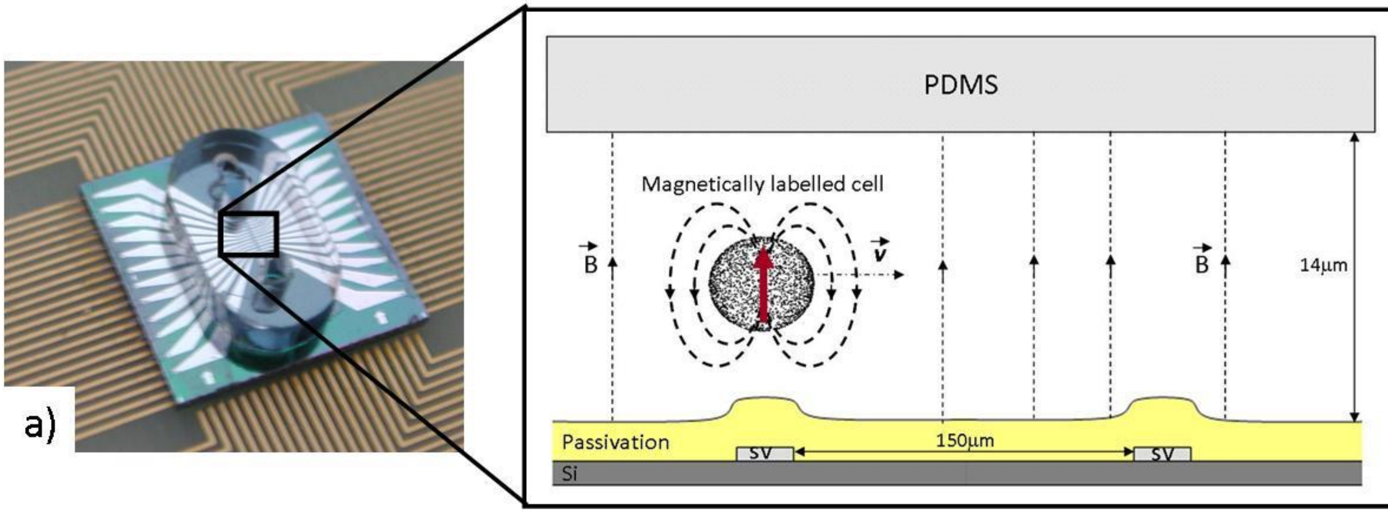

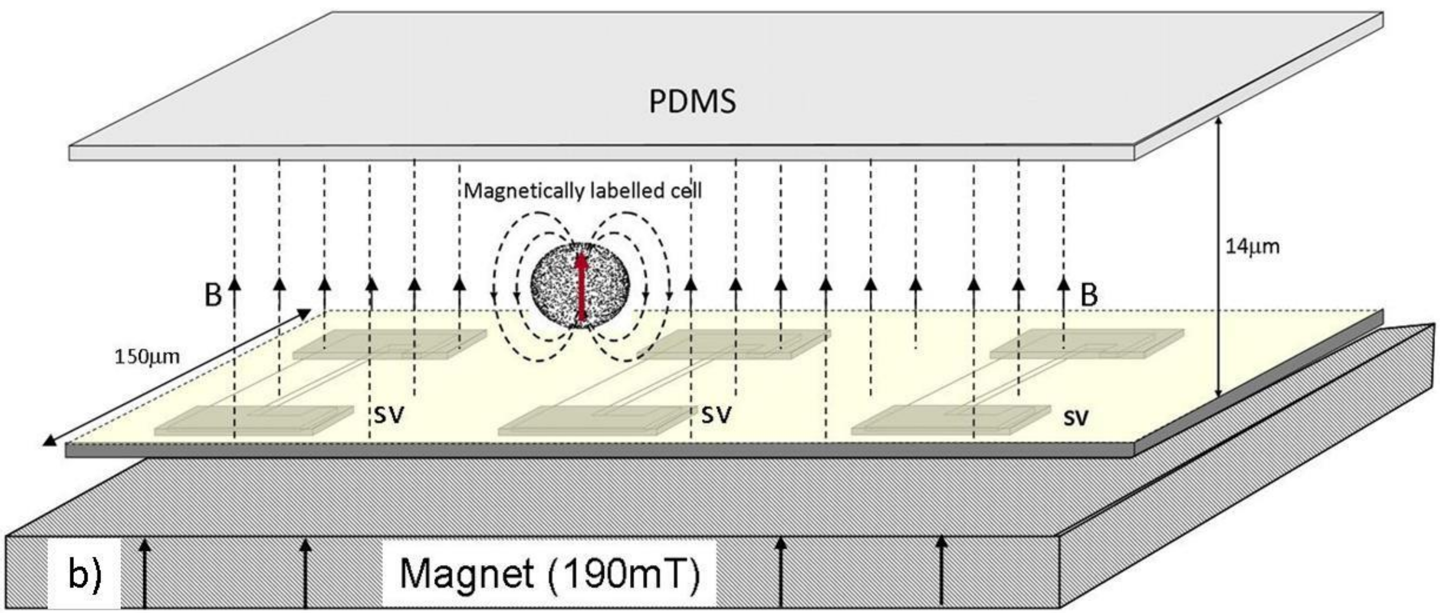

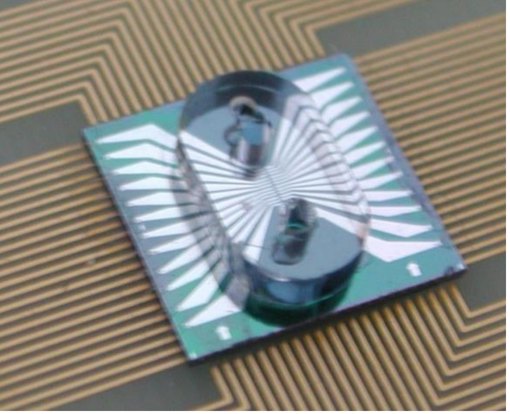

Cell detection – Kg1a cells/CTCs

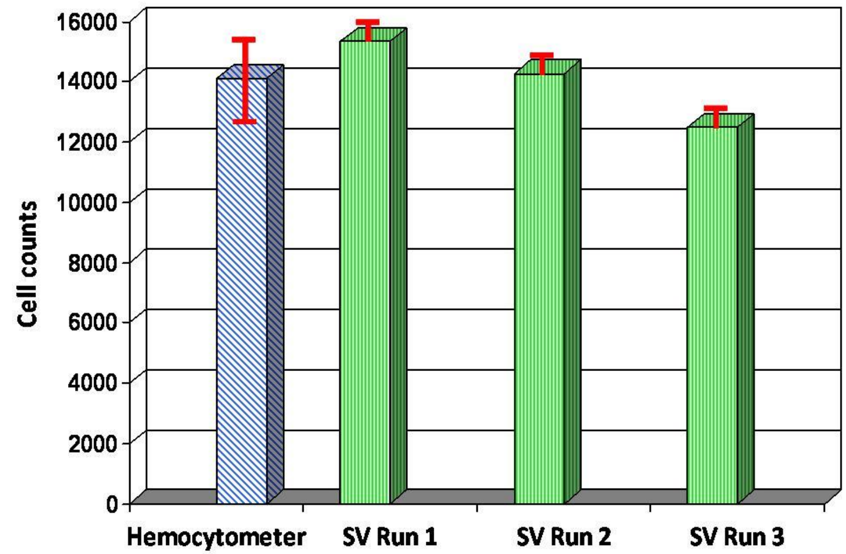

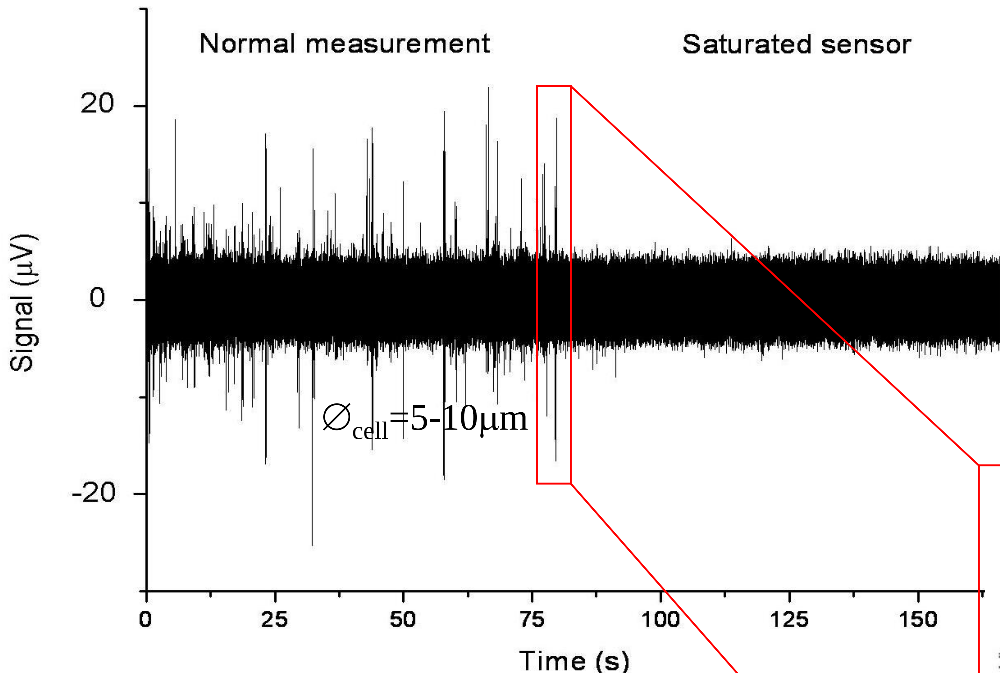

Lab on Chip (2011)

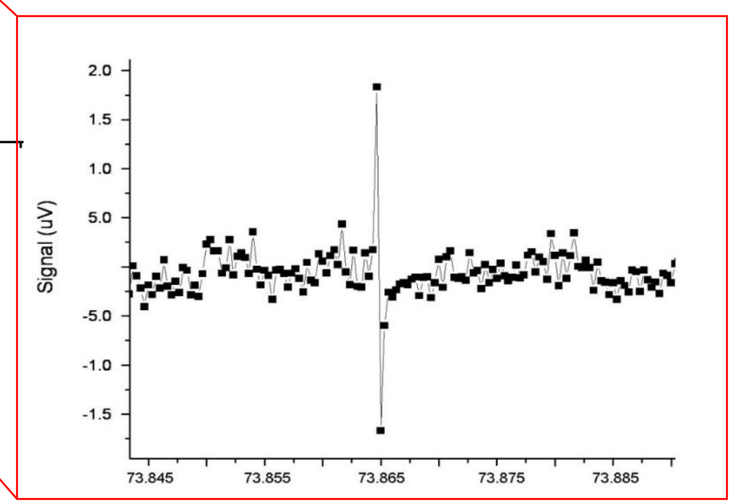

Cells marked with 50nm FeOx particles

NANODEM FP7 (2012-2015)

Synaptic current monitoring with high
Spatial resolution (with A.Sebastiao, IMM, V.Santos, ICVS)

Stimulation electrode

Recording electrode

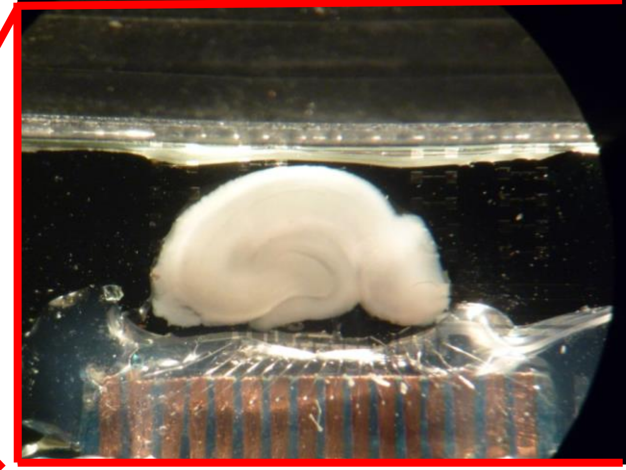

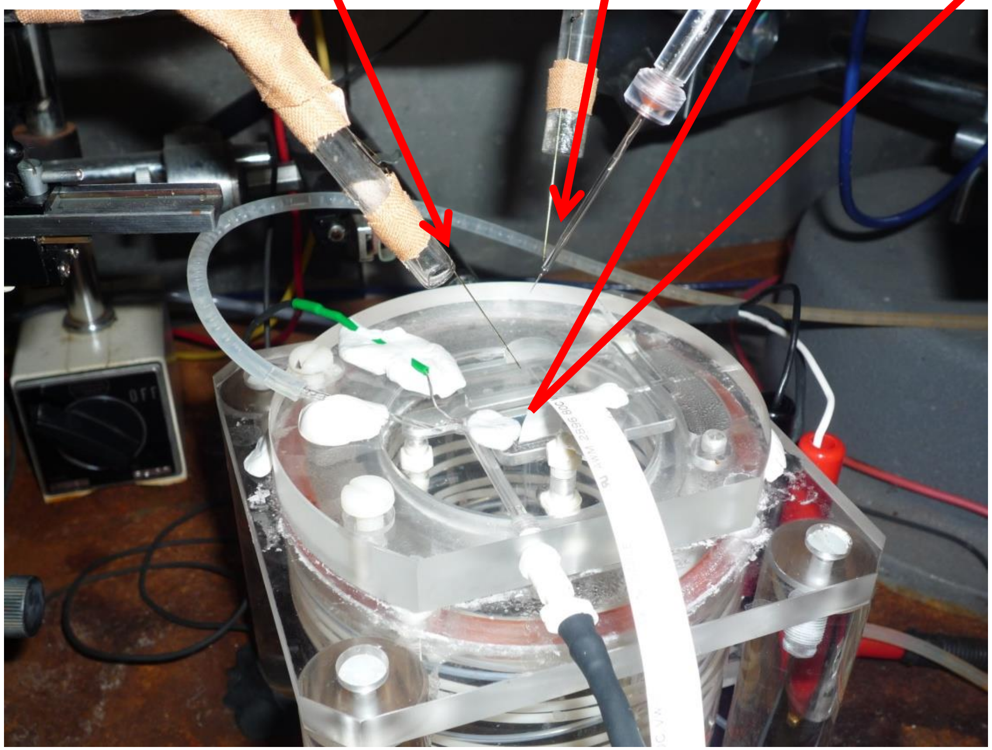

Rat hippocampus

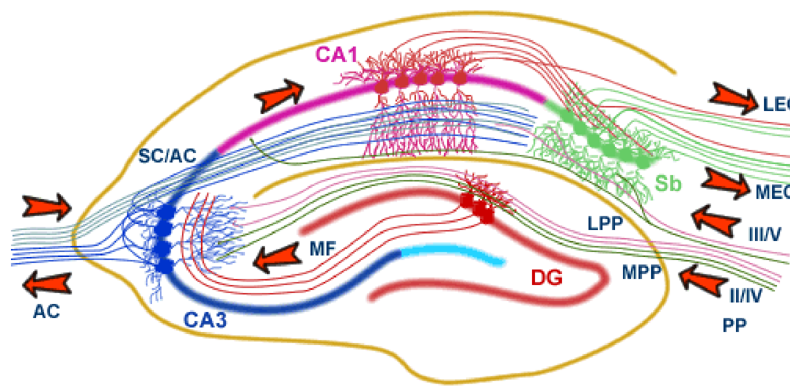

INESC MN and IMM

MAGNETRODES, FP7 (2013-2016)

Si Needles with MR sensors or planar electrode array of MR sensors

Probe design for in-vitro applications

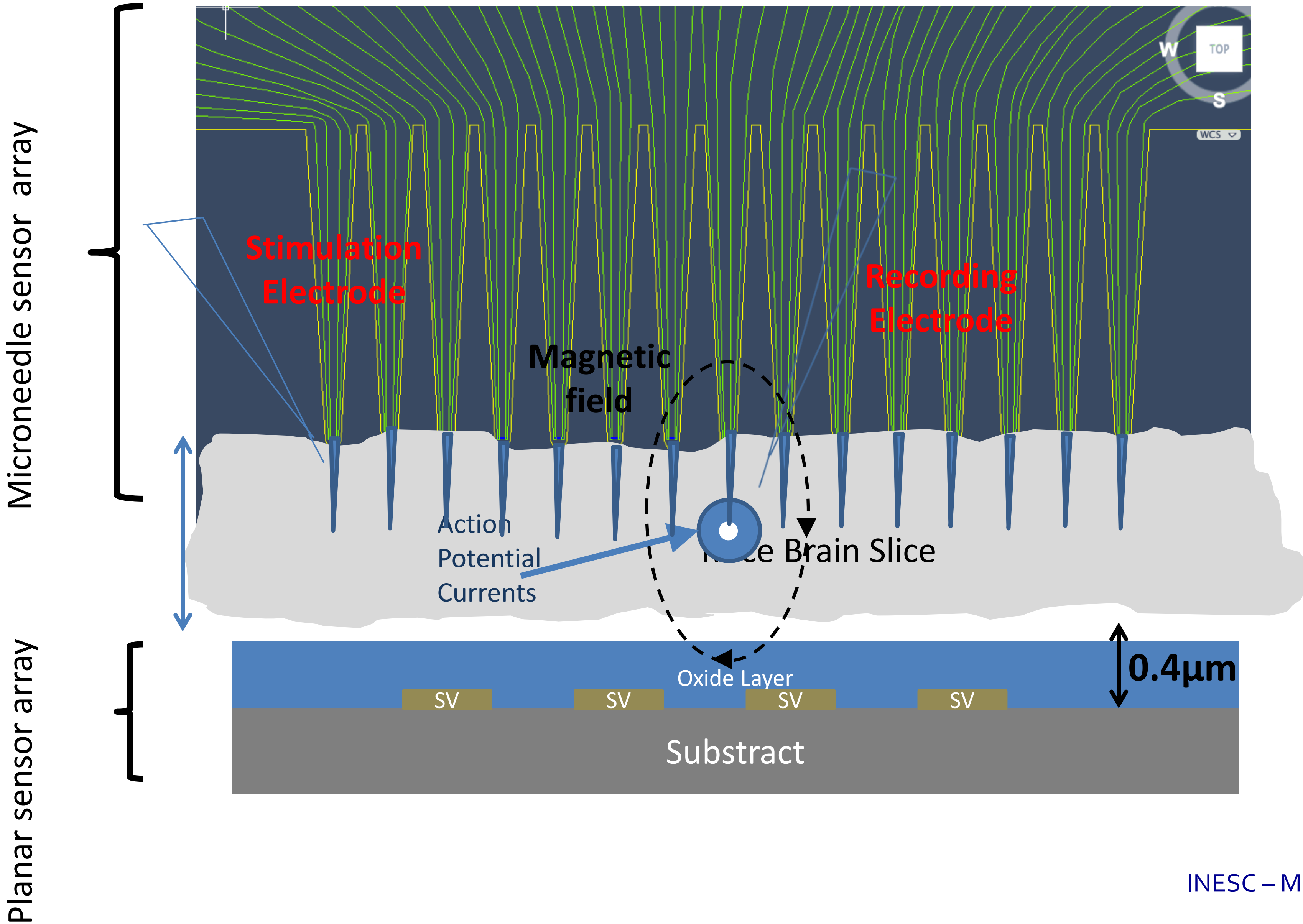

INESC – MN

FP7 MAGNETRODES (2013-2015)
Probe desigb for in-vivo applications

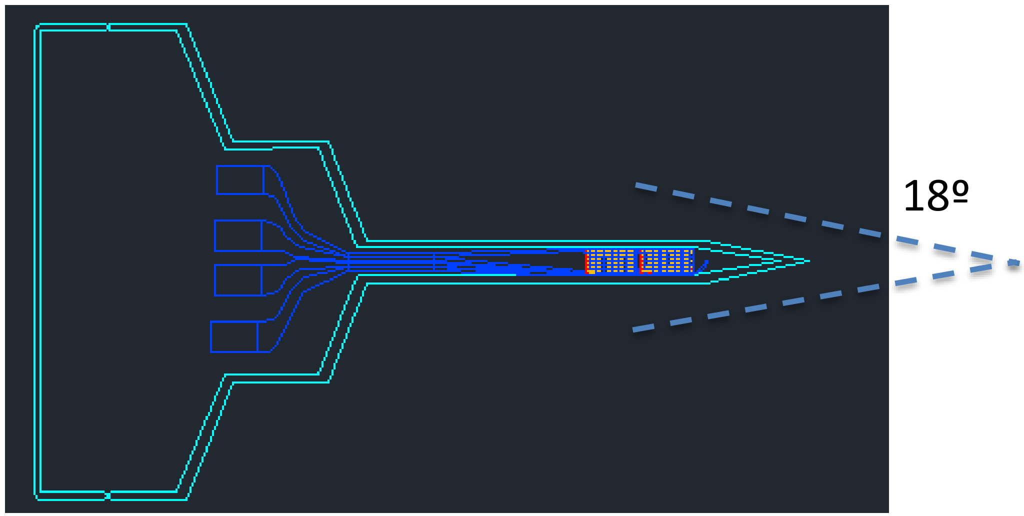

- **Probe specifications:**

1) Shaft angle 18º

2) Thickness < 100 µm

3) Length ~ 1 cm

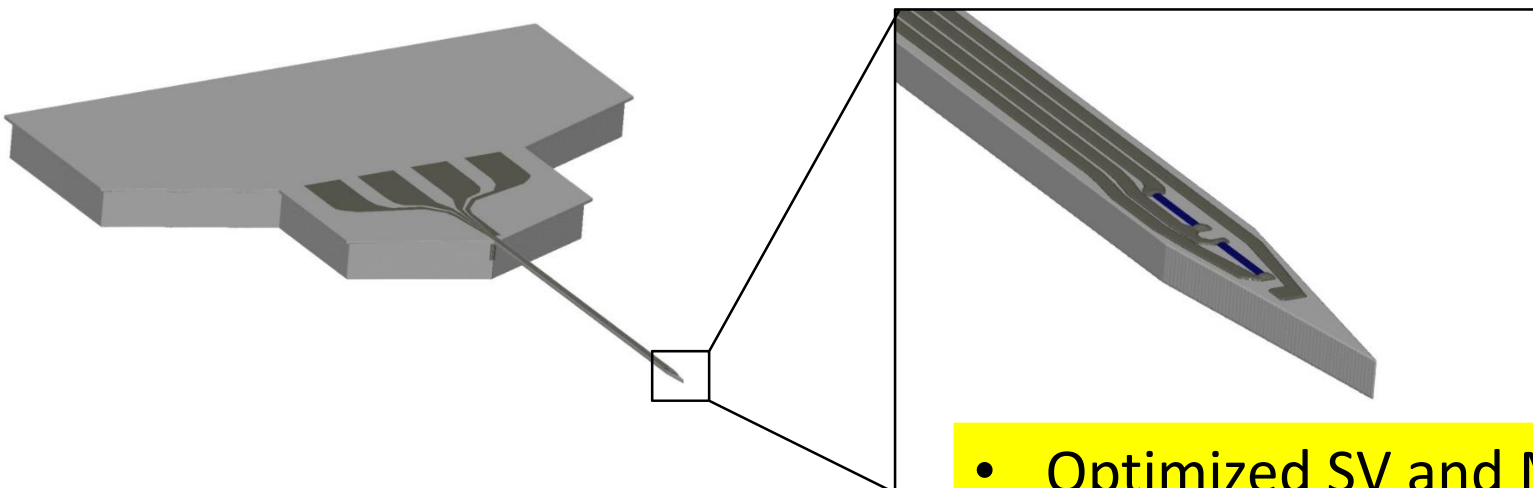

- **Optimized SV and MTJ sensors**

INESC-MN

INL INTERNATIONAL IBERIAN NANOTECHNOLOGY LABORATORY

Silicon probes

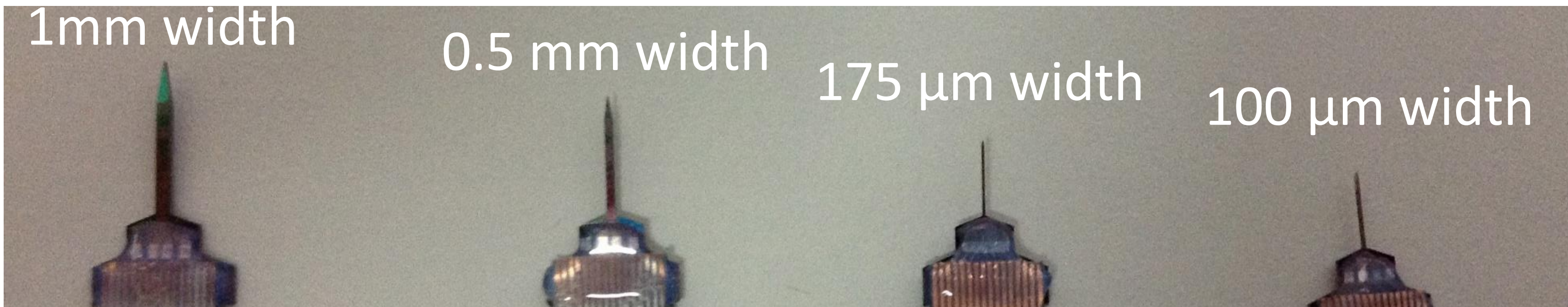

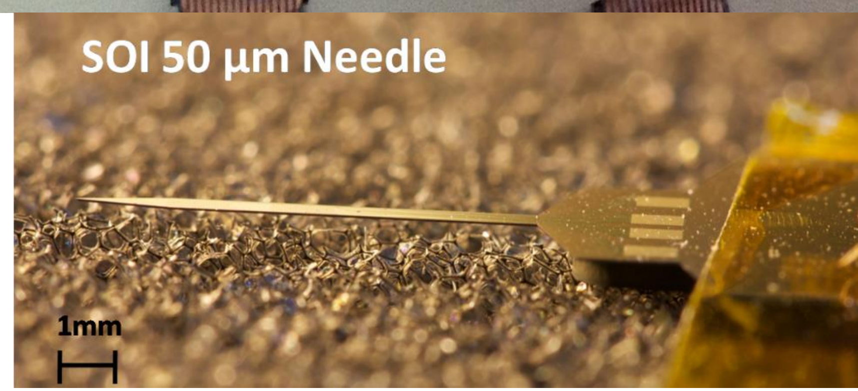

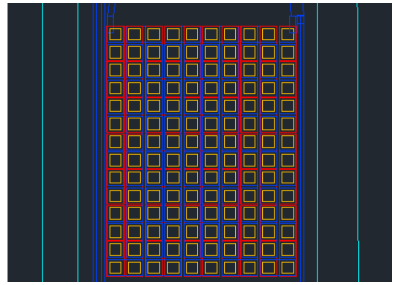

- Probe Tip Area -1000x1000 μm^2
- 140 **Magnetic Tunnel Junction** sensors
- each sensor – 50x50 μm^2

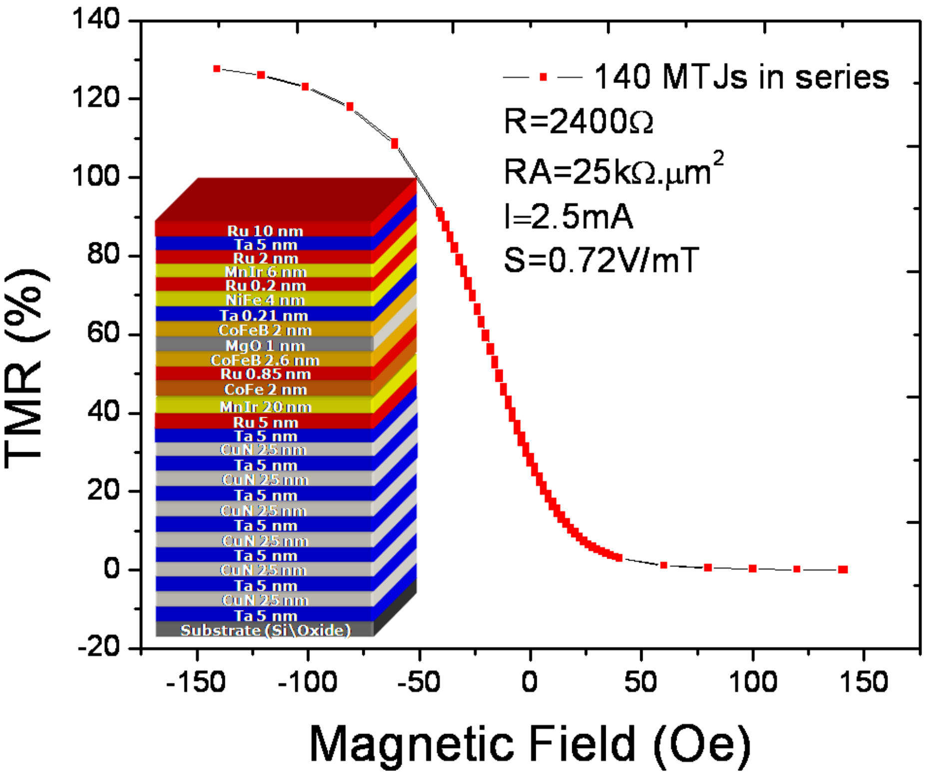

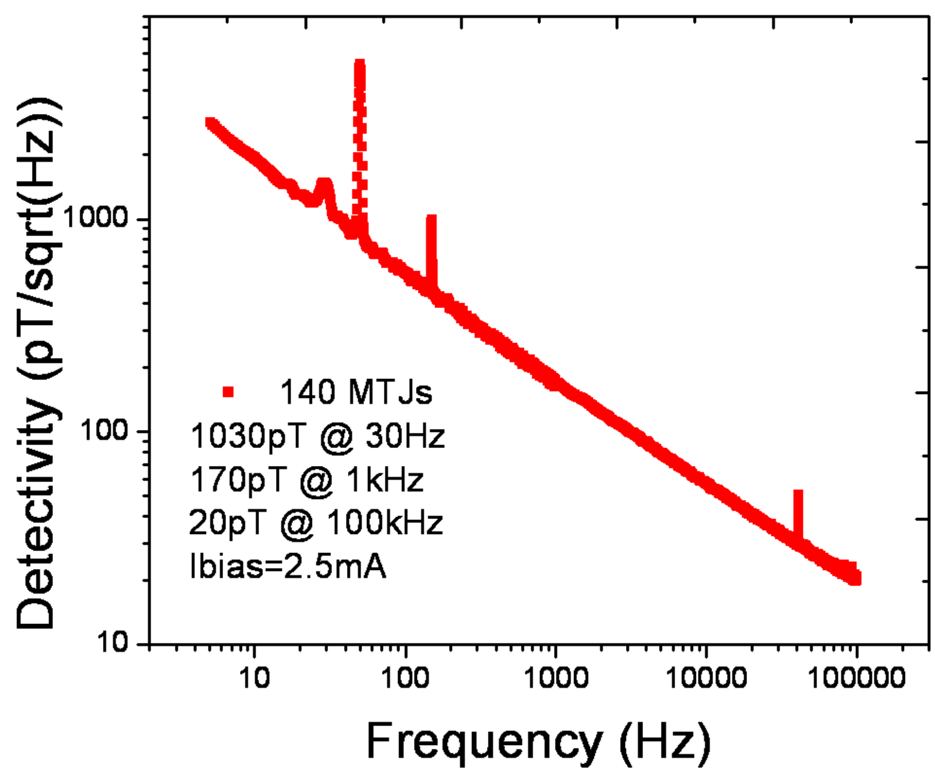

Flexible Probes (polyimide)

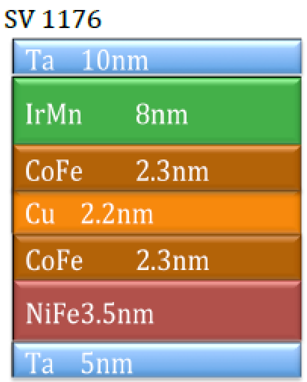

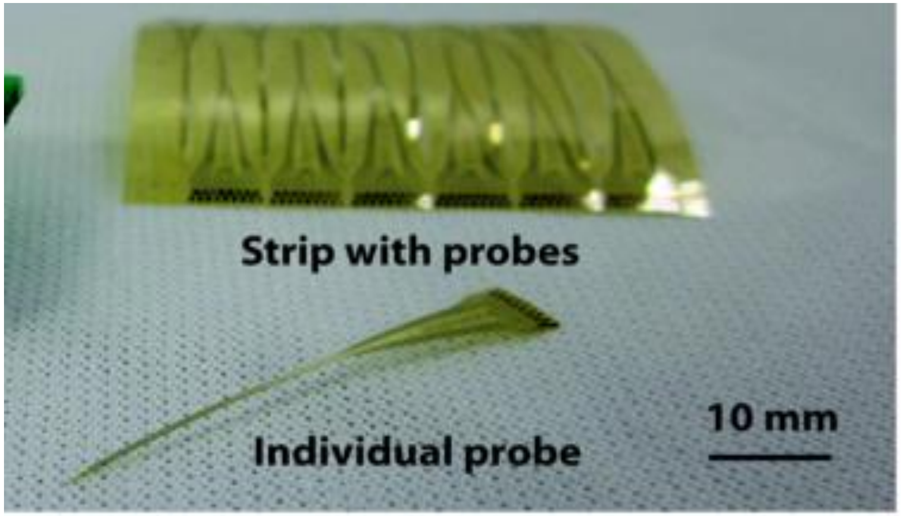

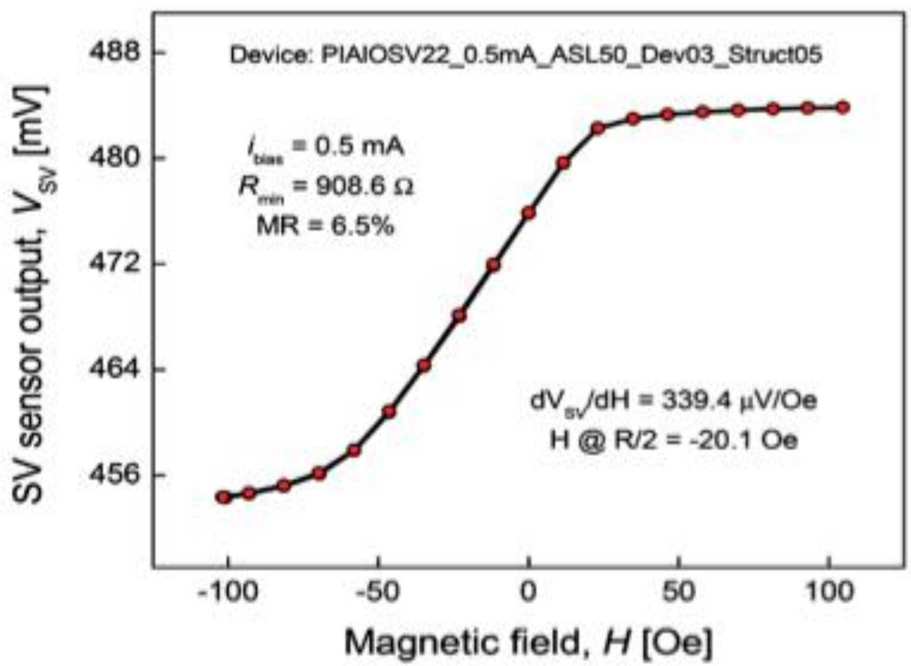

Results – MTJ response

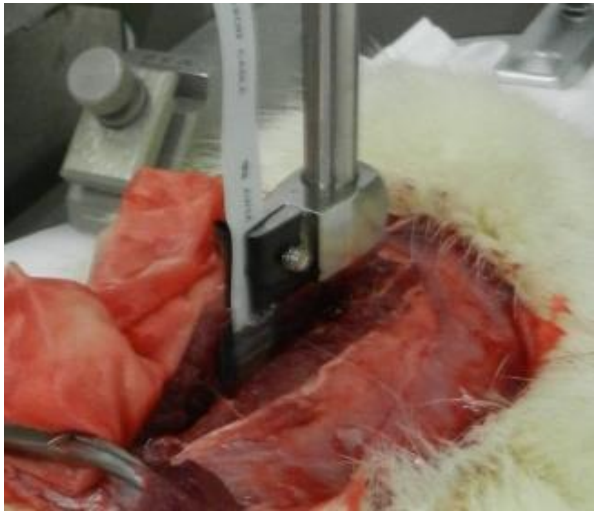

In Vivo - Spinal Cord

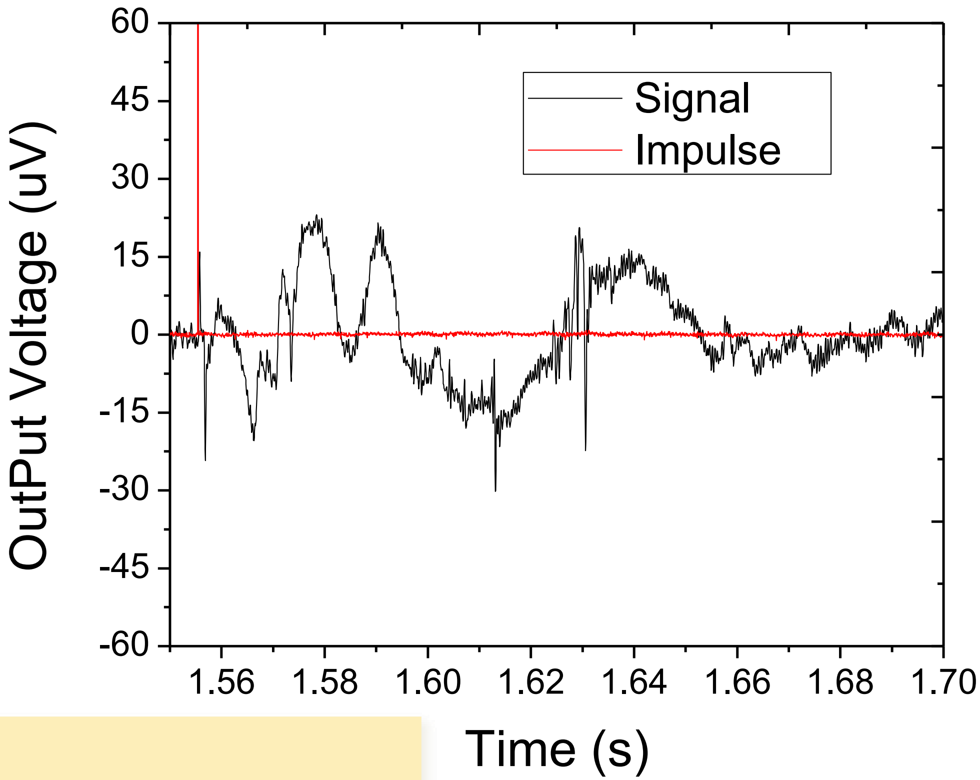

The MTJ sensor readout:

- 20μV amplitude

- 20uV amplitude signal corresponds to a magnetic field of about 3μT.

- Type of signal expected

VI: New spintronic Nanodevices (STT-RAM, Nano Osc., ...)

INESC MN

Applications

Memory Elements

Spin Transfer Torque -MRAMs

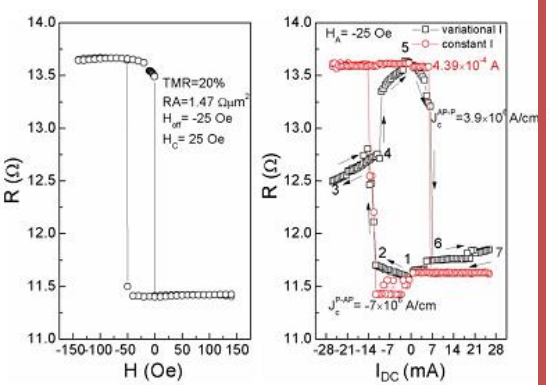

Jie Yang et al. IEEE Trans. Magn., 46, NO. 6 (2010)

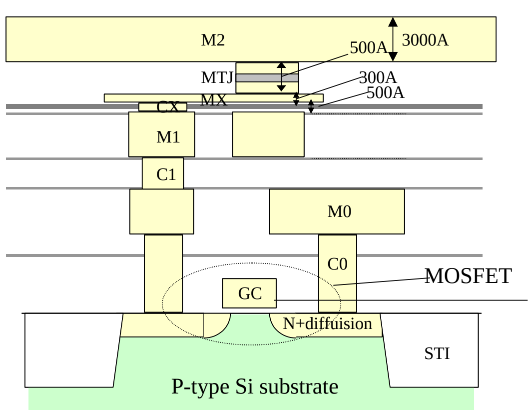

High Frequency Generators

Spin Transfer Torque based NanoOscilators

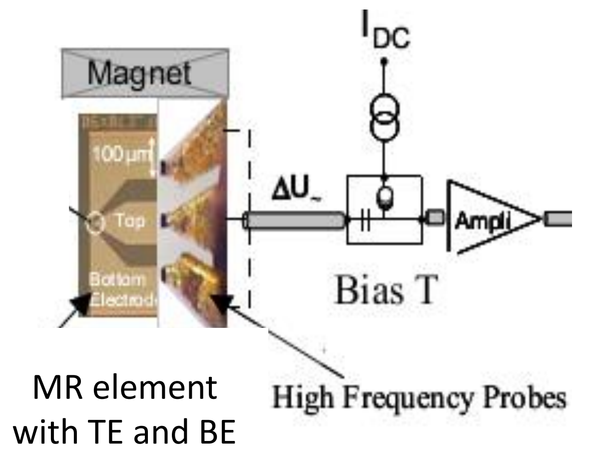

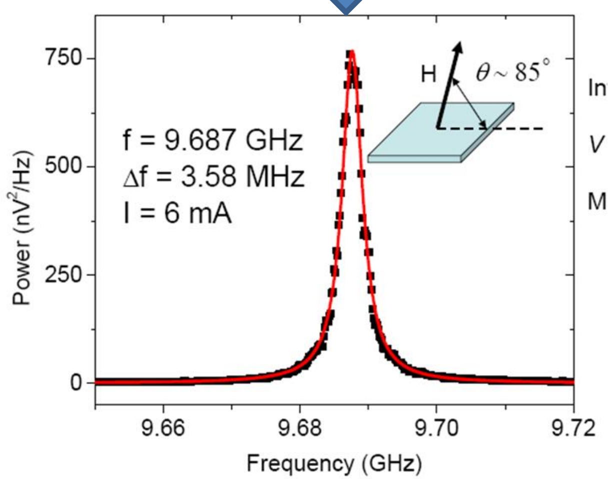

Field Nanosensors

Magnetoresistive Nanosensors with improved spatial resolution

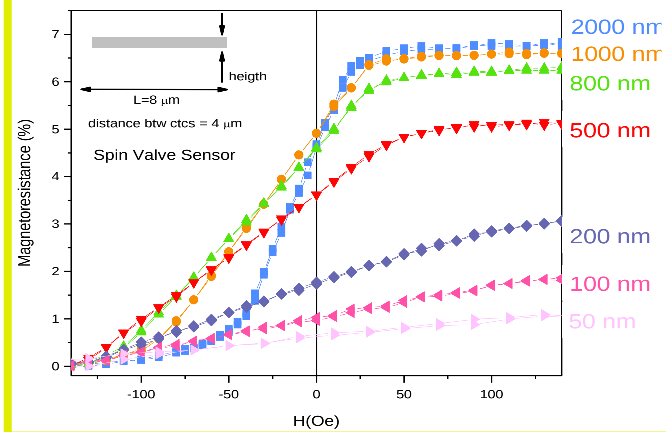

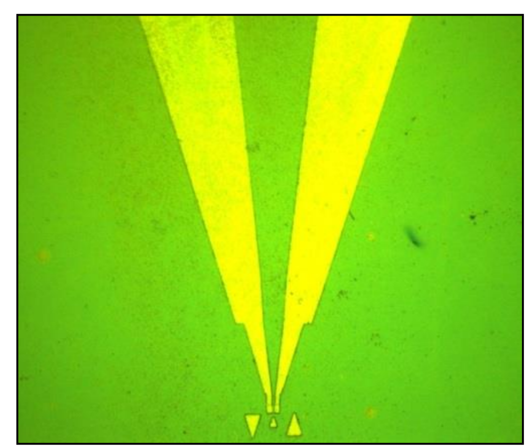

Process for STT Nano-oscilators: Simulations

INESC MN

Micromagnetic Simulations

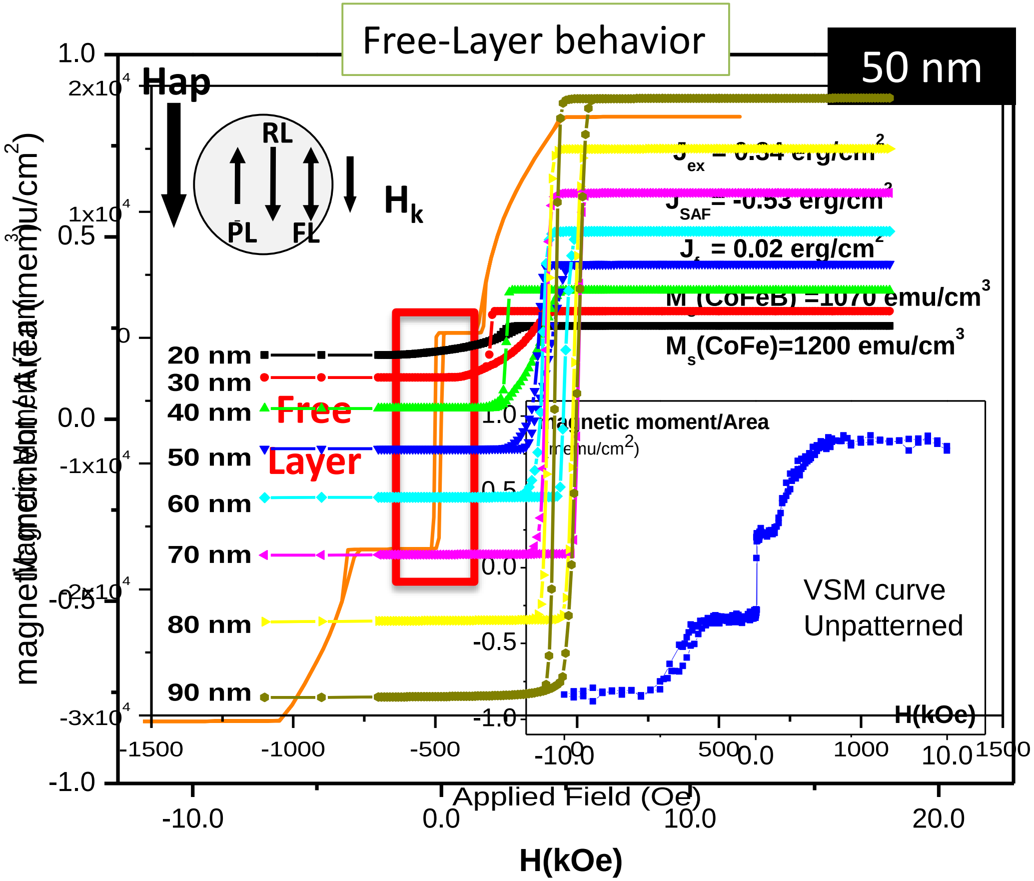

Dot = 50 nm

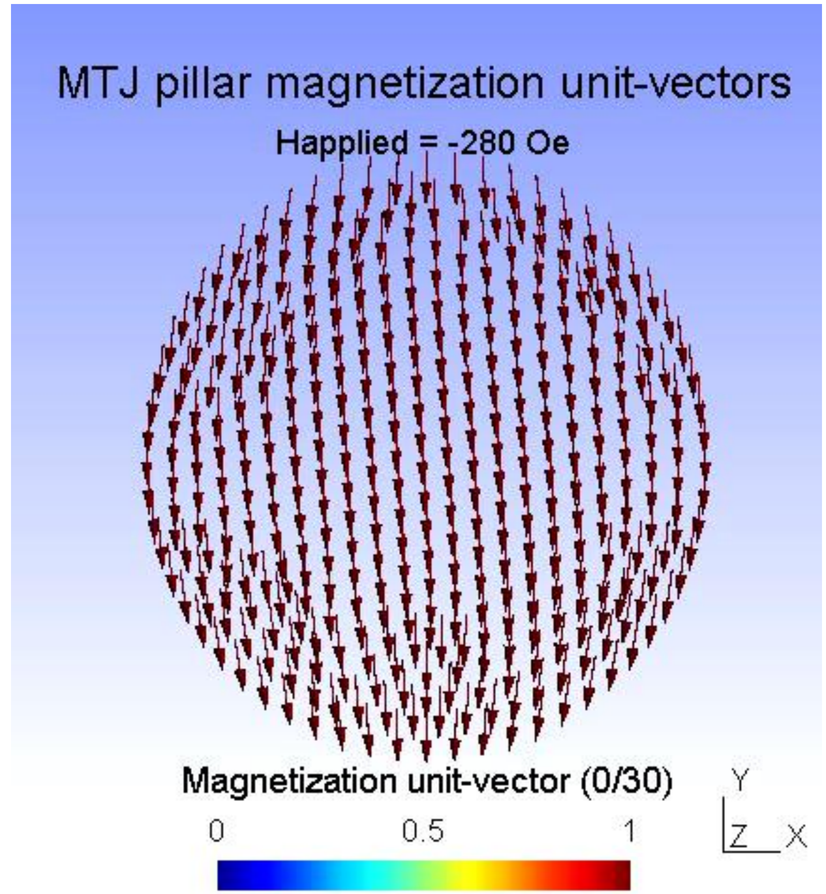

Accurately choose the properties/dimensions of nanostructures to fabricate in accordance with the envisaged application

INESC MN

INL

Obrigado!

MR DEVICE MICROFABRICATION PROCES
Current-perpendicular-to-plane (CPP) device fabrication

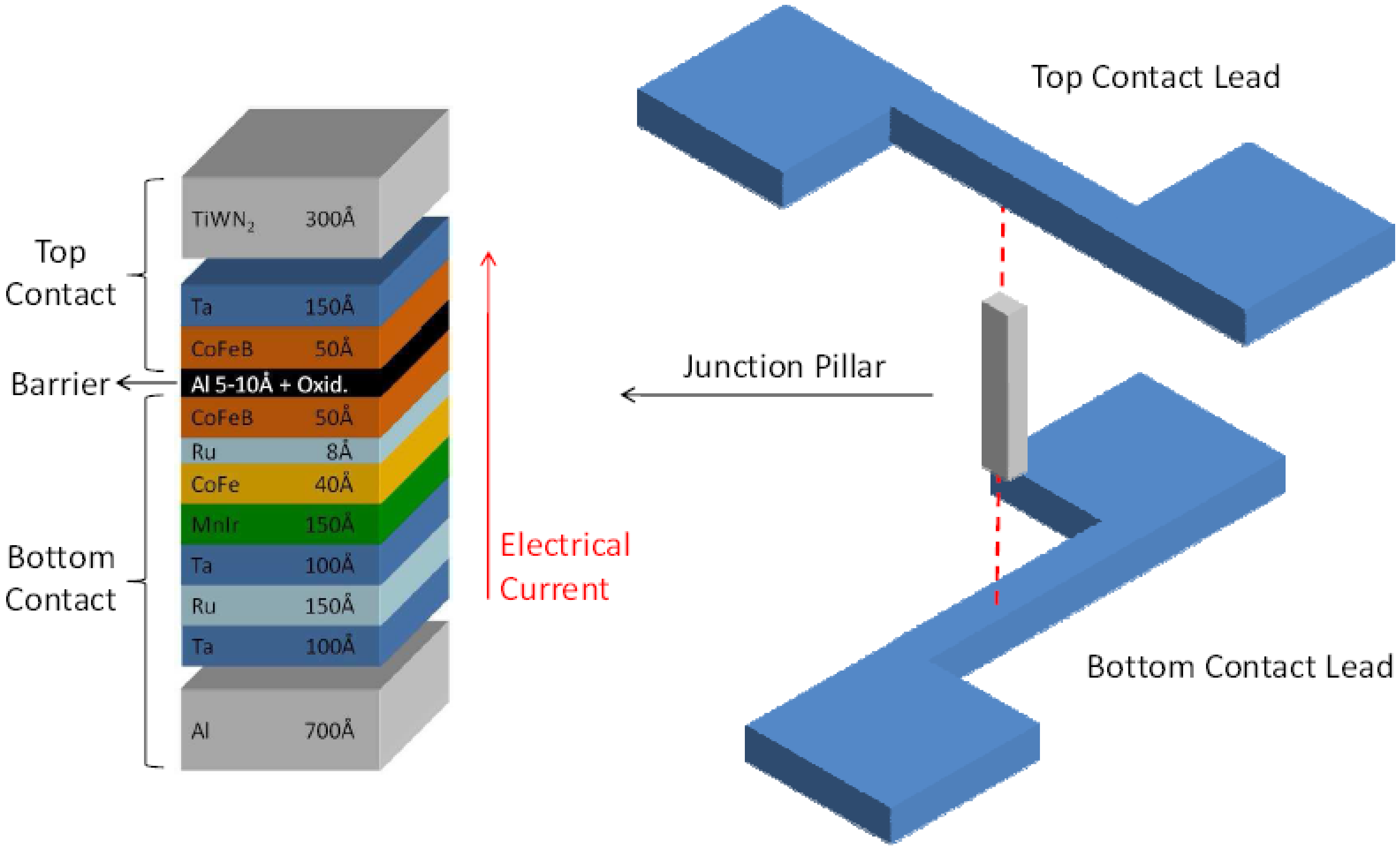

Microfabrication process

1) Deposition of the MTJ Stack

The complete stack is ~1800Å thick

2) 1st. Lithography

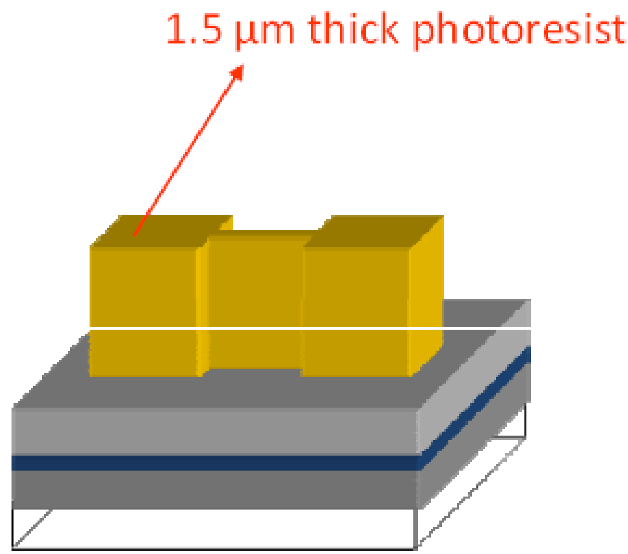

3) Ion Beam Milling

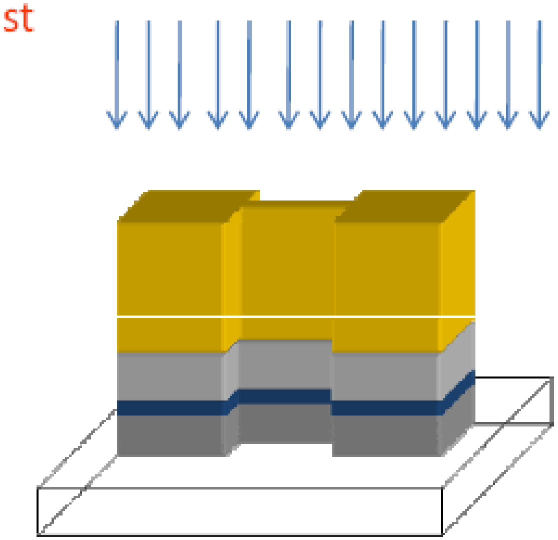

Stop point is signaled by the transparency of the substrate

Optical lithography - DWL

1) Autocad Mask

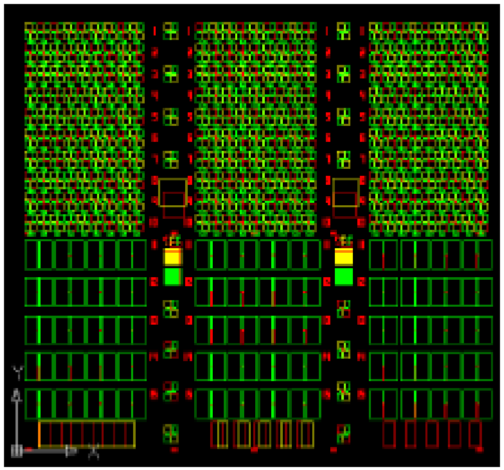

2) Digital Mask Format (LIC)

3) Exposure

Relevant Parameters :

- **Laser Energy**
- **Laser Focus Point**

Laser Energy and Focus Point must be matched with development parameters in order to provide sharp edges in mask

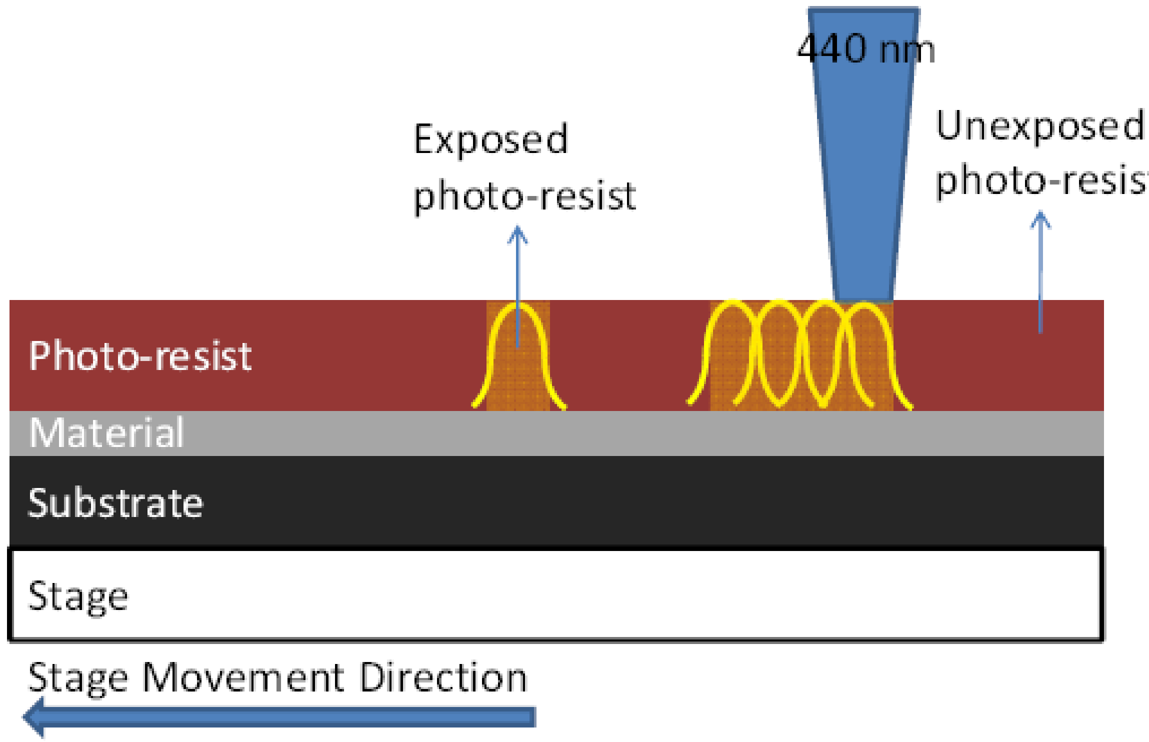

4) Resist Strip

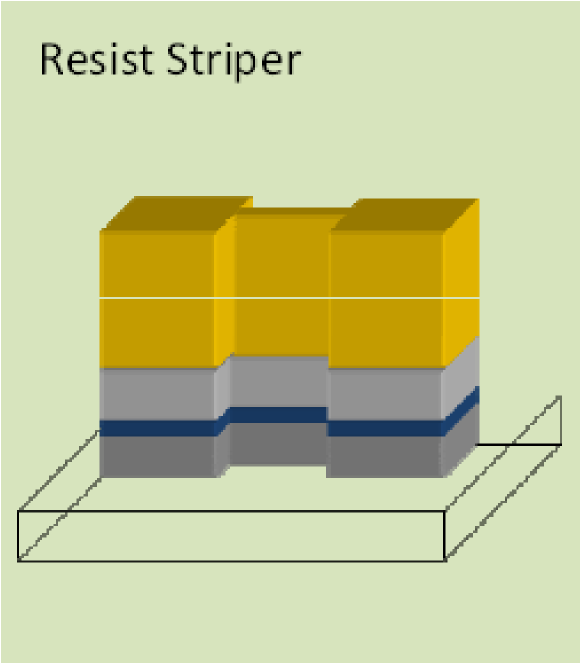

Microstrip 2001 (Fuji) is used to remove the remaining photo-resist

~2 hours in a hot bath (65° C) + Ultrasounds

750µm x 50µm

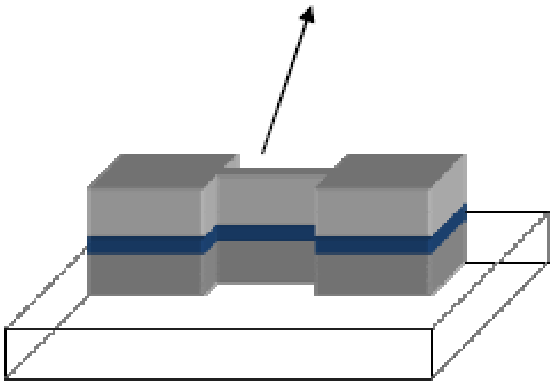

At this point, the shape of what will become the bottom contact lead is defined.

5) 2nd. Lithography : Junction Pillar Definition

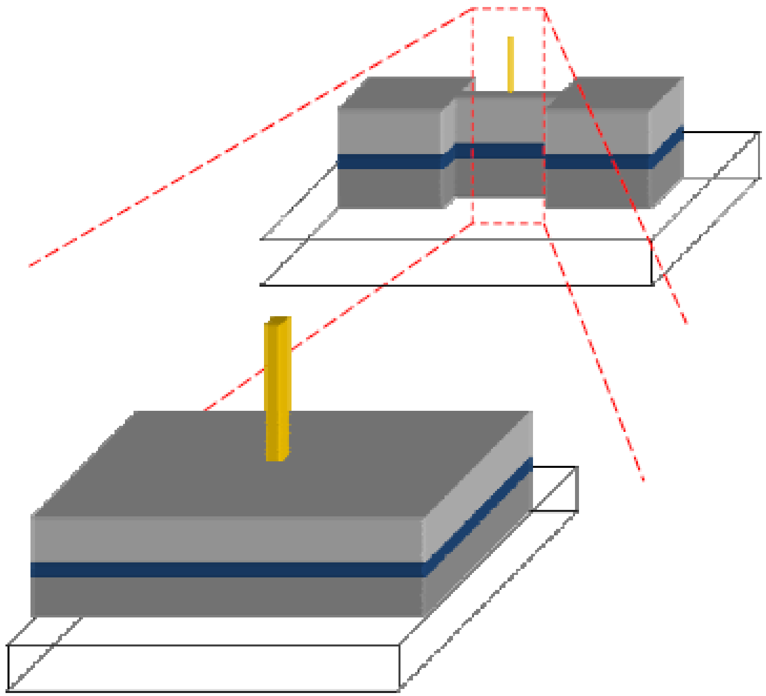

Minimum Junction Area : 1x1 μm^2

6) Junction Pillar Etching

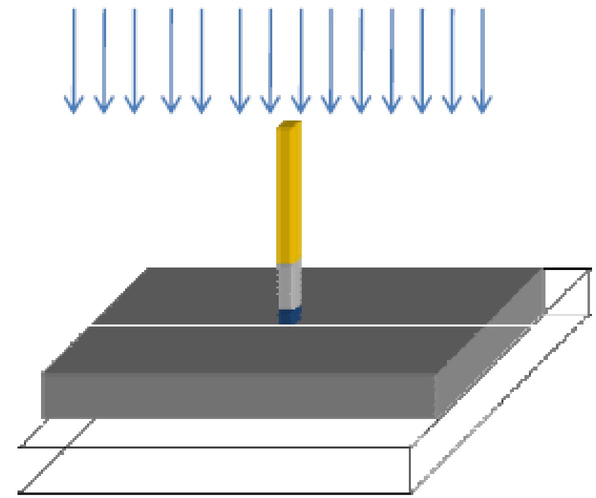

Stop point must be after the barrier and before the substrate. Calibration samples are used to monitor the etching stop point.

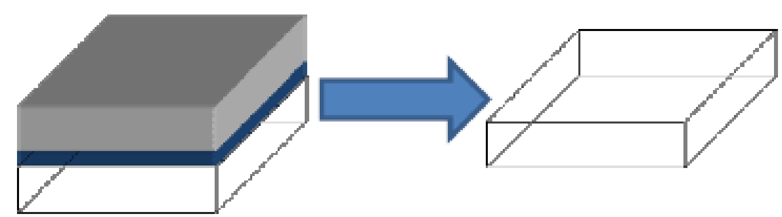

6) Junction Pillar Etching

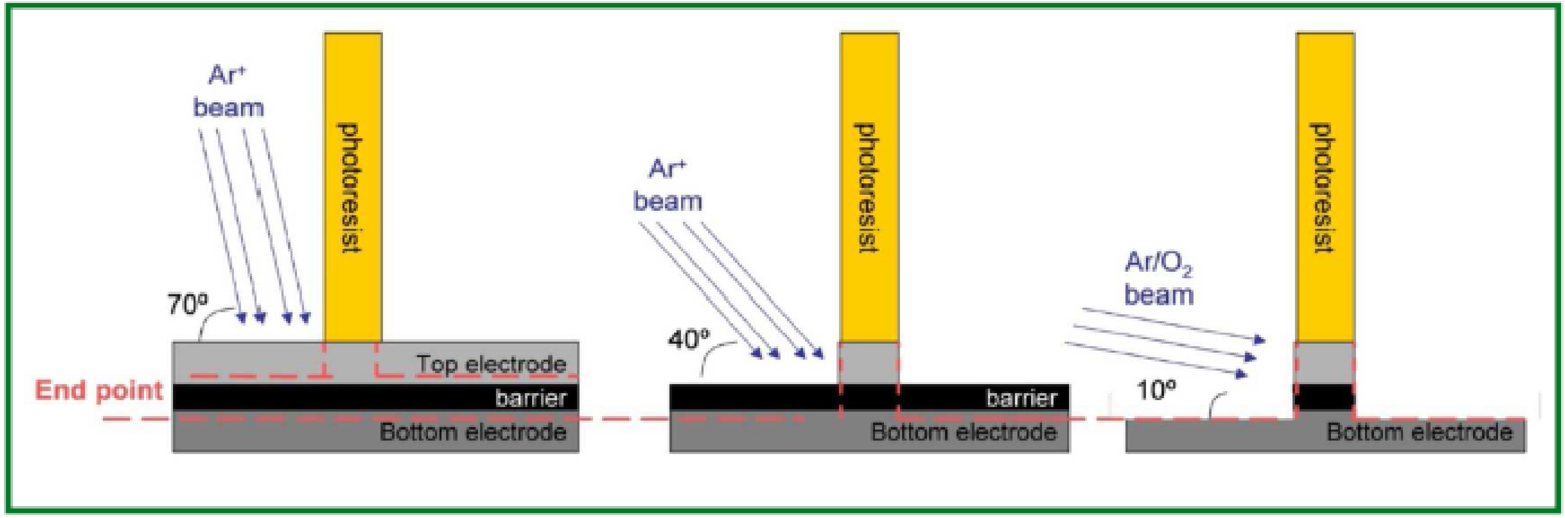

Early Etching Stage :
Large incident angle reduces shadow effects, but results in heavy redeposition

At the level of the barrier:
Shallow incident angle increases the etching in the sidewalls of the pillar, reducing the amount of redeposited material

Final oxidation step:
Any material deposited in the sidewalls of the junction is oxidized, becoming an insulator.

Critical Step #1 : Ion Milling of a NanoPillar

Etch Stop Point Detection

Ion Gun

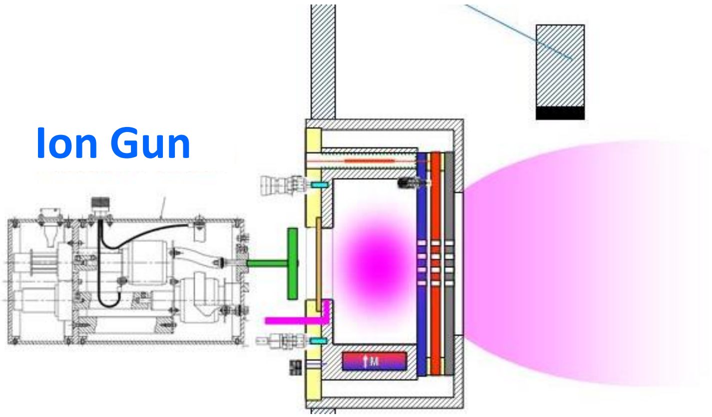

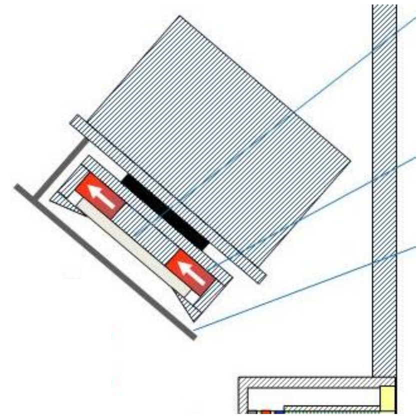

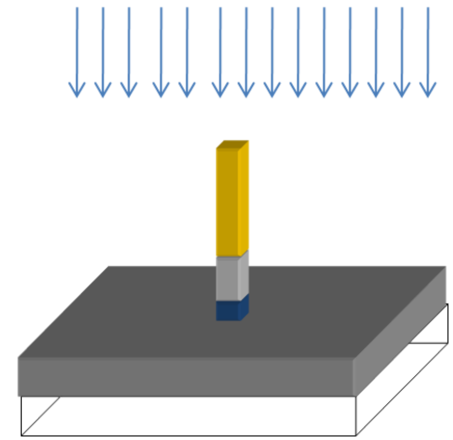

Key Parameters :

RF Power : 190W

V+: +150V

V- : -1500V

I+ : 184mA

I- : -43mA

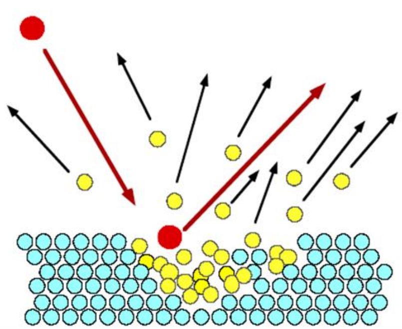

TiW	15nm
Ru	7nm
Ta	10nm
Ru	7nm
Ta	10nm
IrMn	5.5 nm
NiFe	16 nm
Ta	0.21nm
CoFeB	2.6nm
MgO	~ 1.2nm
CoFeB	2.6nm
Ru	0.85nm
CoFe	2.0nm
IrMn	20 nm
Ru	5nm
Ta	5nm
Ru	15nm
Ta	5nm
Ru	15nm
Ta	5nm

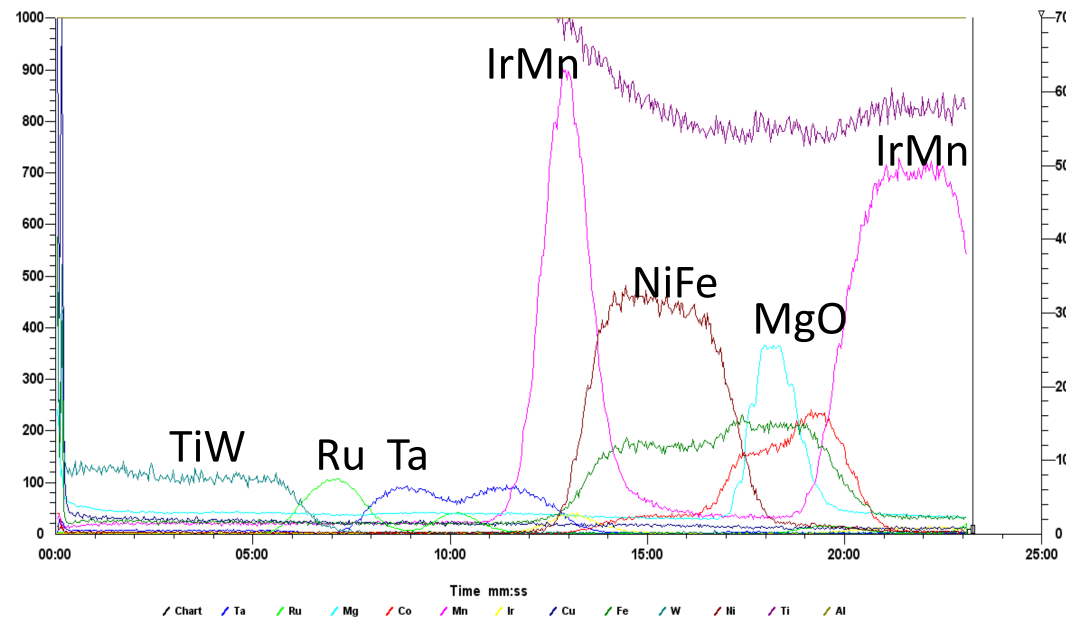

7) Insulating Oxide

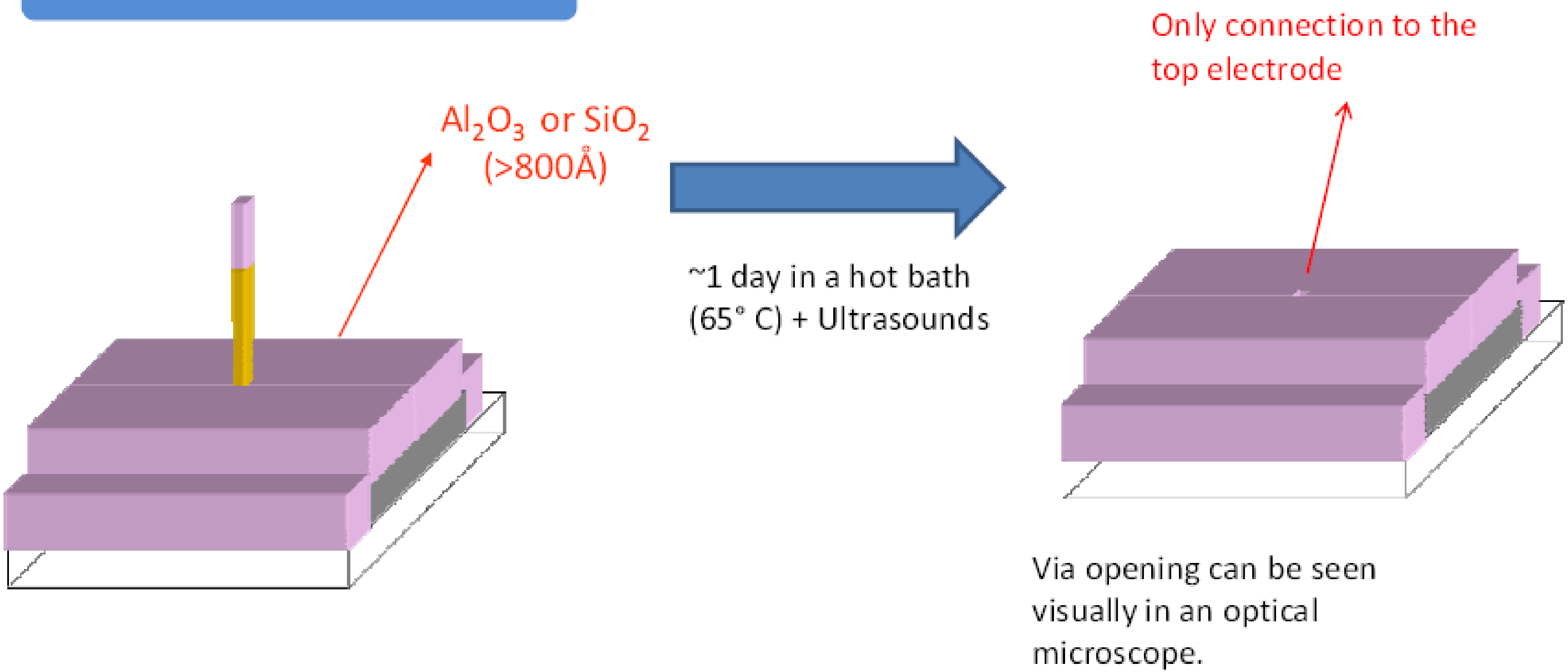

9) 3rd. Lithography : Top Lead Definition

10) Top Lead Definition : Metal deposition + Lift-off

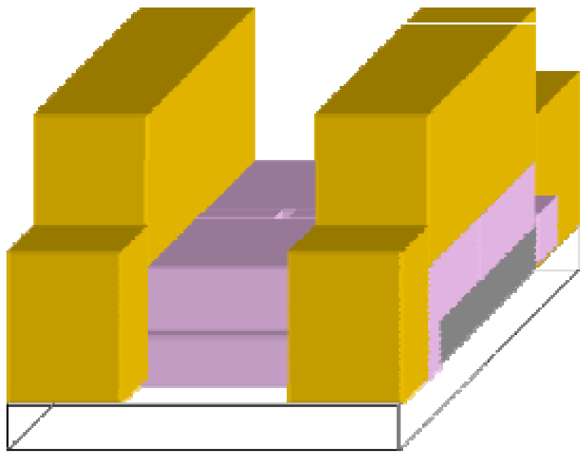

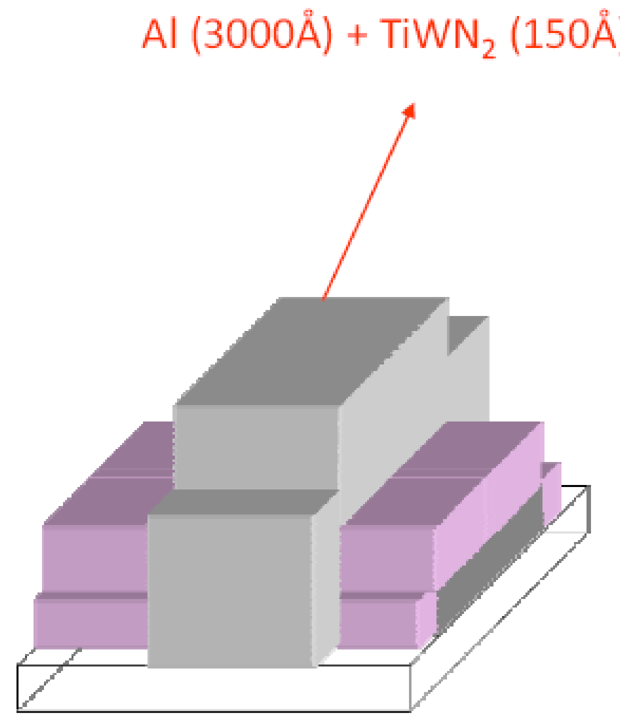

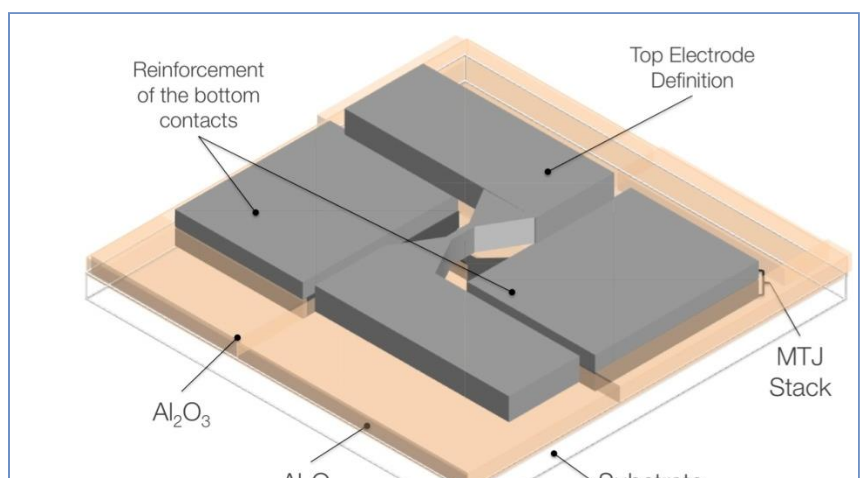

Up to 70,000 sensor devices in a 200mm diameter wafer